ABSTRACT

Title of Dissertation: ESTIMATION OF TROPICAL FOREST ABOVEGROUND BIOMASS USING LARGE-FOOTPRINT LIDAR

Jason Byron Drake, Doctor of Philosophy, 2001

Dissertation directed by: Professor Ralph Dubayah
Department of Geography

Accurate estimates of aboveground biomass provide critical information for modeling carbon dynamics in terrestrial ecosystems. Although aboveground biomass is difficult to quantify over large areas using traditional techniques, large-footprint lidar remote sensing holds great promise for biomass estimation because vertical forest structure is directly sampled. Large-footprint lidar remote sensing techniques have proven successful in accurately estimating forest structural characteristics such as biomass in a variety of temperate forests, however they remained untested in dense, closed-canopy tropical forest ecosystems that contain a large portion of the carbon found in the terrestrial vegetation globally.

The first stage of this research developed relationships between metrics from an airborne scanning lidar instrument and forest structural characteristics in a tropical rainforest in Costa Rica. Lidar metrics were strongly correlated with aboveground biomass, basal area and mean stem diameter through a

successional spectrum of conditions sampled from recently abandoned pasture to primary tropical forest.

The second stage of this research explored the sensitivity of lidar to differences in canopy structure and aboveground biomass at the Costa Rican rainforest. Vertical canopy profiles were developed from field measurements as a basis of comparison with lidar-derived profiles. Metrics from field profiles were highly correlated with both aboveground biomass and corresponding lidar profile metrics. As a result, lidar profile metrics were also highly correlated with aboveground biomass through the entire range of conditions sampled in this Neotropical landscape.

The final stage examined the generality of relationships between lidar metrics and aboveground biomass at two study areas in Central America with different average annual precipitation levels. Lidar metrics were strong predictors of basal area and mean stem diameter at both study areas, however the relationships were significantly different at the two study areas until the deciduousness of canopy trees in Panama was considered. Lidar metrics and aboveground biomass were also strongly correlated, however, relationships remained significantly different between the two study areas primarily due to the different general allometric relationships used to estimate aboveground biomass in tropical wet forests and tropical moist forests. This demonstrates that lidar remote sensing should greatly aid efforts to quantify aboveground biomass in terrestrial vegetation globally.

ESTIMATION OF TROPICAL FOREST ABOVEGROUND BIOMASS USING LARGE-FOOTPRINT LIDAR

by

Jason Byron Drake

Dissertation submitted to the Faculty of the Graduate School of the
University of Maryland, College Park in partial fulfillment
Of the requirements for the degree of
Doctor of Philosophy
2001

Advisory Committee:

Professor Ralph Dubayah, Chair/Advisor
Dr. David Clark
Dr. Robert Knox
Professor Stephen Prince
Dr. Michelle Hofton
Professor Irwin Forseth

DEDICATION

To my parents and grandparents for always believing in me,
and to my loving wife, Betty, whose support and
encouragement made it all
possible.

ACKNOWLEDGEMENTS

This dissertation would not have been possible without the assistance of a great many people. I thank my advisor, Ralph Dubayah, for his vision, advice and support through the past three years. I also thank Ralph Dubayah, Robert Knox, David Clark, Steve Prince, Michelle Hofton and Irwin Forseth for their guidance with this research and for helpful comments related to this dissertation. I thank J. Bryan Blair who designed, developed and operated the LVIS instrument, and Michelle Hofton and David Rabine who helped operate LVIS. I also thank J. Bryan Blair, Michelle Hofton, Nancy Casey-McCabe and Dave Kendig for their tremendous effort in processing the LVIS data. I am deeply indebted to David Clark and Robin Chazdon for the use of field data at La Selva, and to Richard Condit for the use of his field data from Panama. I am grateful to Leonel Ramos, William Miranda, Marcos Molina, Jeanette Paniagua, Braulio Vilchez, Robin Chazdon, Laura Rochio, Birgit Peterson, Steve Prince, John Weishampel and Ralph Dubayah for valuable help in collecting field data at La Selva, and Richard Condit, Suzanne Lao and many others for collecting field data in Panama. I thank Stephanie Bohlman, Chris Pyke and Jerome Chave for sending me copies of their early manuscripts related to Panama field research. My special thanks also go to the La Selva Biological Station, the Organization for Tropical Studies, the Carbono Project (funded by DOE, NSF and the Andrew W. Mellon Foundation), the Center for Tropical Forest Science of the Smithsonian Tropical Research Institute, the Wallops Flight Facility Aircraft Programs Office, the National Geographic Institute of Costa Rica and the Governments of Costa Rica and Panama. This research project was funded by a NASA contract to the University of Maryland for the implementation and execution of the Vegetation Canopy Lidar Mission under the Earth System Science Pathfinder program. I also received funding through a NASA Earth System Science Fellowship.

TABLE OF CONTENTS

TABLE OF CONTENTS (Continued)

TABLE OF CONTENTS (Continued)

LIST OF TABLES

LIST OF FIGURES

LIST OF FIGURES (Continued)

Chapter 1. Introduction and Background

Tropical forests are among the most structurally complex and carbon-rich ecosystems in the world (Dixon et al. 1994, Richards 1996). The way that carbon cycles through these dynamic systems is of interest at local (e.g., landscape-level respiration of woody plants, forest turnover) and global (e.g., deforestation and aforestation of tropical areas) scales. Knowledge of the total carbon content in tropical vegetation provides a crucial initial condition or baseline for studies that examine carbon flux caused by natural and anthropogenic processes.

Field studies typically use biomass (which is approximately 50 percent carbon) as a surrogate for the total carbon that is within terrestrial vegetation. Although field biomass estimation methods are useful for local-scale studies, the total area covered by these studies is small, and many of the field plots are biased in their placement (Brown 1997). This significantly hampers efforts to extrapolate field results over heterogeneous areas of landscapes that were not sampled. In addition, the cost to repeatedly sample field plots is high, which therefore limits the ability to conduct long-term studies over large areas.

As a result, remote sensing techniques are necessary for the measurement of biomass over broad spatial scales. Unfortunately, many types of remote sensing instruments suffer from the same problem: they are sensitive to changes in biomass in relatively young and/or homogeneous forests, but are unaffected by changes in biomass in older or heterogeneous forests (e.g., Luckman et al. 1997, Steininger 2000). As a result, remote sensing techniques have not been successful in estimating biomass in dense closed-canopy tropical forests.

Lidar instruments, or laser altimeters, may be able to overcome some of the limitations of other remote sensing instruments in forest biomass estimation. These instruments have been used to accurately estimate canopy height in a variety of different forest types. As a result, lidar instruments reliably provide an important biophysical characteristic that can then be used to estimate changes in carbon or biomass in forest areas.

In addition to canopy height, new large-footprint, full-digitization lidar instruments also provide data related to the vertical arrangement of forest structure from the top of the canopy to the ground. This data can also be used to improve the prediction of biomass, and to estimate the vertical distribution of forest structure such as vertical foliar profiles (Lefsky et al. 1999a, Harding et al. 2001). As such, lidar instruments provide a wealth of data potentially suited for estimation of biomass in forest ecosystems.

Although large-footprint lidar instruments have proven useful for aboveground biomass estimation in temperate forest environments (Lefsky et al. 1999b, Means et al. 1999), they remain untested in dense, carbon-rich tropical forests. As a result, new empirical relationships between traditional forestry measurements or estimates of forest structure, and metrics from lidar waveforms that may relate to vertical canopy structure must be developed. The generality of the relationships between lidar metrics and forest structure also must be explored in tropical regions with different climatic conditions. If lidar metrics are significantly correlated with tropical forest biomass in different tropical areas then space-borne lidar instruments may be effective for global biomass estimation.

In this chapter I first discuss the importance of estimating the carbon and biomass content of tropical forest ecosystems. Second, I review different techniques for estimating forest biomass, and attempt to illustrate areas where existing techniques are inadequate or remain untested. Finally, I present research questions pertaining to the use of large-footprint lidar instruments for aboveground biomass estimation in closed canopy tropical forests. These research questions are then addressed in the subsequent chapters.

Why is Biomass Important?

Biomass is the total amount of biological materials in a given area at a given time. It is usually expressed in either live or dry weight, for example kilograms of biological material per hectare (kg/ha). Biomass is rarely directly measured, and is instead generally estimated through allometric relationships. As a result, I will typically use “estimated aboveground biomass“ (EAGB) to refer to the estimated total, oven-dried aboveground biomass of a tree or forested area. This will then be a composite of both foliage and woody biomass of a given tree or forested area. EAGB is important in several different ways, some of which are listed below.

Need for Accurate Estimation of Terrestrial Carbon Pools

To more fully explain the degree to which human activity may contribute to global climate change it is necessary to clarify elements of the global carbon cycle (GCC). There are still many uncertainties related to the different portions of the GCC, for example pertaining to the magnitude of carbon pools and fluxes, or transitions, between pools (Smith et al. 1993, Sundquist 1993, Gifford 1994, Kolchugina and Vinson 1995, Gaston et al. 1998, Falkowski et al. 2000).

Although the entire terrestrial carbon pool represents only a fraction of the oceanic carbon pool, the annual flow between the atmosphere and the terrestrial surface is on the same order as the ocean-atmosphere flow (Tans et al. 1990, Smith et al. 1993). Despite their relative importance in the GCC, however, terrestrial carbon pools and fluxes are poorly understood, primarily because of the difficulties associated with estimating the carbon content in terrestrial vegetation (Gifford 1994, Gaston et al. 1998, Potter 1999, Falkowski et al. 2000). These uncertainties limit modeling efforts to link the terrestrial carbon pool to other components of the GCC (Smith et al. 1993) and may undermine major global policy decisions (e.g., management of carbon stocks) that are based on these data (Tans et al. 1990, Dixon et al. 1994, Houghton 1996, Steffen et al. 1998).

Many of the difficulties in identifying the magnitude of terrestrial carbon pools arise from different estimation techniques. Broad-scale carbon modeling efforts often derive terrestrial carbon pool values from data for other portions of the GCC through inversion of atmospheric carbon transport models (e.g., Fan et al. 1998, Battle et al. 2000). However the reliability of this methodology has been questioned (Kaiser 1998, Holland and Brown 1999, Potter and Klooster 1999b). Other methods attempt to use biomass estimates to quantify terrestrial pools of carbon. Because biomass is largely (~50%) carbon, it serves as a useful predictor of the amount of carbon in terrestrial pools (Brown 1997).

Forestry and Ecological Importance of Biomass

Biomass represents the sum of all biological material in a given area, and is a critical component of many forestry and ecological applications. Biomass is also a direct indicator of the total yield from a particular forest stand. As such, foresters often try different management techniques to maximize total biomass. For example by harvesting plantations at different intervals they may identify an ideal time to harvest so as to maximize their return (Franklin et al. 1997). However, many forestry studies may only include commercially valuable species or merchantable timber in their biomass estimates.

Biomass is also an important ecological parameter for describing the productivity and function of forest ecosystems (Spies 1997). The changes in biomass levels during a specified time interval (e.g. one year) help illustrate the productivity of the system. Here an important distinction is necessary. Most techniques estimate only the aboveground component of total biomass (i.e., EAGB), however, the total carbon fixed through photosynthesis after respiration, or net primary production (NPP), is allocated to both aboveground (e.g., branches and leaves) and belowground (e.g., fine and coarse roots) components. In many cases the belowground carbon content may equal or exceed the aboveground component. In addition, many studies also neglect to include the portion of total carbon allocated to materials lost during the measurement interval (e.g., to herbivores). So conclusions about productivity based solely on changes to aboveground components may be missing important details (see Clark et al. 2001). However, because approximately 50% of biomass is carbon, accurate estimation of aboveground biomass levels is an important step in understanding terrestrial ecosystem carbon dynamics.

Additionally, biomass is an indicator of how organisms partition or allocate their resources under different environmental conditions. At the global scale, differences in climate and the total and seasonal variation of incoming solar radiation help to explain biome-level variation in carbon allocation in plants. For example in many tropical environments where there is relatively low seasonal variation in incoming solar radiation, a high total incoming solar radiation, and a warm, wet climate the vegetation is under high competition for light. As a result, individual trees typically allocate a high proportion of carbon resources towards vertical growth and enlargement of crown area. At the local scale, these allocation strategies are further modified by topographic and soil conditions, as well as other environmental factors (Laurance et al. 1999, Clark and Clark 2000). This leads to a hierarchical, heterogeneous distribution of carbon over tropical landscapes or regions. As a result, information pertaining to the spatial patterns of carbon allocation is important for a better understanding of vegetation-environmental interactions.

Methods to Derive Biomass

The only method to directly measure biomass is through destructive sampling of trees or entire forest stands, where all biological material is oven-dried (to remove all water remaining in living tissues) and is then weighed.

Instead, most studies use allometric relationships to estimate biomass from a more easily measurable structural feature. To then convert a biomass estimate to carbon content one typically assumes that approximately 50% of biomass is carbon. This value is an approximation that may be more appropriate for some tree components (e.g., wood) than others (e.g., leaves).

In traditional forestry studies the relationships are typically between a tree component, for example the stem diameter or height, and the aboveground biomass of the tree (Husch et al. 1982, Smith and Brand 1983). More recent attempts have also been made to relate forest biomass to remotely sensed data. In this case the interaction of the vegetation with electromagnetic radiation either from the sun (passive remote sensing) or the instrument itself (active remote sensing) is used to predict field estimated forest biomass. All of these methods are discussed below.

Ground-based Approaches

Methods for estimating biomass on the ground have primarily been developed in forestry and plant ecology studies. Although in some cases intensive destructive sampling and measurement of biomass and other tree parameters is performed (e.g., Whittaker and Woodwell 1968, 1969), this approach is expensive and time-consuming. When destructive techniques are utilized they are typically done in a manner so that allometric equations (e.g., Husch et al. 1982, Smith and Brand 1983, Cannell 1984, Niklas 1994a and b) can be developed to relate total oven-dry aboveground biomass to a particular tree (e.g., height or stem diameter at breast height) or forest stand structural attribute (e.g., basal area or volume over bark). Allometric relationships can often be developed because the growth of different tree components (e.g., stem diameter) is related to the increase in the overall aboveground mass of the tree throughout the growth cycle (Figure 1.1). For example, as trees grow there is typically a geometric increase in biomass per tree with increases in diameter (Brown 1997).

In field studies all stem diameters within a plot that are over a minimum size (e.g., 10 cm) are typically measured at breast height (1.37m) or, in the case of large tropical trees, above buttressing. The diameter measurements can then be used to derive tree biomass using an allometric equation that has been developed for that tree species or for trees within that type of forest ecosystem (e.g., the tropical wet forest equation in Brown 1997). The estimated tree-level aboveground biomass values are then generally summed for all measured trees within the plot. As a result, plot-level EAGB values have both a systematic error component related to components not included (e.g., trees with diameter < 10 cm, shrubs, etc.), and a random error component related to measurement error (see Brown et al. 1995).

Ground-based biomass estimation techniques differ greatly, and are often tailored for the specific need for the data (e.g., Cannell 1982, Smith and Brand 1983, Cannell 1984, MacDicken 1997). In traditional ecological studies the intent is often to characterize local forest structure, therefore, the study sites are often not selected in an unbiased manner. In fact, the placement of plot locations is often biased by the investigators' perception of how an "ideal forest site” should appear (Brown et al. 1995, Brown 1997). Furthermore, the total

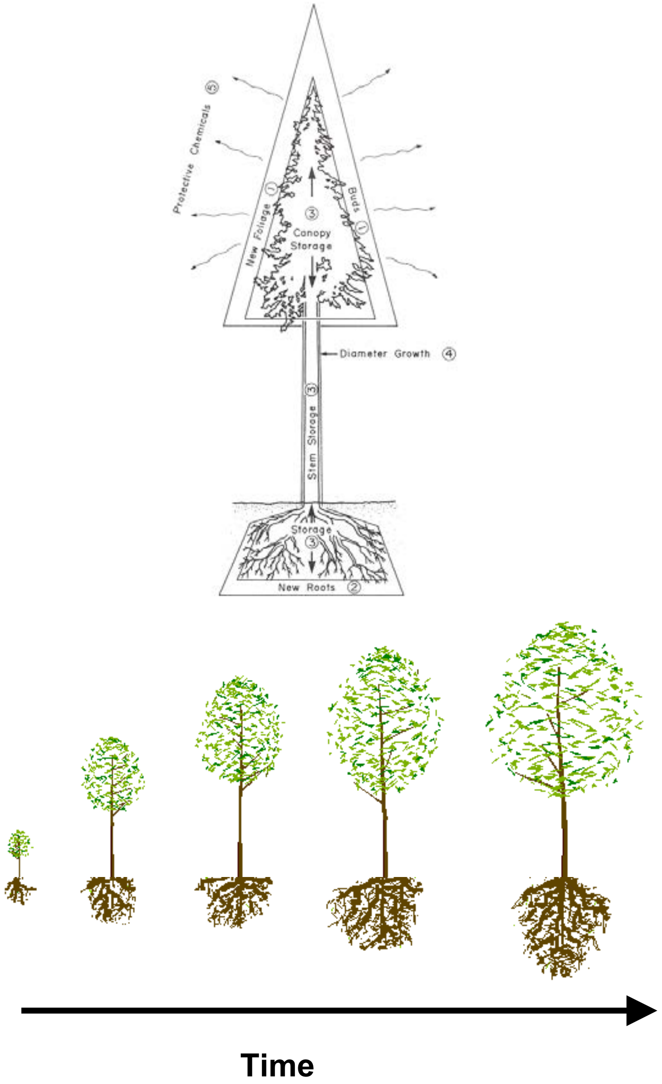

Figure 1.1 Conceptual diagram of tree-level carbon allocation. As trees grow they allocate carbon to roots to increase absorption of water and nutrients, to crown components (e.g., branches, leaves) to increase the amount of carbon which can be fixed into photosynthate, and to stem components to increase the surface area available to transport water and nutrients. Allometric relationships relate the increase in total biomass (or aboveground biomass) of the tree to increases in the size of a component (e.g., stem diameter or height). Upper portion of figure is from Waring and Schlesinger (1985).

area sampled by ecological studies is miniscule. Less than 0.00001% of all tropical forest areas are estimated to have been sampled in field plots (Brown 1997). These studies are effective for quantifying local-scale forest characteristics, but can lead to problems when used to make inferences about surrounding forested regions (Brown and Lugo 1992), and are of particular concern when they are applied globally (Olson et al. 1983).

In addition to ecological studies there are national (e.g., US Forest Service Forest Inventory and Analysis, FIA project; Birdsey et al. 1997) and international (e.g., FAO FORIS; FAO 1995) forest inventory projects that provide EAGB values in forest areas. In many cases, plots in these national and international projects are located using a planned, stratified sampling design. These projects also typically include a large number of plots. Unfortunately, these inventories are relatively scarce in tropical regions (Brown 1997). In addition, there are often different methods used to conduct the inventories in different countries. As a result, current forest inventories are also not ideally suited for global scale forest aboveground biomass estimation.

A large and costly international forest inventory project would be required to obtain accurate estimates of global forest biomass using field techniques. The design of such an international project could resemble the FIA project used by the US Forest Service where a stratified sampling design is implemented globally. The plot network would also need to be resampled periodically through time, which would require enormous resources. As a result, the ability to use remotely sensed data to estimate global forest aboveground biomass is highly desirable.

Passive Optical Remote Sensing of EAGB

Multispectral data collected from airborne (e.g., Airborne Thematic Mapper or ATM) and spaceborne (e.g., Advanced Very High Resolution Radiometer or AVHRR) passive optical remote sensing instruments are generally used to predict forest EAGB in two ways. First, EAGB may be correlated with individual spectral reflectance bands (e.g., near infrared reflectance, middle infrared reflectance) or with spectral indices that incorporate two or more spectral bands (e.g., the normalized difference vegetation index or NDVI). Second, multispectral data may be incorporated into models to infer EAGB.

While some studies have revealed correlation between vegetation indices (e.g., NDVI) and EAGB, this relationship appears to be primarily valid in non-forested areas (Hardisky et al. 1984, Shippert et al. 1995) or in relatively open canopy forests (Running et al. 1986). Other studies (e.g., Sader et al. 1989, Anderson et al. 1993) have shown that there is little or no relationship between NDVI and EAGB in more densely forested regions. Therefore, in some cases passive optical data from tropical regions has instead been used to discriminate between recently cleared and older regenerating rainforest (e.g., Sader et al. 1989, Foody et al. 1996, Kimes et al. 1998, Nelson et al. 2000). This approach to estimate forest EAGB is difficult because spectral indicies (e.g., NDVI) from passive optical sensors are sensitive to changes in leaf area index, or LAI, (Wickland 1991) which may reach an asymptote within 10 years after pastures are abandoned in tropical areas (Brown and Lugo 1990).

Other authors have attempted to estimate forest EAGB using a single spectral band. For example, near infrared reflectance (NIR) was shown to be correlated with EAGB in pine plantations (Danson and Curran 1993) and middle infrared reflectance (MIR) was correlated with tropical forest EAGB (Curran et al. 1997, Boyd et al. 1999). The strength of the relationship between MIR and EAGB varied greatly between and within studies. Steininger (1998) notes that his results for young (<13 years of age) secondary forests from Brazil (R^2= 0.7) and Bolivia (R^2=0.03) cannot be directly compared with the results from Curran et al. 1997 (R^2 =0.2) because the later did not use same atmospheric correction techniques. Steininger (1998) also reports that his results were highly sensitive to different atmospheric correction techniques. The author suggests that the reason the relationships between MIR and EAGB were different in Bolivia and Brazil may have been influenced by differences in sun angles and atmospheric haze over the two study areas where the Landsat TM data were acquired (Steininger 2000).

Spectral reflectance data and spectral indices from passive optical instruments may not be ideally suited for the estimation of tropical forest EAGB. The sensitivity of NDVI to LAI in very young secondary forests, as well as the saturation of MIR in tropical secondary forests older than 13 years confirms the utility of passive optical data for mapping deforestation in tropical regions. However, because the data generally are not strongly correlated with forest EAGB in dense, older tropical forest areas these instruments are of limited use in producing accurate estimates of biomass in areas which contain a large proportion of the carbon in the global terrestrial pool (Dixon et al. 1994).

In addition to direct correlation of passive optical data with EAGB, there are efforts to incorporate this remotely sensed data into models that estimate biomass and carbon globally. Recent models have attempted to simulate the productivity of global terrestrial ecosystems. These models are usually driven by time-series data on the properties of the vegetation cover, such as changes in surface "greenness" (inferred from changes in NDVI) from satellite observations.

The NASA-CASA model (Potter and Klooster 1999a) uses the relationship between NDVI and vegetation parameters such as fraction of absorbed photosynthetically active radiation (fPAR) to predict terrestrial net primary productivity (NPP). The model also simulates the relationship between terrestrial NPP fluxes and atmospheric carbon dioxide fluxes, and has been used to examine potential carbon sinks in the Northern Hemisphere (Potter 1999) at a 1° grid scale. The model also produces global estimates of biomass at the same scale, but these estimates vary greatly from ground-based estimates (Olson et al. 1983) in high latitude, low productivity sites (Potter 1999).

The global production efficiency model (GLO-PEM) is a 'bottom-up' (mechanistic) model of primary production that incorporates remotely sensed estimates of absorbed photosynthetically active radiation (APAR) as well as environmental variables (e.g., temperature) that affect the utilization of APAR (Prince and Goward 1995). Global gross primary productivity (GPP) and NPP values from GLO-PEM are similar to those produced from other approaches (Prince et al. 1995, Prince and Goward 1995, Goetz et al. 1999). In addition, GLO-PEM has been used to produce preliminary estimates of global biomass at the 8X8 km scale, using AVHRR data (Prince et al. 1995).

Even if NASA-CASA, GLO-PEM or other terrestrial ecosystem productivity models can accurately predict net primary production in a given area through time, these models were not intended to predict the total amount of carbon or aboveground biomass in terrestrial ecosystems. The link between productivity and the total biomass is highly variable. As a result, the NASA-CASA model predicts only fifty percent of the ground-derived EAGB that is found in high-latitude, mature coniferous and deciduous forests with low productivity. Although these modeling approaches are important in the effort to go beyond simple linear transforms between vegetation indices and forest production (Prince et al. 1995), the global terrestrial biomass estimations from these models should probably be considered in a relative manner, and not as representative of the absolute values to be used in global policy decisions such as the management of carbon stocks.

Physical canopy reflectance models may also by applied through inversion of reflectance observations to infer physical characteristics, such as biomass (Strahler 1997). Radiative transfer models (e.g., Myneni 1991), consider multiple scattering of photons in canopies, but may not apply well to natural forest and savanna vegetation unless they are heavily calibrated (Wu and Strahler 1994). A more recent type of physical model, geometric-optical models, models vegetation cover as a collection of discrete objects, such as individual plant crowns. An example of this type of model is the Li-Strahler model (Li et al. 1995) that treats individual plant crowns as three-dimensional objects. This model has been inverted to estimate forest structural characteristics, including EAGB with somewhat successful results (Wu and Strahler 1994, Yang and Prince 1997). Similarly, geometric models have been used to relate crown shadow characteristics to forest EAGB in boreal regions (Hall et al. 1995).

Recently, hybrid physical reflectance models (e.g., Li et al. 1995) have been developed that combine geometric-optical and radiative transfer principles. Early validation efforts from conifer forests in Maine (Li et al. 1995) and at BOREAS (Ni et al. 1997) show good agreement between modeled and observed reflectance data (Strahler 1997). Further advances in this field, coupled with a new suite of EOS sensors should radically improve the ability to predict land surface characteristics from satellite observations. However, the degree to which physical models will help with retrieval of forest biomass globally is uncertain because of the dependence of these models to knowledge of local forest canopy characteristics (Strahler 1997).

Passive Optical Summary

Passive optical remote sensing instruments have proven to be extremely useful for global land cover classification (e.g., DeFries et al. 1995), and deforestation (Skole et al. 1994, Kimes et al. 1998) studies, primarily because of the sensitivity of spectral regions to differences in LAI associated with different forest types (e.g., deciduous vs, broadleaf) and ages (e.g., clear-cut, vs. regenerating). However, because LAI in closed canopy (>80% cover) forest ecosystems typically reaches an asymptote early in succession while biomass may continue to increase for hundreds of years (Saldarriaga et al. 1988), these types of instruments may not be ideally suited for global estimation of terrestrial biomass, particularly in dense tropical forests. As a result, models that use this data will also be limited in producing accurate biomass estimates in dense tropical forest areas. Although products from existing and new EOS-era passive optical systems play a vital role in the realm of earth system science, there is currently a need to use alternative remote sensing technology to accurately estimate forest biomass.

Radar Remote Sensing of EAGB

Radar remote sensing examines the interaction of long wavelength microwave energy (typically between 1 and 150 cm) with vegetation structure. The majority of radar systems used to estimate forest structural characteristics are active (i.e., the energy is emitted and received by the instrument) systems. Passive microwave instruments have primarily been limited to estimating characteristics of agricultural crops (Ferrazzoli et al. 1992, Paloscia and Pampaloni 1992, Wigneron et al. 1993, Wigneron et al. 1995, Jin and Liu 1997, Wigneron et al. 1999), however the possibility of using these instruments to study forests has been addressed in theoretical framework (Ferrazzoli and Guerriero 1996).

Active radar systems have a resolution that is proportional to the antenna length of the instrument, therefore synthetic aperture radar (SAR) techniques are generally used for terrestrial land surface applications (Waring et al. 1995, Kasischke et al. 1997). Most SAR instruments emit energy in specific wavelength bands (e.g., C, L and P), each of which interact differently with particular components of the vegetation structure (see Waring et al. 1995 for a detailed discussion). The radar signal that is reflected back in each of these bands is referred to as "backscatter". The amount of reflected energy, or backscatter, that is received corresponds to the particular wavelength that is emitted, the spatial resolution of the instrument, and the interaction of the energy at that wavelength with vegetation structure. Unfortunately, radar imagery often contains speckle (or radar fading), which generally requires the user to average pixels from a particular land cover type (Kasischke et al. 1997). One of the greatest benefits of radar, however, is that it is not greatly affected by atmospheric clouds and haze.

Numerous studies have found relationships between radar backscatter and forest EAGB. From the relatively large body of literature that exists on the topic a few trends emerge. First, all radar bands are highly sensitive to water, and therefore may not operate well without relatively dry canopy and soil conditions (e.g., Dobson et al. 1995a, Harrell et al. 1997). Second, shorter radar wavelengths (X- and C-bands) are scattered and attenuated by canopy elements and are usually not effective for forest aboveground biomass estimation (e.g., Baker et al. 1994). Third, longer radar wavelengths (L- and P-bands) tend to be most sensitive to changes in forest EAGB (e.g., LeToan et al. 1992, Green et al. 1996). Fourth, multiple band sensors (e.g., AIRSAR, SIR-C) are more sensitive to changes in forest EAGB than single band sensors (e.g., Dobson et al. 1992, Ranson et al. 1997). And finally, cross-polarized (e.g., horizontally transmitted, vertically received or HV) signals are usually more sensitive to changes in EAGB than single polarized (HH) signals (e.g., Kasischke et al. 1995, Harrell et al. 1997).

Many studies report that radar backscatter is highly correlated with forest EAGB, and therefore report that radar is an effective tool for forest biomass estimation. These kinds of conclusions may be justified, but from the available literature it appears that a few qualifications need to be included with the above statement. First, these studies typically have been conducted in forest plantations (e.g., LeToan et al. 1992, Baker et al. 1994, Green et al. 1996) or in managed or natural forest ecosystems with low woody species diversity (e.g., Kasischke et al. 1995, Wang et al. 1995, Harrell et al. 1997, Hyyppa et al. 1997). In these relatively uniform, homogenous forests it is much easier to develop multiple-step approaches which first estimate individual components of the total forest aboveground biomass (e.g., crown biomass) and then apply these components in a secondary regression to estimate total EAGB (e.g., Dobson et al. 1995b, Kasischke et al. 1995, Harrell et al. 1997, Kasischke et al. 1997). Kasischke et al. (1997) state "the complexities of these methods and the uncertainties are greater in landscapes where there are…multiple tree species." As a prime example, Luckman et al. (1997) found a weak relationship between a long radar wavelength band (L-band) and tropical forest EAGB in Brazil.

A second qualification relates to a disagreement in the radar community about radar saturation in high biomass areas. Even in relatively homogeneous forest plantations radar instruments have been reported as insensitive to increases in forest EAGB beyond a certain threshold. In some cases this threshold has been listed as between 100-150 Mg/ha (Imhoff 1995, Waring et al. 1995) for longer radar wavelengths, and even lower for shorter radar wavelengths. This “saturation threshold" varies a great deal depending on both the forest type and the analytical techniques used in a given study. For example, some studies have reported that the more elaborate multi-step techniques mentioned above were sensitive to EAGB levels up to 400 Mg/ha in managed loblolly pine forests (Kasischke et al. 1995) and to 250 Mg/ha in mixed coniferous/deciduous forests in Michigan (Dobson et al. 1995b). However, in the dense tropical forests of Brazil (Luckman et al. 1997) the saturation point was 60 Mg/ha, which is approximately the level found in a 10 year old secondary tropical forest.

A final qualification relates to the general applicability of the results in the radar studies that are cited above. Although the studies have demonstrated that radar backscatter is empirically related to forest EAGB in particular plantations or forest ecosystems, it is unclear how general these relationships are outside of those study areas. This site specificity problem is not unique to radar remote sensing, however it is a clear obstacle in the attempt to estimate forest biomass over broad spatial regions or globally.

Despite these issues, radar has been used in several studies to effectively estimate aboveground biomass, especially in high latitude forests. Although the saturation levels of most SAR instruments would prohibit global biomass estimation (Imhoff 1995), recent studies using a low-frequency SAR instrument (CARABAS-II) are encouraging. Studies in deciduous and spruce forests in southern Sweden have illustrated that the backscatter coefficient from CARABAS-II is significantly correlated (R^2= 0.87), and does not saturate through EAGB levels of 375 Mg/ha (Fransson et al. 2000, Smith and Ulander 2000). However, there are currently no low frequency radar results available from tropical forests.

Several studies have also attempted to use physical models to help construct relationships between radar backscatter and forest EAGB. Most of these studies utilize physical models of how microwave energy scatters through different components of forest canopies (e.g., Ulaby et al. 1990, Sun et al. 1991, Sun and Ranson 1995, Lin and Sarabandi 1999b). For example a recent Monte Carlo coherent scattering model that uses fractal-generated trees (Lin and Sarabandi 1999a) produced very similar results to SAR data from a boreal forest thus suggesting the need for more realistic models of forest structure. Future modeling efforts will certainly aid attempts to understand the complex interaction between microwave energy and forest structure. However, as was the case with physical models for passive optical remote sensing, the applicability of these models over broad spatial regions is uncertain because of the dependence of these models on knowledge of local forest canopy characteristics.

Another study (Ranson et al. 1997) made an attempt to go beyond site-specific limitations from both empirical relationships and physical models of the interaction of forest structure with radar backscatter. The authors used output from a gap-type forest succession model for a northern hardwood-boreal transitional forest area to drive a 3-D canopy backscatter model. Unfortunately, the relationship between the modeled forest structure and the simulated radar backscatter was still found to underestimate EAGB and required field data for calibration, in particular the results were highly dependent on soil moisture levels.

Radar Summary

Radar remote sensing is an effective tool for land surface characterization (Kasischke et al. 1997), however its utility in global biomass estimation remains unclear (Imhoff 1995). Although saturation levels often differ in different forest conditions, it is still uncertain how applicable these relationships are outside of the study areas where they were developed. The insensitivity of radar backscatter to moderate and high forest biomass levels globally has led to a call to 1) move from attempts to correlate forest EAGB with radar backscatter to using radar to identify recently cleared and regenerating forest areas, 2) develop new technology to estimate EAGB in dense forests (Imhoff 1995). However it is likely that new low frequency SAR instruments will expand the applicability of radar instruments, especially if they are proven to be effective for biomass estimation in other areas.

Another consideration is the sensitivity of radar backscatter to water on vegetation. Studies by Harrell et al. (1997) and others have revealed very different relationships between forest EAGB and radar backscatter from two different time periods, one after a rain shower and one in relatively dry conditions. Some tropical regions may receive more than 4000 mm of rainfall per year, thus creating a spectrum of moisture conditions in their canopies. It is likely that radar backscatter from the same tropical forest canopy with different moisture conditions would also be very different. The degree to which this moisture problem may have contributed to the poor results in Luckman et al. (1997) was not detailed. Similarly, how this problem may affect backscatter from new low frequency radar instruments in tropical forest has not been addressed.

Lidar Remote Sensing of Forest EAGB

Lidar (**li**ght **d**etecting **a**nd **r**anging) remote sensing, sometimes also called “laser altimetery,” is a relatively new technology that may greatly improve estimates of biomass in dense forest ecosystems. Whereas radar data are quite complex to process and interpret (Dobson 2000), data from lidar instruments are conceptually quite simple (Dubayah and Drake 2000). Lidar instruments measure the roundtrip time for pulses of laser energy to travel between the sensor and the target. From this travel time, the distance between the sensor and the target(s) can be derived. By subtracting the differences in timing of canopy and ground reflections, canopy height is derived. Although the way in which different lidar instruments operate varies (discussed below), the ability to measure canopy heights is a major benefit over other remote sensing techniques because it is a biophysical characteristic with a field legacy.

Some lidar instruments emit short duration pulses of laser energy from low-flying aircraft and record the distance to the first intercepted surface within a relatively small (less than 1 m in diameter on the ground) sampling area, or footprint (Weishampel et al. 1996). Other versions of these “small-footprint” lidar instruments record the distance to both the first and last returns within each footprint, and the distance between these two elevations is inferred to be the vegetation or "canopy" height for each footprint (Lefsky et al. 1999b). In many cases, energy from small footprint lidar instruments does not consistently reach the ground, which may reduce the apparent vegetation height (Weishampel et al. 1996).

Next-generation, large-footprint lidar instruments (Blair et al. 1994, 1999), overcome many of the problems associated with small footprint instruments. By increasing the footprint size to at least the average crown size of a canopy-forming tree (10-25 m), laser energy consistently reaches the ground even in dense forests (Weishampel et al. 1996). In addition to the traditional canopy height measurement, these instruments also digitize the entire time history of the outgoing and return laser pulses, thus providing a vertical profile of intercepted surfaces (or "waveform") from the top of the canopy to the ground (Blair et al. 1999).

The ability of lidar instruments to recover canopy heights is important because of the strong link between the height and biomass of trees. In this case the allometric relationship moves from the level of the individual plant (Niklas 1994b) to the plot or stand level (Figure 1.2). It is this type of allometric relationship that has allowed researchers to use lidar instruments to estimate forest aboveground biomass and/or volume in mixed hardwood-softwood (Maclean and Krabill 1986, Lefsky et al. 1999b), southern pine (Nelson et al. 1988a, Nelson et al. 1988b), Scots pine (Nilsson 1996), Norwegian spruce-pine

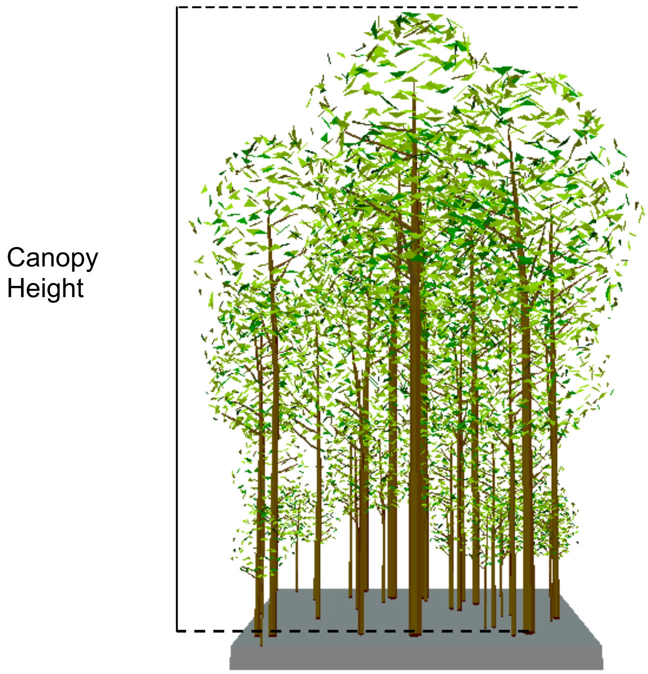

$$\text{Biomass}_{\text{Plot}} = \Sigma\, \text{Biomass}_{\text{Stem}}$$

$$\text{Biomass}_{\text{Plot}} = f\,(\text{Canopy Height})$$

Figure 1.2 In laser altimeter remote sensing plot-level allometric relationships can be developed to relate the total biomass (or aboveground biomass) of all trees within the sampling area to the laser altimeter-derived canopy height.

(Naesset 1997b), Douglas fir/ Western hemlock (Lefsky et al. 1999a, Means et al. 1999) and to a limited degree in tropical rainforests (Nelson et al. 1997). When canopy height is accurately measured, these instruments are generally able to estimate forest EAGB in a statistically significantly way.

The accuracy of canopy height recovery from lidar instruments is influenced by many factors. Prior to kinematic differential global positioning systems, many of the earlier studies were significantly hindered by the problem of obtaining precise position of the aircraft. As a result the location of the lidar footprint within a forest stand was uncertain, thus making ground validation exercises difficult. The wavelength of the laser is also critical because of the spectral response of vegetation. Generally near-infrared wavelength (700-1150 nm) lasers are used because vegetation is highly reflective in this region. Nelson et al. (1984) used an ultraviolet laser, designed for bathymetric work, which may have negatively affected their results.

Another critical factor that affects canopy height recovery from lidar instruments is the ability to consistently penetrate through the canopy to the ground. Many small-footprint sensors tend to yield ground return only in relatively open forest canopies (Weishampel et al. 1996). In more dense forests these small footprint sensors typically provide information pertaining only to canopy roughness and do not reveal accurate canopy heights. As a result small-footprint lidar instruments tend to yield poor EAGB estimates in dense forest areas such as in tropical rainforests (Nelson et al. 1997).

Because of their ability to consistently penetrate to the ground, and to record complete waveforms from the canopy top to the ground, large footprint lidar instruments are ideally suited for the estimation of forest structural characteristics such as EAGB. In addition to canopy height, waveform metrics from large-footprint lidar instruments, which are related to the vertical distribution of canopy elements within the sampled area, can also be used to improve the prediction of EAGB (Figure 1.3).

An early airborne large footprint lidar instrument that has been used to estimate forest structural characteristics is the Scanning Lidar Imager of Canopies by Echo Recovery, or SLICER (Blair et al. 1994). As the name indicates, SLICER scans across its track to produce images of forest structure. A typical SLICER swath is comprised of five, contiguous 10 m diameter footprints and is therefore approximately 50 m across-track. In addition, the footprints are spaced contiguously along track.

SLICER data has been correlated to forest EAGB in tulip poplar, and oak-hickory stands in the coastal plain of eastern Maryland (Lefsky 1997, Lefsky et al. 1999b) and Douglas fir-western hemlock stands in western Oregon (Lefsky et al. 1999a, Means et al. 1999). In both cases, canopy height data from SLICER were incorporated into empirical regression equations to derive stand-level aboveground biomass estimates. For both studies, these relationships were found to be highly significant. For example, Means et al. (1999) could predict total stand EAGB with r^2 values of up to 0.90 with a canopy height metric from the SLICER data. This relationship was non-asymptotic through forest EAGB levels of 1300 Mg/ha, exceeding the normal saturation point of SAR instruments by approximately an order of magnitude. These studies illustrate

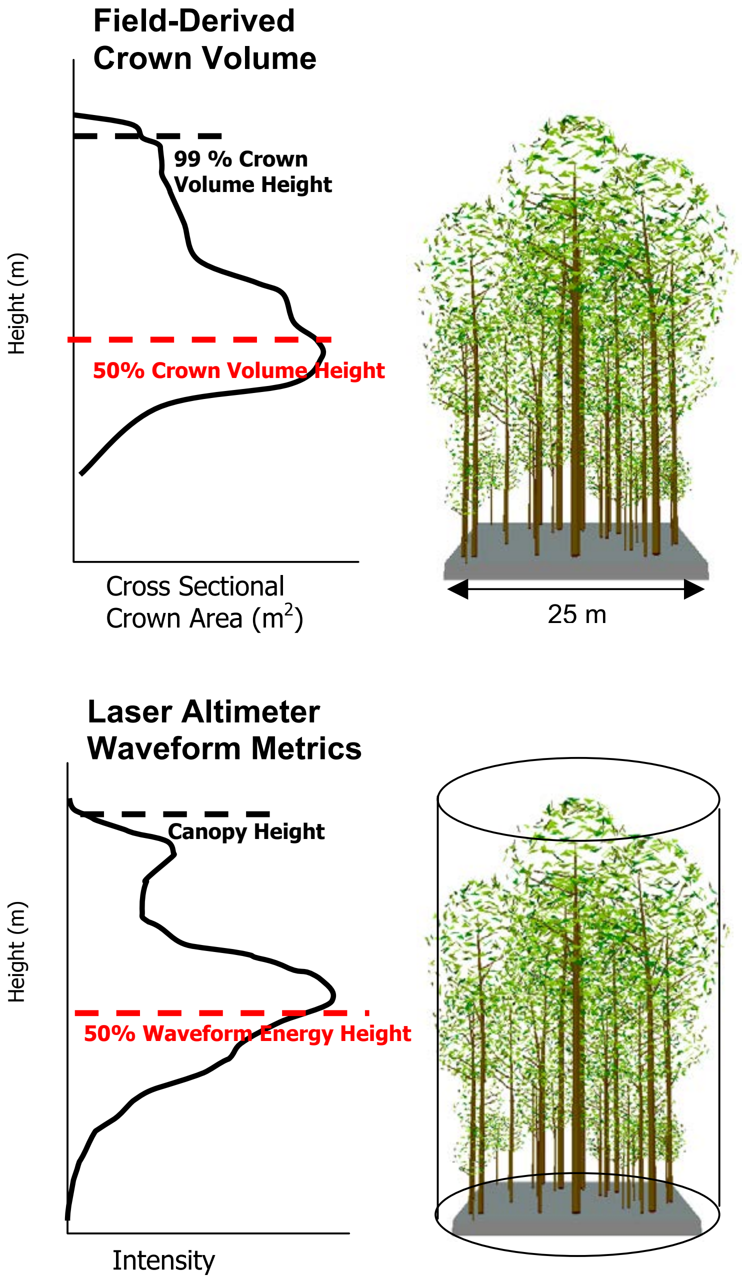

Figure 1.3 Conceptual representation of the relationship between laser altimeter waveform metrics and crown volume. Because of this relationship, laser altimeter metrics (in addition to canopy height) are helpful to predict biomass levels in forest ecosystems.

that new large-footprint lidar instruments are capable of accurately estimating aboveground biomass in some of the most carbon-rich temperate forests in the world. However, a thorough examination of the utility of lidar instruments in dense closed-canopy tropical forests is still necessary.

Unlike passive optical and radar remote sensing work, there is a paucity of studies that model the physical interaction between laser energy and forest structure. A study by Nelson et al. (Nelson 1997) explicitly examined the affect of physical canopy characteristics on lidar metrics. Using this modeling approach, the authors demonstrated that simulated lidar heights differ by as much as 25% if different crown shapes (e.g., conical, elliptical) are used. Similarly, Magnussen and Boudewyn (1998) used two "models" of laser penetration into vertical forest structure to illustrate that the distribution of canopy heights from lidar instruments are a function of the vertical distribution of foliage area.

Recent studies have also extended assumptions from a methodology developed to model foliar height profiles (FHP) from optical point quadrats (MacArthur and Horn 1969) to waveforms from large-footprint lidar instruments (Lefsky 1997, Lefsky et al. 1999a, Lefsky et al. 1999b, Means et al. 1999). The MacArthur-Horn transformation assumes a constant leaf angle for all trees, a random distribution of all leaves, and a logarithmic decrease in energy from the top of the canopy to the ground to produce a "canopy height profile" or CHP (Lefsky 1997, Harding et al. 2001). Metrics from the CHP have also been used to estimate aboveground biomass, however they generally have not improved on the empirical relationship with canopy height (Means et al. 1999).

A recent study also illustrated that elevations from a scanning small footprint lidar instrument can be used to model large footprint lidar waveforms (Blair and Hofton 1999). For this particular case, the small footprint data densely covered the same area that was sampled with a large footprint instrument. This helps illustrate that large footprint lidar provide a "statistical sample" of forest surface elevations within each large (10-25 m) footprint.

There is still a need to develop physical models of the interaction between laser energy and forest structure. Although these physical models, which are in the early stages of development (Ni et al. 1999, Sun et al. in preparation), may also not be applicable over broad spatial regions, they will provide vital information about the utility and limitations of this new technology.

Lidar Remote Sensing Summary

Unlike radar and passive optical sensors, lidar instruments can recover biophysical characteristics that have a "field legacy" such as canopy height. Foresters and botanists have related stand EAGB and volume to heights of trees and forest stands for several decades (Husch et al. 1982, Niklas 1994a). As such these instruments have been used to accurately estimate forest aboveground biomass in a variety of forest conditions.

Beyond the recovery of canopy height, large-footprint lidar instruments also record information pertaining to the distribution of foliar and woody structural elements from the top of the canopy to the ground. Although these measurements do not have a direct analog in traditional forestry techniques, they provide even more potential metrics to relate to forest structure such as EAGB.

Strong linear, non-asymptotic relationships between lidar metrics and EAGB in coniferous forests in Oregon and temperate deciduous forests in Maryland reveal that this technology can accurately estimate aboveground biomass in a variety of temperate forests. However, large-footprint lidar instruments remain untested in dense closed-canopy tropical forests.

There is also a need to explore the nature and generality of relationships between lidar metrics and aboveground biomass. Even across a wide range of conditions in tropical regions throughout the world there is a strong relationship between stand height and EAGB illustrated in Figure 1.4 (data from Cannell 1982). It is important to note that the relationship in Figure 1.4 only uses canopy top height. Data pertaining to vertical distribution of canopy elements (either field- or lidar-derived) could potentially improve upon this relationship.

Research Questions

The research in this dissertation will attempt to develop relationships between large-footprint lidar data and forest structural characteristics in dense closed-canopy tropical forest ecosystems. Although the primary motivation is to use lidar data to accurately estimate tropical forest aboveground biomass, there is an underlying need to understand the fundamental nature of the relationship between lidar data and the forest structural components that together comprise

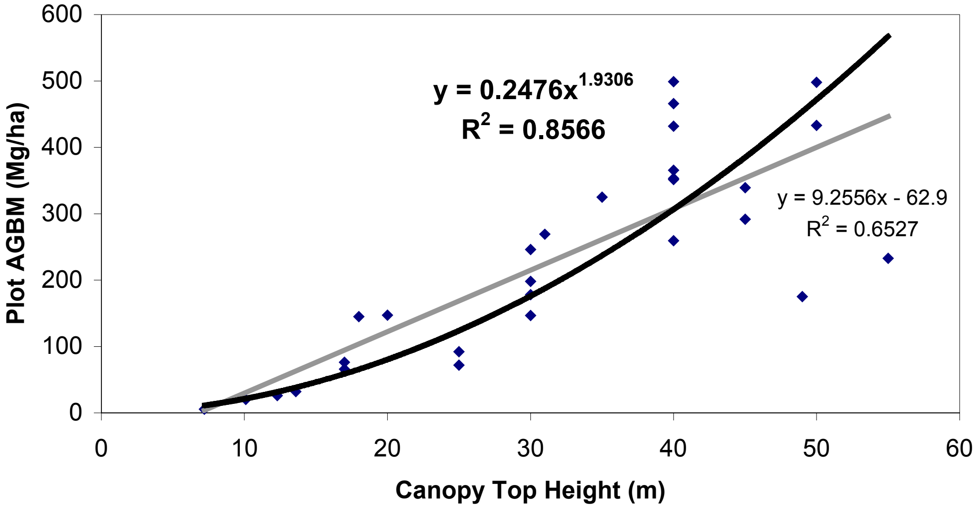

Figure 1.4 Relationship between total plot aboveground biomass (AGBM) and canopy top height (height of tallest tree in plot) for neotropical and paleotropical forest locations in M.G.R. Cannell (1984) *World Forest Biomass and Primary Production Data,* Academic Press, New York. Minimum plot size was 150m^2. Plots that listed only a mean value for all tree heights sampled were not included. The black line in the figure is the regression line corresponding to the power equation (bold). The gray line is the regression line corresponding to the simple linear regression equation.

that biomass. In addition, the generality of the relationship between lidar data and forest structure throughout a broad range of environmental conditions found in the tropics must be examined. The specific questions that this research will address are listed below, followed by a brief overview.

1. Can lidar data be used to accurately estimate biomass in a dense tropical forest?

Although large-footprint lidar has been shown to be an effective new tool for estimating biomass in temperate forest sites (Lefsky et al. 1999a, Lefsky et al. 1999b, Means et al. 1999), it remains an untested technology in dense tropical forest regions where over 40% of the carbon in the terrestrial pool may be located (Dixon et al. 1994). This is a potentially difficult biome for lidar instruments because in many dense tropical forests less than 1-2% of the total sunlight at the canopy top may reach the ground (Baldocchi and Collineau 1994). This represents much greater canopy cover levels than most temperate forest areas where lidar has already been successfully tested.

In the first stage of this research, relationships between field-estimated aboveground biomass and metrics derived from coincident lidar waveforms will be developed for a dense tropical forest landscape in Costa Rica. The field data will be from forest areas in different stages of succession (i.e., secondary and primary forests), and with different local environmental conditions (e.g., different soil types).

2. Are lidar metrics sensitive to differences in the vertical arrangement of forest structure over a tropical forest landscape?

If lidar metrics are significantly correlated with differences in aboveground biomass in a tropical rainforest, then the fundamental nature of these relationships must be further examined. The strength of these relationships primarily will be determined by the ability of large-footprint lidar to record differences in canopy structure that are related to differences in aboveground biomass. For example, canopy height is a relatively straightforward lidar metric to relate to traditional field measurements, and should be correlated with changes in aboveground biomass through succession. Although other metrics that can be extracted from large-footprint lidar waveforms do not have a direct analog in traditional field techniques, they too may be highly correlated with changes in aboveground biomass through succession and in areas with different environmental conditions.

The second stage of this research will involve a more detailed analysis of the sensitivity of lidar waveform metrics to differences in the vertical arrangement of forest canopy structure. The relationship between field-derived vertical canopy profiles and biomass first will be examined to provide a baseline for comparison to lidar-biomass relationships. In addition, both lidar- and field-derived vertical canopy profiles will be compared to examine the sensitivity of lidar to important differences in vertical forest structure.

3. How general are the relationships between lidar metrics and forest structural characteristics (such as aboveground biomass) across closed-canopy tropical forests with different environmental conditions?

The remaining challenge is to explore the generality of relationships between metrics from lidar data and forest structural characteristics such as aboveground biomass and basal area. Thus far, the relationships that have been developed between lidar metrics and forest structural characteristics are site specific and there have been no attempts to compare relationships developed in areas with different environmental conditions. It will be necessary to examine the generality of these relationships in different areas so that global terrestrial biomass estimates can be made using data from future spaceborne lidar instruments such as the Vegetation Canopy Lidar (Dubayah et al. 1997).

The primary goal in the final chapter is to examine the relationship between lidar metrics and aboveground biomass in closed-canopy Neotropical forest areas with different annual precipitation amounts. I will focus on a tropical wet forest (sensu Holdridge et al. 1971) area in Costa Rica, and on a tropical moist area in Panama that receives 50-75% less rainfall on average. First I will examine the relationships between lidar metrics and allometrically estimated aboveground biomass in the two study areas. Next I will develop relationships between lidar metrics and directly measured forest structural characteristics (e.g., basal area) at the two study areas. I will also look for additional factors (e.g., environmental characteristics) that could help explain any differences in the relationships at the two study areas.

Chapter 2. Estimation of Tropical Forest Structural Characteristics using Large-footprint Lidar

Abstract

Quantification of forest structure is important for developing a better understanding of how forest ecosystems function. Additionally, estimation of forest structural attributes such as aboveground biomass is an important step in identifying the amount of carbon in terrestrial vegetation pools and is central to global carbon cycle studies. Although current remote sensing techniques recover such tropical forest structure poorly, new large-footprint lidar instruments show great promise. As part of a pre-launch validation plan for the Vegetation Canopy Lidar (VCL) mission, the Laser Vegetation Imaging Sensor (LVIS), a large-footprint airborne scanning lidar, was flown over the La Selva Biological Station, a tropical wet forest site in Costa Rica. The primary objective of this study was to test the ability of large-footprint lidar instruments to recover forest structural characteristics across a spectrum of land cover types from pasture to secondary and primary tropical forests. LVIS metrics were able to predict field-derived quadratic mean stem diameter, basal area and aboveground biomass with R^2 values of up to 0.93, 0.72 and 0.93 respectively. These relationships were significant and non-asymptotic through the entire range of conditions sampled at the La Selva. Our results confirm the ability of large-footprint lidar instruments to estimate important structural attributes, including biomass in dense tropical forests, and when taken along with similar

results from studies in temperate forests, strongly validate the VCL mission framework.

Introduction

Tropical forests are among the most structurally complex and carbon-rich ecosystems in the world. This complexity is related both to the size-frequency distribution of woody stems (Denslow and Hartshorn 1994, Clark and Clark 2000) and to the three dimensional arrangement of canopy elements (e.g., leaves, branches, trunks) from the top of the canopy to the ground (Richards 1996). Variation in tropical forest structure is influenced by underlying environmental conditions (Clark et al. 1998, Laurance et al. 1999, Clark and Clark 2000), and in turn creates microclimatic (e.g., light, temperature, humidity) gradients (Parker 1995). These fine-scale gradients modify biological processes such as competition and growth (Oberbauer et al. 1993, Rich et al. 1993, Clark et al. 1996, Nicotra et al. 1999) that further modify organization of forest structural components.

Quantification of forest canopy structure provides information about the primary surfaces of energy and matter exchange between the atmosphere and one of the largest reserves of terrestrial aboveground carbon (Dixon et al. 1994, Perry 1994). Knowledge of the total carbon content in tropical vegetation provides a critical initial condition for studies at multiple scales which examine carbon flux caused by natural (e.g., landscape-level respiration of woody plants) and anthropogenic (e.g., deforestation and aforestation) processes. However, the accurate estimation of structural characteristics (e.g., aboveground biomass or total amount of carbon within living tissues) of tropical forest vegetation remains a major obstacle (Dubayah et al. 1997).

Most studies use forest aboveground biomass (AGBM), which is approximately 50 percent carbon, as a surrogate for total aboveground carbon. Because biomass can only be directly measured through destructive sampling, it is usually estimated through a relationship with other measurable properties. Field studies typically use allometric relationships between total biomass and the height or bole diameter of trees. Although field biomass estimation methods are useful for local scale studies, remote sensing techniques are necessary for the recovery of biomass over broader spatial scales.

Most remote sensing studies illustrate the empirical correlation between forest biomass and the intensity of EM energy (or the ratio of energy at different wavelengths) that is received by the instrument. Unfortunately, many types of remote sensing instruments suffer from the same problem: they are sensitive to changes in biomass in relatively young and/or homogeneous forests, but in older or heterogeneous forests the signal becomes less predictable with respect to changes in biomass.

Several studies have shown that passive optical instruments are insensitive to changes in tropical forest structural characteristics such as AGBM beyond secondary forests of 10-15 years (Sader et al. 1989, Foody and Curran 1994, Moran et al. 1994, Steininger 1996, Curran et al. 1997). Metrics from synthetic aperture radar (SAR) such as backscatter also tend to saturate in dense forest conditions (Imhoff 1995, Waring et al. 1995, Kasischke et al. 1997) and have been shown to be insensitive to changes in AGBM for secondary tropical forests with AGBM levels >60 Mg/ha (Luckman et al. 1997).

New large-footprint lidar instruments (Blair et al. 1994, Blair et al. 1999) may be able to overcome the saturation problems of other remote sensing instruments. These instruments estimate canopy height as well as other parameters related to the vertical arrangement of canopy elements from the top of the canopy to the ground by directly measuring vertical structure (Weishampel et al. 1996, Blair et al. 1999, Lefsky et al. 1999b). However, this technology has not been applied to tropical forests. The objective of this study was to test the ability of a new airborne large-footprint mapping laser altimeter instrument to accurately estimate tropical forest structural characteristics such as aboveground biomass and basal area in a dense, wet tropical forest. Related large-footprint laser altimetery technology will soon be incorporated in the spaceborne Vegetation Canopy Lidar (VCL) mission (Dubayah et al. 1997, Dubayah et al. 2000).

In this paper we first provide a brief background on lidar remote sensing, including previous lidar studies of forest structure, and highlighting some differences between existing systems. Next we describe our study site and the new lidar instrument used in this study. Finally we present the results from this lidar instrument and discuss these results in relation to previous remote sensing efforts to estimate tropical forest structure.

Lidar Remote Sensing

Lidar (**li**ght **d**etection **a**nd **r**anging) is an active remote sensing technique using laser light. Lidar systems measure the roundtrip time for a pulse of laser energy (usually with a near-infrared wavelength for vegetation studies) to travel between the sensor and the target. This incident pulse of energy interacts with canopy (e.g., leaves, branches) and ground surfaces, and is reflected back to the instrument. The travel time of the pulse, from initiation until it returns to sensor, is measured and provides a distance or range from the instrument to the object (hence the common use of the term "laser altimetry" which is now generally synonymous with lidar).

Current lidar systems for terrestrial applications differ in: (1) whether they record the range to the first return, last return, multiple returns or fully digitize the return signal; (2) footprint size (from a few centimeters to tens of meters); and, (3) sampling rate/scanning pattern. Most commercial airborne lidar systems are low-flying, small-footprint (5-30 cm diameter), high pulse rate systems (1,000-10,000 Hz). In addition, most commercial lidar systems record the range to the highest, and/or lowest, reflecting surface within the footprint, and are not fully imaging, using instead many laser returns in close proximity to each other to recreate a surface.

Small-footprint lidar sensors may not be optimal for mapping forest structure for several reasons. First, small diameter beams frequently miss the tops of trees (see Nelson 1997). Secondly, because of their small beam size, mapping large areas requires extensive flying. Finally, with systems that only record first and/or last returns, it is difficult to determine if a particular shot has penetrated the canopy all the way to ground. In areas of high canopy only one in several thousand returns may be from the ground (Blair and Hofton 1999). If this topography cannot be recovered, accurate height determination is impossible because canopy height is measured relative to the ground.

Large-footprint lidar systems (Blair et al. 1994, Blair et al. 1999) have several advantages that help avoid these problems. First, by increasing the footprint size to the approximate crown diameter of a canopy-forming tree (~10-25 m), laser energy consistently reaches the ground even in dense forests (Weishampel et al. 1996). Second, the larger footprint size also avoids the biases of small-footprint systems that frequently miss the tops of trees. Third, large-footprint systems fly at higher altitudes and enable a wide image swath, which reduces the expense of mapping large areas on the ground (Blair et al. 1999). Finally, large-footprint lidar systems also digitize the entire return signal (or "waveform"), thus providing data on the vertical distribution of intercepted surfaces (i.e., canopy and ground elements) from the top of the canopy to the ground.

The conceptual basis for a large-footprint lidar return is illustrated in Figure 2.1. The time history of the reflected energy is fully digitized, and is converted to units of distance (accounting for the speed of light through the atmosphere). The first energy return above a threshold is used to derive the distance to the canopy top, and the midpoint of the last energy return is used to find the range to ground, the subtraction of which yields laser-derived canopy height. The return waveform gives a record of the vertical distribution of nadir-

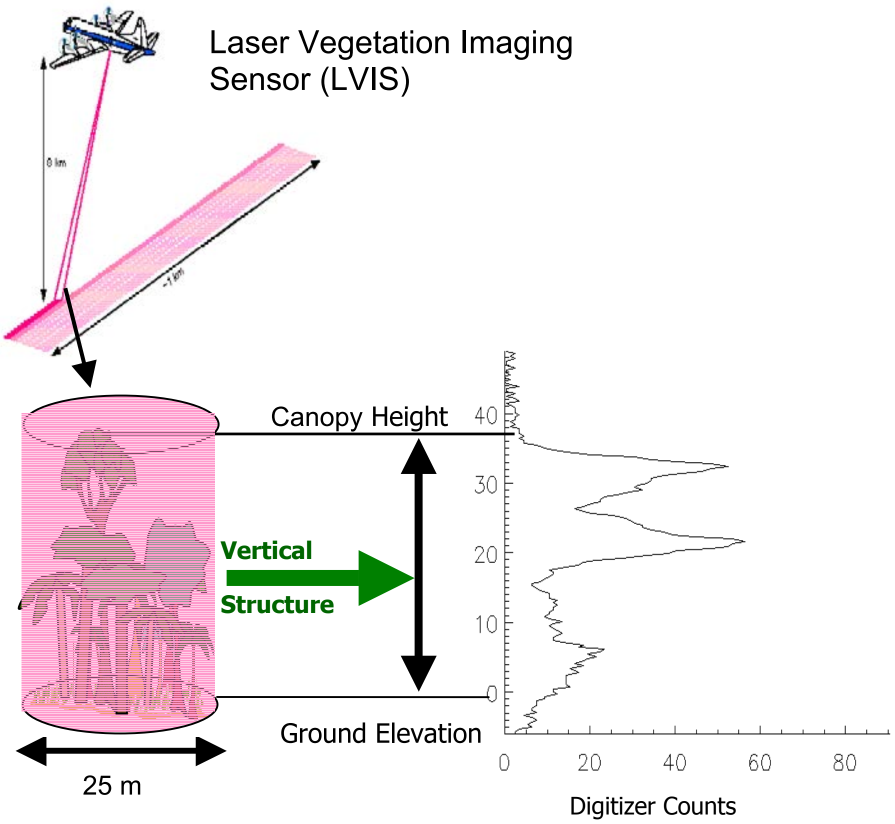

Figure 2.1 Conceptual basis of lidar remote sensing. Incident Gaussian-distributed pulses of laser energy from airborne or spaceborne instruments reflect off various portions of the canopy, resulting in a return waveform where the amplitude of the pulse is a function of the area of reflecting surfaces (leaves and branches) at that height. The entire waveform gives the vertical distribution of surfaces intercepted by the incident beam. Some of the incident light penetrates all the way through the canopy to produce the last large-amplitude Gaussian-shaped spike in the waveform known as the ground return. Lidar systems do not measure canopy height, but rather a target range determined by measuring the travel time of the pulse (accounting for the speed of light through the atmosphere). Canopy height is determined by subtracting the range to the ground from that to the first detectable return or some threshold above that return. The Laser Vegetation Imaging Sensor (LVIS), a large-footprint airborne scanning lidar instrument that was used in this study, is illustrated in the top portion of the figure.

intercepted surfaces (i.e. leaves and branches). At any particular height, the amplitude of the return waveform measures the strength of the return. Thus, for surfaces with similar reflectance values and geometry within a footprint (and under similar atmospheric conditions), a larger amplitude indicates more canopy material and a smaller amplitude less. The waveform provides only an apparent canopy profile (leaves and branches) because of attenuation of the beam through the canopy, and must be adjusted to approximate the true canopy profile (Lefsky et al. 1999b, Ni et al. 1999).

Previous Lidar Studies of Forest Structure

Measurements from small-footprint laser altimeter instruments have been useful in estimating tree heights (Nelson et al. 1988b, Nilsson 1996, Naesset 1997a, Magnussen and Boudewyn 1998), percent canopy cover (Weltz et al. 1994), timber volume (Naesset 1997b) and in some cases forest aboveground biomass (Nelson et al. 1988b). However, these fine-resolution sensors typically yield consistent ground returns only in relatively open forest canopies (Weishampel et al. 1996), thus making AGBM estimation difficult in dense tropical forests. Previous attempts to estimate tropical forest AGBM using small-footprint laser altimeters have also been complicated by the incompatibility of data sets, for example the lack of coincident field- and laser-derived data (Nelson 1997, Nelson et al. 1997, Nelson et al. 1998).

Large-footprint lidar measurements, incorporating information contained in the laser return waveform, have been used to derive canopy height and structure in a variety of canopy closure conditions (e.g., Means et al. 1999 and

Lefsky et al. 1999b). Because these large-footprint lidar instruments consistently measure subcanopy topography, even under conditions of high canopy closure, they have been shown to recover forest canopy structure that is statistically indistinguishable from field measurements (Lefsky 1997), and are able to accurately capture spatial patterns of canopy heights (Drake and Weishampel 2000). These instruments have also accurately estimated AGBM in both Douglas fir/western hemlock (Lefsky et al. 1999a, Means et al. 1999) and temperate mixed-deciduous forests (Lefsky et al. 1999b). In both cases, data from the lidar instruments were incorporated into regression models to derive plot-level forest structural (e.g., AGBM) estimates. These relationships were found to be significant even through dense structural conditions. For example, Means *et al*. (1999) predicted total plot AGBM with R^2 values of up to 0.96 using lidar-based AGBM estimation models through biomass levels of 1300 Mg/ha, far exceeding the normal saturation point of radar (≈150 Mg/ha from Dobson et al. 1992; (Waring et al. 1995); Imhoff 1995; Ranson et al. 1997). These results suggest that data from the upcoming (2001) spaceborne VCL (Dubayah et al. 1997) mission will greatly improve global biomass estimates.

Methods

La Selva Biological Station

The La Selva Biological Station (Figure 2.2; also see (Clark 1990, Matlock Jr. and Hartshorn 1999)) is located near the Sarapiquí River in northeast Costa Rica. Over its 46 year history, La Selva has become one of the

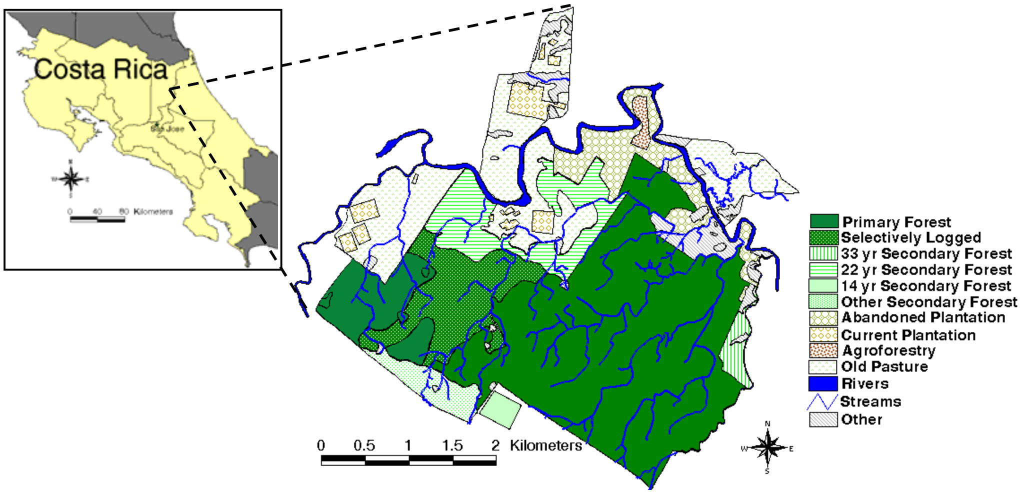

Figure 2.2 La Selva Biological Station is located near the Sarapiquí River in northeast Costa Rica. This 1536 ha area is a mixture of primary and secondary wet tropical tropical forest, pasture, plantations, and agroforestry plots.

most heavily studied tropical field stations in the world (McDade et al. 1994). This 1536 ha area is comprised of a mixture of lowland primary and secondary tropical wet forest (Holdridge et al. 1971), abandoned pasture, current and abandoned plantations, and agroforestry plots. The elevation range at La Selva is approximately 35-135 m above sea level, with a north to south gradient resulting in higher elevations and steeper slopes to the south where it borders on the 47,000 ha Braulio Carrillo National Park. The soils at La Selva are primarily a mixture of inceptisols (particularly in alluvial terraces in the north), and residual ultisols to the south (Clark et al. 1998, Clark and Clark 2000).

The primary forest estimated AGBM and basal area values at La Selva are low in comparison with other primary tropical rainforests (Saldarriaga et al. 1988, Brown et al. 1995, Brown 1997, Laurance et al. 1999). This may be due to differences between tropical moist forests (where the majority of studies are conducted) and tropical wet forest such as La Selva (see Clark and Clark, 2000 for a more detailed discussion). Nevertheless the variety of land cover types, and the wealth of ancillary data (e.g., soil, topography, forest structural data) available, makes La Selva an ideal study site for this study.

Field Data

Forest structural data (Table 2.1) were collected across a successional spectrum ranging from abandoned pasture to primary wet tropical forests (Figure 2.2.). Primary tropical forest data were collected in 18, 0.5-ha plots that are part of an ongoing landscape-scale carbon storage and flux study (Clark and Clark 2000). The plots were stratified over three edaphic conditions:

Table 2.1 Forest structural summaries for all field data used in this study by land cover types sampled at La Selva Biological Station

Land Cover Type	**Approximate Age (year)**	**Number of Sites**	**Plot Size (ha)**	**Quadratic Mean Stem Diameter* (cm)**	**Basal Area (m^2 ha^{-1})**	**Mean Estimated AGBM (Mg ha^{-1})**	**Related Study/ Data Source**
Primary Forest	Old-growth	18	0.5	20.76	23.6	160.5	Clark and Clark (in press)
Secondary Forest	31	6	0.05**	22.24***	26.71	147.7	VCL****
	22	1	0.25	12.85	22.05	129.4	Nicotra et al. 1999
	14	1	0.25	10.46	14.28	78.5	Nicotra et al. 1999
Agroforesty	7	6	0.12	9.03	14.48	34.3	Menalled et al. 1998 (literature values)
Pasture	<5	2	0.05**	N/A	N/A	8	Olson, 1983 (literature values)

* See equation 1.

** Size of a LVIS footprint

*** Stem diameters not measured above buttressing, median stem diameter= 18.70

**** Data collected as part of 1998 pre-launch VCL field campaign at La Selva relatively fertile flat inceptisols on old alluvial terraces (A plots); relatively infertile ultisols areas on ridgetops (L plots); and ultisol areas on steep slopes (P plots). All 18 plots were geolocated without knowledge of existing forest structure. This approach eliminates placement biases that can lead to large inaccuracies when AGBM values are extrapolated over a landscape-scale (Brown et al. 1995, Clark and Clark 2000).

Secondary forest data were collected in three different areas that were approximately 14, 22 (Chazdon 1996, Guariguata et al. 1997, Nicotra et al. 1999) and 31 (Pierce 1992) years old respectively as of March 1998. The 14 and 22 year old secondary forest plots are each approximately 0.5 ha. Within the 31 year old secondary forest area, 6 circular plots of 12.5 m radius were geolocated so as to approximately coincide with LVIS footprints.

In each primary forest plot, all stem diameters greater than 10 cm were measured in a marked location on each tree, either at breast height (1.37m) or, when necessary, above buttressing (Clark and Clark 2000). In the 31 year old secondary forest plots, all stem diameters greater than 10 cm at breast height were measured. In the 14 and 22 year old secondary forest plots all stem diameters greater than 5 cm at breast height were recorded. These measurements were taken both as a part of a March 1998 VCL calibration/validation campaign, and as a part of the separate long-term studies.

Stem diameters were used to calculate quadratic mean stem diameter (QMSD, Equation 2.1) basal area and aboveground biomass using an equation for tropical wet forests (Brown 1997). Quadratic mean stem diameters were calculated to compensate for the different (i.e. 5 cm vs. 10 cm) minimum diameter thresholds that were used in the existing studies. In addition, published aboveground biomass values from agroforestry plots at La Selva (Menalled et al. 1998) and for tropical pastures (Olson et al. 1983) were used in this study.

Equation 2.1 $\mathbf{QMSD} = ((\Sigma \mathbf{D}^2) / \mathbf{n})^{1/2}$ where QMSD is the quadratic mean stem diameter, **D** is stem diameter and **n** is the number of stem diameters in the area

Lidar Data

The airborne instrument used in this study is the Laser Vegetation Imaging Sensor (LVIS, Blair *et al.*, 1999). LVIS is a medium-altitude imaging laser altimeter, designed and developed at NASA's Goddard Space Flight Center. Variable-sized footprints and a randomly positionable laser beam and 7 degree telescope field of view allow LVIS to operate in a variety of modes. Footprint diameters can be varied from 1 to 70 m, and footprint spacing can be varied both along and across track. The return signal, or waveform, is digitally recorded and converted to units of distance (by accounting for the speed of light through the atmosphere). In this study the vertical resolution was approximately 30 cm, as determined by the digitization rate. Ancillary information such as the pointing direction and position of the laser at the time of each pulse (provided using an inertial navigation system and GPS unit) are also recorded. The combination of these data post-flight enables the geolocation of the laser footprint on the ground within a global reference frame (usually to better than 1 m horizontal accuracy) (Hofton et al. 2000a).

In March 1998 LVIS was flown in a NASA C-130 airplane to map the La Selva Biological Station and surrounding regions of NE Costa Rica. LVIS was in VCL emulator mode and operated at an altitude of 8 km above the ground to produce eighty, 25 m diameter footprints separated by ~25 m along- and ~9 m across-track (See Figure 2.1). Unlike previous laser altimeter instruments which record narrow transects of data, LVIS is able to map entire landscapes with relatively few flights. Only LVIS footprints that were coincident with field study plots (see below for details) were selected.

Four metrics were derived from the waveforms (see Figure 2.3). Lidar canopy height (LHT) was calculated by identifying 1) the location within the waveform when the signal initially increases above a mean noise level/threshold (the canopy top) and 2) the center of the last Gaussian pulse (the ground return), and then calculating the distance between these locations. Second, the height of median energy (HOME) was calculated by finding the median of the entire signal (i.e., above the mean noise level) from the waveform, including energy returned from both canopy and ground surfaces. The location of the median energy is then referenced to the center of the last Gaussian pulse to derive a height. The HOME metric is therefore predicted to be sensitive to changes in both the vertical arrangement of canopy elements and the degree of canopy openness (including tree density). Third, the height/median ratio (HTRT) is simply the HOME divided by canopy height. The HTRT provides an index of how the location of HOME may change relative to the canopy top height (LHT) through succession. Finally, a simple ground-return ratio (GRND) was calculated by taking the total intensity (i.e., the number of

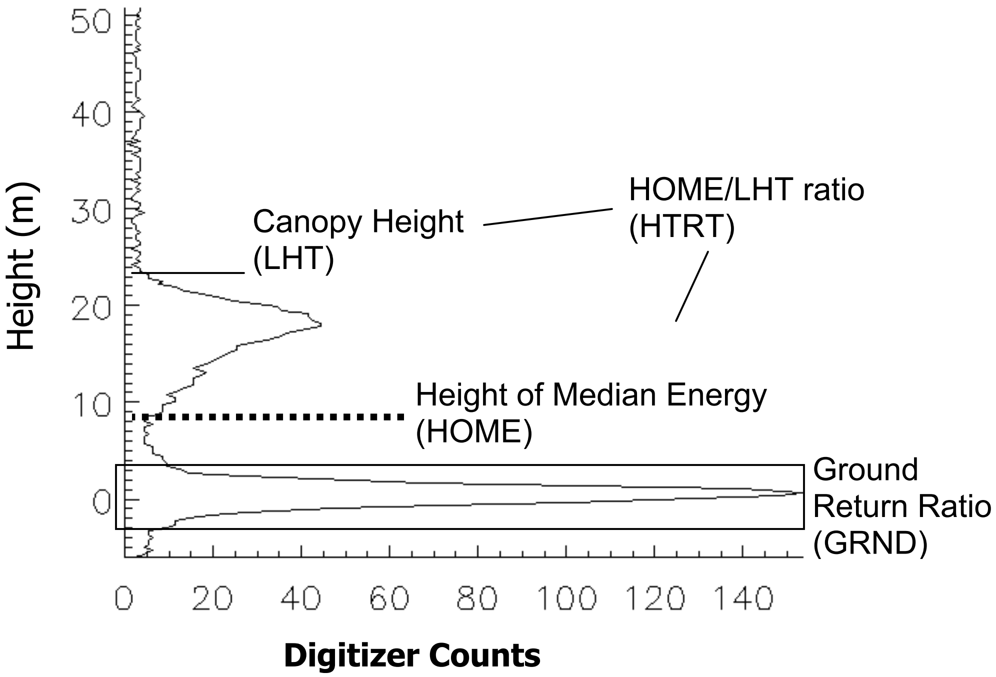

Figure 2.3 Metrics derived from lidar waveforms. See text for discussion. These metrics are then used to estimate forest structural characteristics such as aboveground biomass at both the footprint and stand levels.

digitizer counts) contained in all 30 cm vertical bins contained in the last Gaussian peak (Hofton et al. 2000b) divided by the sum of the intensity of all other canopy vertical bins of the waveform (see Figure 2.3). Thus, GRND provides an approximation of the degree of canopy closure (note that the canopy closure can be directly derived from the waveform under suitable canopy assumptions, as found in Means et al. 1999). These four metrics were then incorporated into a stepwise regression procedure to predict field measured basal area and QMSD and field estimated AGBM.

Analysis

The analysis involving ground and laser altimeter derived data was performed at both the level of individual LVIS footprints (25 m diameter circle) and at the level of the average plot size (0.5 ha) for areas with coincident LVIS and field data (Figure 2.4a and b). For each field plot, only LVIS footprints that are located entirely within the plot (i.e., footprint center over 12.5 m from plot edge) were selected to avoid the affects of outside canopy structure that was not measured on the ground (Figure 2.4).

In all plots where stem maps were available (18 primary plots and the six 31 year old secondary forest plots), footprint-level analysis was performed. All stems located within each LVIS footprint were selected and used to calculate forest structural characteristics (see below). In addition, a plot-level analysis was performed using all stems and LVIS footprints that fell entirely within each field plot (or in the case of pasture, using shots falling within an area of

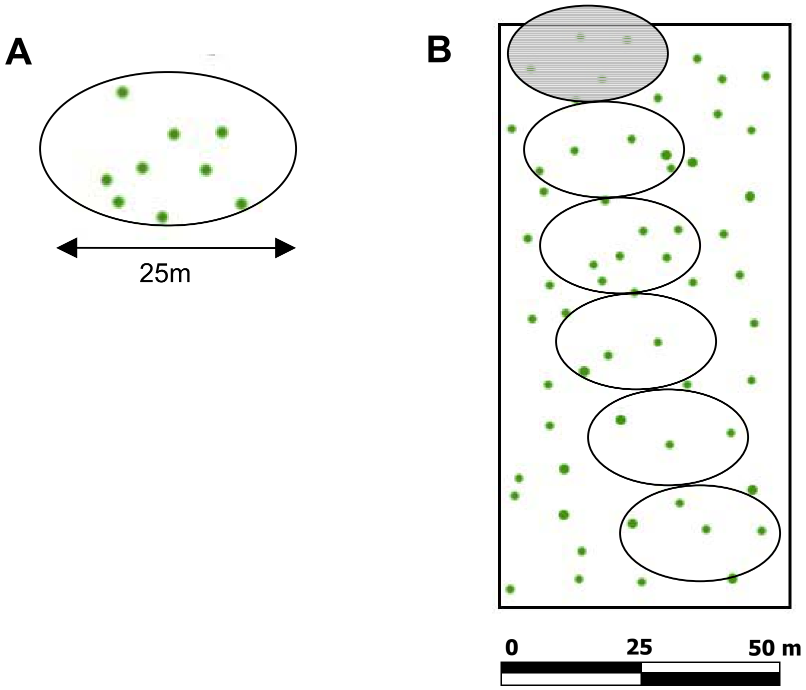

Figure 2.4 (A) Footprint-level (0.05 ha) analysis involved all stems that were located within LVIS footprints. **(B)** Plot-level analysis involved all stems that were located within a plot, and all LVIS shots that fell entirely within the same plot (i.e., 12.5 m from the plot edge). In this case the clear LVIS shots would be included, but the gray shot would not be included. At both the footprint and plot level, the stems that fell within the designated areas were used to calculate forest structural characteristics such as basal area and aboveground biomass. The relationships between these field values were then compared to metrics from individual footprints (A) or means of metrics for all footprints within the plot (A).

pasture)(Figure 2.4). Field and lidar data from the six footprint-sized plots, were combined into two (0.15 ha) plot-scale subsets.

The diameters of all stems within the respective footprints or plots were used to calculate stem basal area. These stem diameters were also used to estimate aboveground biomass using the tropical wet allometric equation of Brown (1997):

Equation 2.2 $\mathbf{AGBM_s} = 21.297 - 6.953(\mathbf{D}) + 0.740(\mathbf{D}^2)$ where **D** is stem diameter in cm, and $\mathbf{AGBM_s}$ is the estimated oven-dried AGBM for the stem

Basal area and estimated AGBM were then summed within the footprint or plot and were converted to standard units of area, m^2/ha and Mg/ha respectively. Additionally, the quadratic mean diameter (Equation 2.1.) within each footprint or plot was also calculated.

At the footprint-level, the lidar metrics were derived from individual waveforms. Plot-level values were calculated as the means of metrics for all footprints within the plot. For example, plot-level LHT was calculated for each plot by taking the mean of LHT values for all footprints within the plot (Figure 2.4).

Metrics derived from LVIS waveforms (Figure 2.3) were then used to estimate the field-derived forest structural summaries at both the footprint and plot levels using stepwise multiple linear regression. During this process transformations of dependent and independent variables (including square, square root and logarithmic) were also explored. Those models that were found most predictive were then cross-validated (Cressie 1991) to define a generalization error. Finally, these models were applied to all of the LVIS data over La Selva to produce landscape-level maps of forest structural characteristics.

Results

The assortment of plots from different land cover types that are incorporated in this study span the range of forest structural characteristics for the La Selva landscape. Additionally because the 18 primary forest plots are evenly stratified over the main upland edaphic and topographic conditions at La Selva (Clark and Clark 2000), the primary forest data are an unbiased, representative sample of the structural conditions found in this primary tropical wet forest.

In general all of the forest structural characteristics increase through the range of land cover types that were sampled (Table 2.1). There is a trend of increasing estimated AGBM and QMSD from pasture through secondary forest and into primary tropical forests. The exception to this trend is for the average QMSD value for the six 31 year old secondary forest sites, which is larger than the average QMSD of the primary forest sites. This exception is likely the result of large remnant trees (i.e., those not cut-down when the area was originally deforested), which are found within the 31 year old forest area (D.B. Clark, pers. obs.) and strongly influence the QMSD values

Overall, the lidar metrics from these areas (Table 2.2) are sensitive to changes in forest structure in the different land cover types included in this study. The height metrics (i.e., LHT, HOME and HTRT) are the most sensitive,

Table 2.2 Summaries for all lidar data used in this study by land cover types sampled at La Selva Biological Station

Land Cover Type	**Age (years)**	**Lidar Height (m) [LHT]**	**Height of Median Energy (m) [HOME]**	**HOME/LHT Ratio [HTRT]**	**Ground Ratio [GRDRT]**
Primary Forest	Old-growth	31.33	20.14	0.64	0.014
Secondary Forest	31	25.48	16.65	0.65	0.016
	22	17.68	11.32	0.63	0.013
	14	23.67	9.21	0.38	0.023
Agroforesty	7	9.47	1.68	0.17	0.067
Pasture*	<5	5.09	0.54	0.11	0.740

*-Data from two LVIS shots from abandoned pasture sites at La Selva were compared to tropical pasture AGBM data from Olson (1983)

and increase with increasing forest age, basal area and biomass. Ground return ratio is generally insensitive to changes in forest structure beyond a secondary forest age of approximately 14 years.

At the footprint-level (0.05 ha) metrics from LVIS are able to significantly estimate all three forest structural attributes throughout the range of conditions at La Selva, though in most cases logarithmic transformations of dependent variables was necessary. The HOME metric is the best single predictor of both QMSD (Table 2.3, equation 1) and AGBM (Table 2.3, equation 5), and explains 59% and 53% of the variation in these attributes respectively. The ground-return ratio metric was the best single-term predictor of basal area (Table 2.3, equation 3), and explained 27% of the variation.

For all three structural characteristics, multiple-term equations (Table 2.3, equations 2, 4 and 6) explain much higher levels of variation (R^2) than the single-term equations. The level of variation of basal area that is explained by both single and multiple-term equations is over 40% lower than the levels for AGBM and QMSD.

At the plot level (~0.5 ha) all of the relationships between forest structural summaries and lidar metrics are much stronger than at the footprint level. For all single-term equations the levels of variation in forest structural summaries explained (R^2 values) are over 35% higher at the plot level than at the footprint level, and range from 0.72 to 0.92. Again, the R^2 values for AGBM and QMSD are higher than for basal area.

The metric that is the best single-term predictor of both plot-level QMSD (Table 2.4, equation 1) and AGBM (Table 2.4, equation 4) is HOME, as is the

Table 2.3 Regression equations and values for footprint-level (0.05 ha) forest structural characteristics

Forest Structural Characteristic	**Equation**	**R^{2*}**	**RMSE**
Quadratic Mean Stem Diameter (cm)	(1) QMSD = 10.39+0.72*HOME	0.59	3.84 cm
	(2) Log(QMSD) = 1.14+0.05*LHT-0.05*HOME-0.72*GRND+2.43*HTRT	0.77	3.74 cm
Basal Area (m^2/ha)	(3) Sqrt(BArea) = 5.11-6.28*GRND	0.27	7.88 m^2/ha
	(4) Sqrt(Barea) = 3.24 +0.04*LHT-4.12*GRND+1.15*HTRT	0.39	7.16 m^2/ha
Estimated Aboveground Biomass (Mg/ha)	(5) Log(AGBM) = 3.58+ 0.07* HOME	0.53	63.17 Mg/ha
	(6) Log(AGBM) = 2.06+0.07*LHT-0.08*HOME-1.05*GRND+3.51*HTRT	0.73	60.02 Mg/ha

*All values significant ($p<0.01$)

Table 2.4 Regression equations and values for plot-level (0.25-0.5 ha) forest structural characteristics

Forest Structural Characteristic	Equation	R^2*	RMSE**
Quadratic Mean Stem Diameter (cm)	(1) QMSD = 8.19+0.81*HOME	0.92	2.09 cm
	(2) QMSD =5.97+0.15*LHT+1.05 *HOME-0.01*[LHT*HOME]	0.93	2.00 cm
Basal Area (m^2/ha)	(3) Barea = 11.09+20.10*HTRT	0.72	3.00 m^2
Estimated Aboveground Biomass (Mg/ha)	(4) AGBM = 26.28+ 6.77*HOME	0.89	22.54 Mg/ha
	(5) AGBM = 15.64+9.54*HOME-0.01*HOME^3	0.93	18.39 Mg/ha

* All values significant ($p<0.01$)

** Numbers are cross-validated

case at the footprint level (Table 2.4). The HOME metric explains 89% of the variation in estimated AGBM and 92% of the variation in QMSD with no transformation of the dependent or independent variables. The best single-term predictor of plot-level basal area is HTRT (R^2=0.72), instead of GRND, which is the best predictor of basal area at the footprint level.

Multiple-term equations (Table 2.4, equations 2 and 5) only marginally improve the relationship for both QMSD (R^2= 0.93 vs 0.92) and estimated AGBM (R^2=0.93 vs. 0.89). For basal area, the single-term equation (Table 2.4, equation 3) was selected through all combinations and transformations in the stepwise multiple regression procedure.

To further examine the nature of the single-term relationships, they are graphically represented in scatter plots (Figures 2.5-2.7). In all three cases the metrics significantly estimate forest structural summaries without reaching an asymptote throughout the entire range of conditions at La Selva. In addition, the cross-validated generalization error (RMSE) for all three single-term relationships (Table 2.4) is low. As a result these relationships were applied to LVIS data over the entire La Selva landscape to produce images of estimated QMSD (Figure 2.8), basal area (Figure 2.9) and AGBM (Figure 2.10) with a resolution equal to the plot level used in this study (~0.5 ha). In addition, the footprint-level (~0.05 ha) equation for AGBM (Table 2.3, equation 5) was applied to a subset of the LVIS data within a primary forest area to produce a high-resolution image of estimated AGBM variability (Figure 2.10, inset).

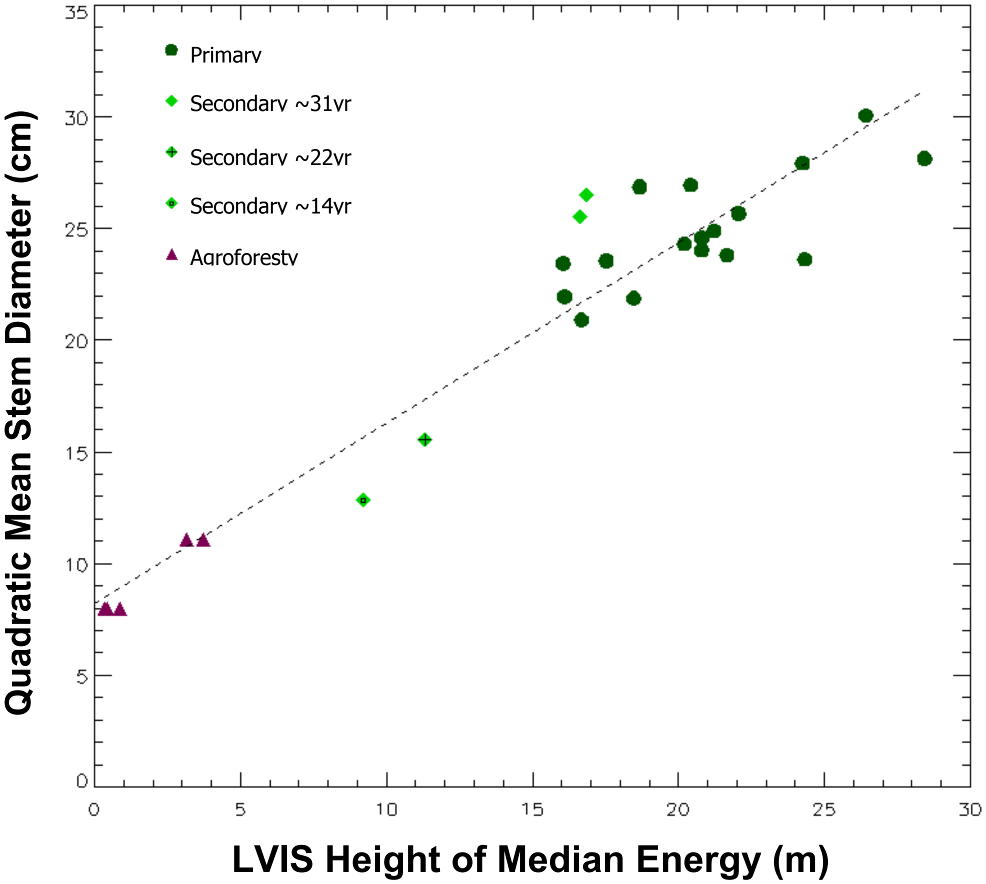

Figure 2.5 Plot-level quadratic stem diameter predicted from the LVIS height of median energy (HOME, Figure 2.4) metric. The regression line is equation 1 in Table 2.4.

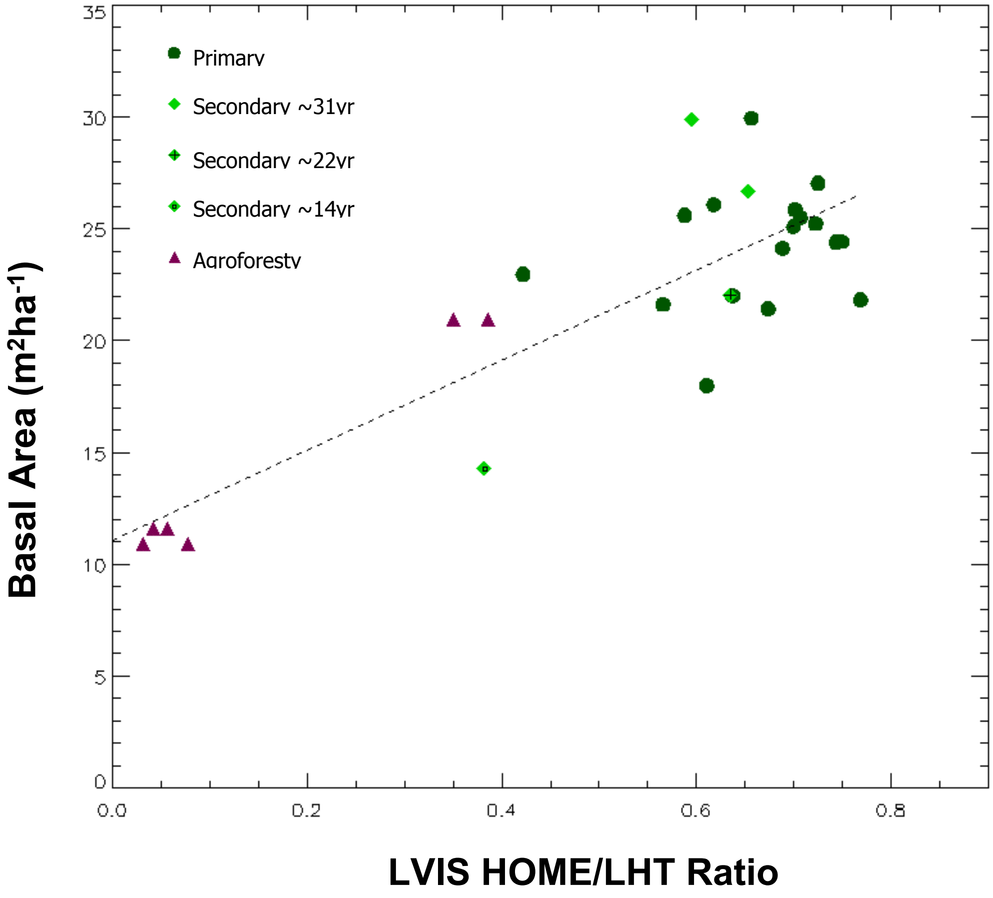

Figure 2.6 Plot-level basal area predicted from the LVIS height ratio (HTRT) metric (Figure 2.4). The regression line is equation 3 in Table 2.4.

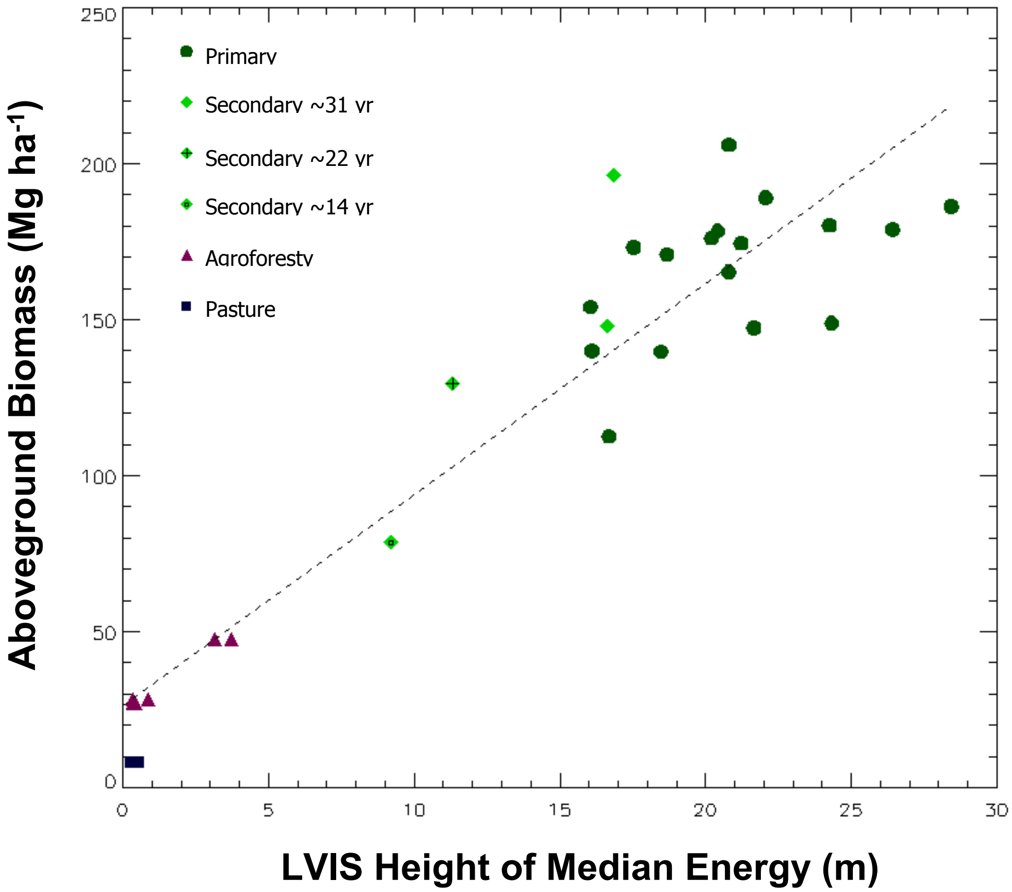

Figure 2.7. Plot-level aboveground biomass (AGBM) predicted from the LVIS height of median energy (HOME, Figure 2.4) metric. The regression line is equation 4 in Table 2.4.

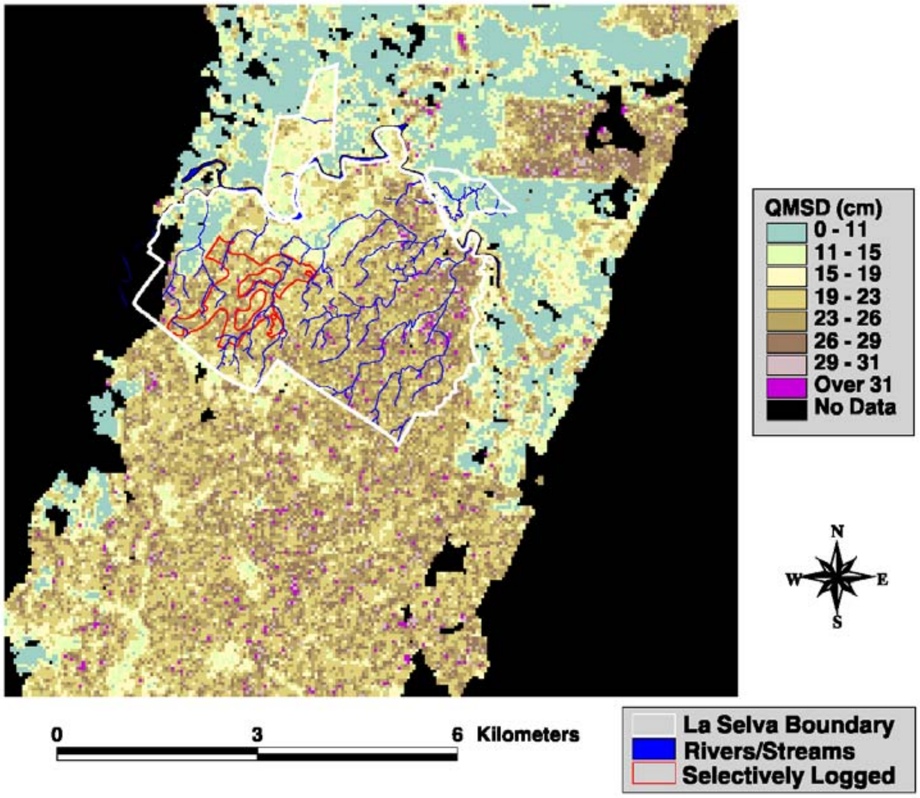

Figure 2.8 Image of quadratic mean stem diameter (QMSD) predicted from LVIS data over La Selva Biological Station using equation 1 in Table 2.4. Note the areas of lower QMSD in western portions of La Selva that were selectively logged in the late 1970s, and the clustering of high QMSD values near streams.

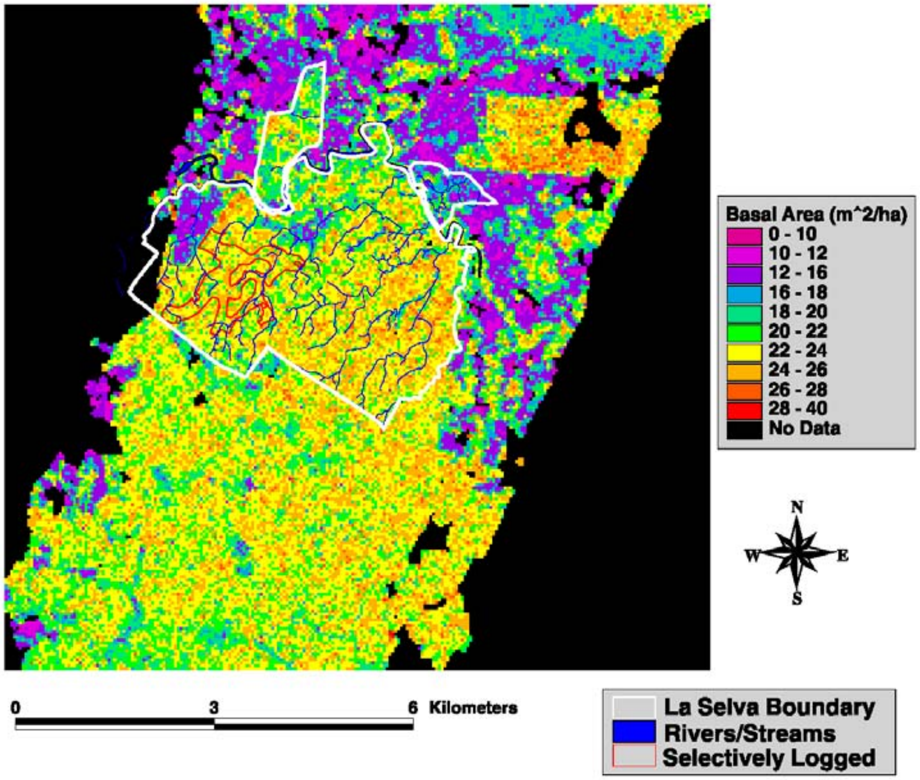

Figure 2.9 Image of basal area predicted from LVIS data over La Selva Biological Station using equation 3 in Table 2.4. Note the differences in basal area between younger secondary forest areas and primary forests (see land cover data in Figure 2.2).

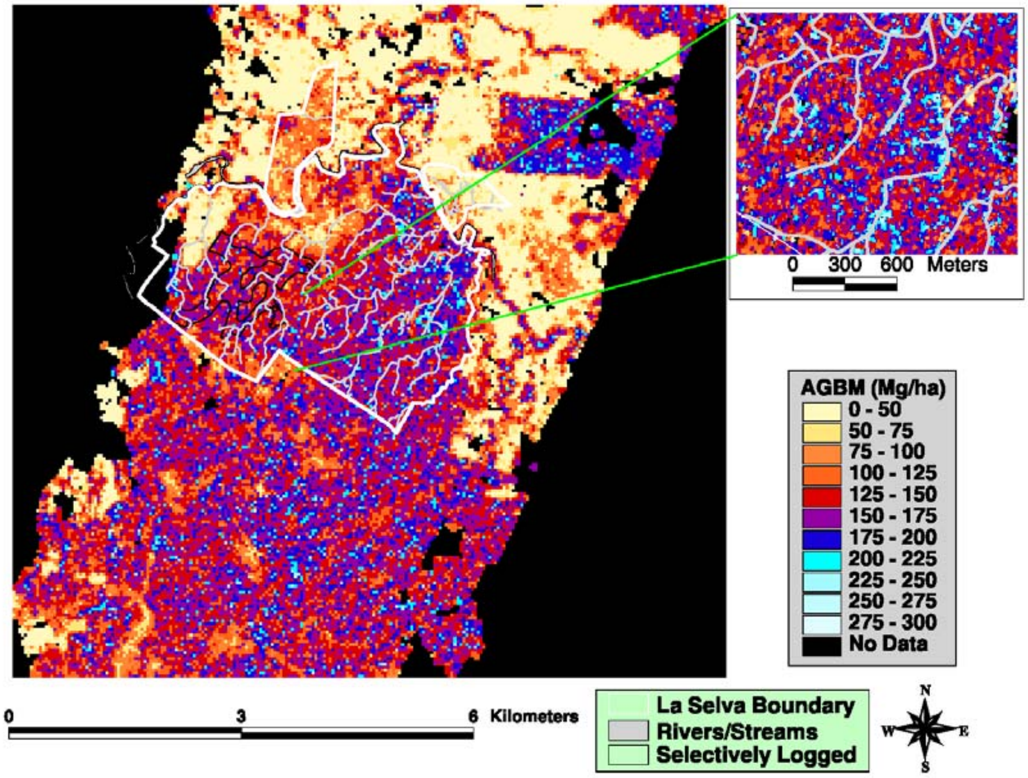

Figure 2.10 Image of aboveground biomass (AGBM) predicted from LVIS data over La Selva Biological Station using equation 4 in Table 2.4. Note the areas of lower AGBM in western portions of La Selva that were selectively logged in the late 1970s. In the right inset, AGBM predicted using the footprint level (~0.05 ha) equation (Table 2.3, equation 5) clearly reveals the clustering of high AGBM values near streams.

Discussion

Field and Lidar Summaries

The trends in forest structural summaries (Table 2.1) are primarily in agreement with results from other studies for La Selva. As has been reported in other studies at La Selva (e.g., Guariguata et al. 1997) basal area does not significantly differ between older (i.e. ~22 yr) secondary and old-growth forests. The large remnant stems in the 31 year old secondary forest area result in the exception to the trend of increasing QMSD size through secondary forests and into primary forest plots, as mentioned above. Estimated AGBM is not as sensitive to remnant stems in secondary forest areas, and increases through the range of successional conditions sampled at La Selva.

Lidar-derived metrics are quite sensitive to changes in forest structure, particularly LHT, HOME and HTRT (Table 2.2). The canopy height metric (LHT) from the 14 year old secondary forest plot is higher than expected, which could be the result of two factors. First, large remnant stems, which can account for as much as 15% of the total basal area in secondary forests at La Selva (Guariguata et al. 1997), coupled with the sensitivity of LVIS canopy height to the maximum detectable canopy surface may explain why these values are higher than expected. Second, precise plot boundary coordinates were not available for the 14 year old secondary plot, so the LVIS shots may not be entirely coincident with the actual plot location.

Footprint-level Relationships

The relationships between lidar metrics and field-derived forest structural summaries at the footprint scale (~0.05 ha), though not as strong as the plot-level relationships (Tables 2.3 and 2.4), are significant. The multiple-term equations (Table 2.3, equations 2 and 6) selected through a stepwise multiple regression procedure explain 77% of the variation in QMSD and 73% of the variation in estimated AGBM across the range of conditions sampled in this dense tropical landscape. Still the footprint scale R^2 values are less than 65% of the plot-level single-term equations and less than 80% of the plot-level multi-term regression equations (Tables 2.3 and 2.4).

The footprint-level relationships could be negatively affected by two factors. First, the level of variability in forest structure at the scale of an LVIS footprint (0.05 ha) is much higher than at the plot level (~0.5 ha). The level of variation in forest structural characteristics (as determined by calculating the coefficient of variation or CV) is 2-3 times higher at the footprint scale as the plot level (Table 2.5). This agrees with other studies that have reported that a plot size of approximately 0.35-0.5 ha is necessary for sampling tropical forest estimated aboveground biomass and other structural characteristics (Brown et al. 1995, Clark and Clark 2000).

A second factor that contributes to the weaker relationship between forest structural attributes and lidar metrics at the footprint-level is geolocation of LVIS observations and stems in each forest area. Although LVIS shots may be geolocated to within 1-2 meters (Blair and Hofton 1999, Hofton et al. 2000a), the location of stems within primary and the 31 year old secondary forest plots

Table 2.5 Coefficients of variation in forest structural characteristics at the footprint-level (0.05 ha) and at the plot-level (0.5 ha, old-growth and 0.3 ha for 6 combined 31 year old secondary forest plots).

Forest Structural Characteristic	Footprint-level CV*	Plot-level CV*
Quadratic Mean Stem Diameter	22.54	9.60
Basal Area	33.56	11.94
Estimated Aboveground Biomass	43.41	14.01

*These values were calculated using only primary and 31 year old secondary forest were referenced to a plot corner using a compass and fiberglass measuring tapes. As a result stem locations may be off by 5-10 m in random (i.e., approximately unbiased) directions. Thus, stems that were included in particular LVIS footprints for this analysis may be as many as 12 m (LVIS shot geolocation uncertainty + stem geolcation uncertainty) outside of the footprint area, and stems that are up to 12 m outside of the footprint area and were not included may have truly been within the footprint.

Plot-level Relationships

The relationships between lidar metrics and forest structural characteristics at the plot level are strong (Table 2.4). Metrics from LVIS are able to explain very high levels of variation (R^2 up to 0.93) in tropical forest aboveground biomass, basal area and quadratic mean stem diameter. These relationships are non-asymptotic (Figures 2.5-2.7) through the entire range of conditions sampled at La Selva, and permit estimates of AGBM to approximately the same level of accuracy as related large-footprint lidar studies in temperate coniferous forests (Lefsky et al. 1999a, Means et al. 1999).

The slightly weaker relationship between basal area and lidar metrics is caused by the lack of significant differences in basal area between secondary and primary forest areas that has been reported in field studies at La Selva (Guariguata et al. 1997). Although the frequency distribution of basal area (i.e., number of stems in different size classes) does change, the overall total basal area at La Selva is not significantly different beyond a secondary forest age of approximately 16 years since abandonment (Guariguata et al. 1997). As a result, lidar metrics such as LHT, HOME and HTRT which continue to increase with increasing forest age (Table 2.1) may not be as predictive of changes in total basal area compared to changes in estimated AGBM and QMSD. This may explain why ground return ratio (which is also insensitive to changes beyond a young secondary forest) was the best single-term predictor of basal area at the footprint-level (Table 2.3).

The height of median energy (HOME) is perhaps the metric with the strongest potential for estimating tropical forest structural characteristics. It is the best single-term predictor of both footprint- and plot-level QMSD and AGBM (Tables 2.3 and 2.4). The canopy height (LHT) metric is strongly influenced by the highest detectable canopy surface within a footprint. The HOME metric, however, may be more sensitive to both the vertical arrangement and density of canopy elements. In areas with densely packed canopy materials less lidar energy will reach the ground, thereby increasing HOME. Conversely in more open or disturbed areas (e.g., a treefall gap), more lidar energy will reach the ground, thus reducing HOME. Because primary tropical forests represent a spectrum from newly-created treefall gaps to mature patches with high canopy closure (Lieberman et al. 1989), the sensitivity of HOME to these changes make it an excellent predictor of forest structural attributes such as biomass.

The generalization error (RMSE) of 22.54 Mg/ha for the aboveground biomass (Table 2.4, equation 4) level is 13.75% of the mean (160.5 Mg/ha) plot-level AGBM for all primary forest areas sampled at La Selva. This value is also comparable to a recent study in temperate coniferous forests where RMSE levels (131 Mg/ha) were approximately 14% of the mean (965 Mg/ha) primary coniferous forest AGBM level (Means et al. 1999). Additionally this value (the generalization error divided by the mean primary forest AGBM level) is approximately equal to the coefficient of variation of field-estimated AGBM at La Selva (Table 2.5) and is approximately equal to the level of error from field measurements (Brown et al. 1995).

The images of forest structural characteristics (Figures 2.8-2.10) over the entire La Selva landscape allow for an unprecedented examination of the relationship between forest structural characteristics and environmental (e.g., edaphic and topographic) conditions. Field based efforts (Clark and Clark 2000) have shown that although the AGBM summaries from primary forest plots in areas with different soil and topographic conditions do not significantly differ, the way in which this AGBM is distributed (i.e., the distribution of stem sizes) does vary. In future work we hope to fully explore the variability in AGBM arrangement over the entire La Selva landscape.

The landscape-scale images of tropical forest structural characteristics (Figures 8-10) reveal several trends. First, through comparisons with a map of La Selva land cover (Figure 2.2) secondary and primary forest areas are clearly distinct in terms of estimated AGBM (Figure 2.10) and QMSD (Figure 2.8), but not in terms of basal area (Figure 2.9), as expected from field studies (Guariguata et al. 1997). Secondly, an area of primary forest in western La Selva that was selectively logged (i.e., commercial stems >70 cm diameter were removed) in the late 1970s is also distinct from the undisturbed primary forest in eastern La Selva (with approximately the same edaphic and topographic conditions). Third, high estimated AGBM (Figure 2.10), basal area

(Figure 2.9) and QMSD (Figure 2.8) values are clustered around stream valleys throughout the La Selva landscape, consistent with field data (Clark and Clark 2000).

Previous remote sensing studies using passive optical and SAR instruments have had great difficulty in estimating tropical forest structural characteristics such as AGBM. Metrics from passive optical instruments such as Landsat are highly sensitive to leaf area index, or LAI (Running et al. 1986, Hall et al. 1995) but in the tropics LAI and leaf biomass levels may become asymptotic in secondary forests less than 10 years old (Brown and Lugo 1990, Foody et al. 1996). This may explain why passive optical instruments are insensitive to changes in AGBM beyond secondary forests of 10-15 years (Sader et al. 1989, Steininger 1996). Similarly, SAR backscatter tends to saturate in dense forest conditions (Imhoff 1995, Waring et al. 1995, Kasischke et al. 1997) and has been shown to be insensitive to changes in AGBM for secondary tropical forests with AGBM levels >60 Mg/ha (Luckman et al. 1997). Consequently, the ability of a large-footprint lidar to accurately predict tropical forest structural characteristics across a dense, structurally complex, dense tropical forest landscape is extraordinary.

Conclusions

Metrics derived from a large-footprint lidar instrument were significantly correlated with tropical forest structural characteristics at both footprint and plot levels across the entire range of conditions in a structurally complex tropical wet forest. Although the majority of the field-measured forest structural data are from the high-end of the biomass and basal area spectrum at La Selva, the instrument nonetheless successfully measured the structural heterogeneity within this dense primary forest at both footprint (0.05 ha) and plot (~0.5 ha) levels.

At the level of individual LVIS footprints (0.05 ha) the relationship between lidar metrics and forest structural characteristics is weakened by problems of geolocation (stems and LVIS footprints) and the level of variation in forest structure at that scale. Nevertheless, even with these factors the relationships between lidar metrics and tropical forest structural attributes are strong through the entire range of conditions sampled.

At the plot level (0.5 ha) these factors are negligible and the relationship among plot-level forest structural summaries and lidar metrics are extremely strong. The levels of variation explained by metrics from the LVIS instrument at this scale are significantly higher than for any other remote sensing instrument for tropical forests areas to our knowledge. The level of generalization error of the relationships between lidar metrics and QMSD and estimated AGBM is approximately the same as from previous studies in more open temperate forests. As a result, when these relationships are applied to LVIS data over the entire landscape at La Selva, it is possible to examine the relationship between forest structural characteristics and environmental conditions (e.g., topography) and past land use (e.g., selective logging).

Although several of the forest structural characteristics used in this study from La Selva are lower than many moist tropical rainforests (Saldarriaga et al. 1988, Brown et al. 1995, Brown 1997, Laurance et al. 1999) this is not the case for all forest characteristics at La Selva. For example, the heights of emergent (>50 m) and average canopy-forming trees (~33 m) at La Selva are approximately equivalent to those found in other Neotropical rainforests (Richards 1996).

Perhaps more important from a lidar remote sensing point of view is the light availability at ground level. The degree of canopy closure in primary and secondary forest areas at La Selva is approximately 98-99% at 1m above ground level (Fetcher et al. 1994, Nicotra et al. 1999). This is among the highest canopy closure values found in tropical and extra-tropical forests (Baldocchi and Collineau 1994). Thus, although large-footprint lidar has proven effective for estimation of forest structure in temperate forests with higher AGBM levels than La Selva, the ability of this technology to recover forest structural characteristics in a dense tropical forest with 3-4 times higher canopy closure than most temperate forests (Baldocchi and Collineau 1994) is critical. This ability is particularly important at a global scale because tropical forests are estimated to contain approximately 40% of the carbon in the terrestrial vegetation pool (Dixon et al. 1994). The combination of the previous efforts in temperate forests along with this study in tropical forests strongly confirm that next-generation lidar technology, as found on the Vegetation Canopy Lidar (VCL) mission, will greatly improve global estimates of aboveground biomass and other forest structure.

Chapter 3. Sensitivity of large-footprint lidar to canopy structure and biomass in a Neotropical rainforest

Abstract

Accurate estimates of the total biomass in terrestrial vegetation are important for carbon dynamics studies at a variety of scales. Although aboveground biomass is difficult to quantify over large areas using traditional techniques, lidar remote sensing holds great promise for biomass estimation because it directly measures components of canopy structure such as canopy height and the vertical distribution of intercepted canopy surfaces. In this study our primary goal was to explore the sensitivity of lidar to differences in canopy structure and aboveground biomass in a dense, Neotropical rainforest. We first examined the relationship between simple vertical canopy profiles derived from field measurements and the estimated aboveground biomass (EAGB) across a range of field plots located in primary and secondary tropical rainforest and in agroforestry areas. We found that metrics from field-derived vertical canopy profiles are highly correlated (R^2 up to 0.94) with EAGB across the entire range of conditions sampled. Next, we found that vertical canopy profiles from a large-footprint lidar instrument were closely related with coincident field profiles, and that metrics from both field and lidar profiles are highly correlated. As a result, metrics from lidar profiles are also highly correlated (R^2 up to 0.94) with EAGB across this Neotropical landscape. These results help to explain the nature of the relationship between lidar data and EAGB, and also lay the

foundation to explore the generality of the relationship between vertical canopy profiles and biomass in other tropical regions.

Introduction

The total biomass of terrestrial vegetation is an important variable for studies at multiple scales. As biomass (i.e., the total biological material or mass in a given area at a given time) is approximately 50% carbon, changes in the total biomass through time are important both at local (e.g., forest carbon dynamics) and regional to global scales (e.g., carbon release from large forest fires). Because tropical areas contain a large proportion of the total carbon in terrestrial vegetation globally (Dixon et al. 1994), knowledge of the biomass content in tropical ecosystems can provide an initial condition or baseline for studies that examine carbon flux related to natural (e.g., disturbances) and anthropogenic (e.g., deforestation) processes. However, the estimation of terrestrial vegetation biomass, especially in dense tropical forests, has proven difficult.

Most remote sensing techniques to estimate biomass are empirical, and illustrate the correlation between biomass and the intensity of electromagnetic radiation (or the ratio of energy at different wavelengths) that is received by the instrument (e.g., Sader et al. 1989, Moran et al. 1994, Foody et al. 1996, Curran et al. 1997, Luckman et al. 1997, Steininger 2000). In some cases a modeling approach is also incorporated to explain the physical interaction between the electromagnetic radiation and forest canopy structure (Strahler 1997). Many remote sensing instruments, however, have the same problem: they are able to detect differences in biomass in relatively young and/or homogeneous forests, but are not as sensitive to changes in biomass in older or heterogeneous forests (Wickland 1991, Imhoff 1995, Waring et al. 1995, Weishampel et al. 1996). As a result, estimating terrestrial biomass, especially in dense primary tropical forests has proven difficult (e.g., Sader et al. 1989, Moran et al. 1994, Foody et al. 1996, Curran et al. 1997, Luckman et al. 1997, Steininger 2000).

Lidar (Light Detecting and Ranging) remote sensing is a relatively new active remote sensing technique with potential for estimation of terrestrial vegetation biomass (Lefsky et al. 1999a, Means et al. 1999, Dubayah and Drake 2000, Dubayah et al. 2000, Drake et al. In press). Lidar instruments have been used to accurately estimate canopy height (Nelson et al. 1988b, Lefsky et al. 1999b, Magnussen et al. 1999, Drake and Weishampel 2000, Peterson 2000) and vertical structure (Harding et al. 2001, Parker et al. 2001) in a variety of different forest types. As a result, lidar instruments reliably provide important biophysical characteristics that can then be used to estimate changes in biomass in forests.

The empirical relationships between lidar-derived canopy height and forest biomass are conceptually similar to the allometric relationships used in field studies (Niklas 1994a). The primary difference is that instead of relating changes in the height or diameter of individual trees to the changes in biomass, the relationship is between lidar-derived canopy height (or other lidar metrics) and the total aboveground biomass of all trees within the area of interest (e.g., a field plot). The changes in canopy height and structure through succession are also affected by ecological processes (e.g., competition, stand-thinning) operating on individual trees through time. The net result is that the vertical growth of forest stands also correlates with an overall increase in stand biomass levels.

In addition to canopy height, new large-footprint, full-digitization lidar instruments also provide data related to the vertical arrangement of forest structure from the top of the canopy to the ground (Dubayah et al. 1997, Dubayah and Drake 2000, Dubayah et al. 2000, Harding et al. 2001). This data can also be used to improve the prediction of biomass (Lefsky et al. 1999a, Lefsky et al. 1999b, Means et al. 1999, Drake et al. In press), and to estimate the vertical distribution of forest structure such as vertical foliar profiles (Harding et al. 2001) and the vertical distribution of light transmittance (Parker et al. 2001). As such, lidar instruments provide a wealth of data potentially suited for estimation of biomass in carbon-rich tropical forest ecosystems.

Drake et al. (In press) showed that metrics from an airborne large-footprint lidar instrument were correlated with the estimated aboveground biomass across a successional spectrum of sites ranging from abandoned pasture to dense primary tropical forest. However, there is still a need to examine the nature of this empirical relationship to understand why metrics from lidar data are highly correlated with aboveground biomass in tropical forests. The generality of these relationships will bear on global applications of these types of lidar data such as the Vegetation Canopy Lidar (VCL) mission (Dubayah et al. 1997) and on the design of future lidar instruments.

The primary goal of this study is to explore the sensitivity of lidar to vertical canopy structure and biomass across a Neotropical rainforest landscape. We hypothesize that the strong relationship between metrics from large-footprint, full-digitization lidar instruments and aboveground biomass in tropical forests is the result of: 1) the sensitivity of lidar to differences in vertical canopy structure and 2) the correlation between vertical canopy structure and total aboveground biomass. In both cases, the relationships may be valid across a wide range of successional and environmental conditions. To test these assertions we take a three-step approach.

First, we examine the relationship between field-derived vertical canopy profiles and biomass. Metrics from the distributions of stem heights (e.g., maximum stem height) and from vertical canopy profiles derived from field measurements in a series of plots located in a dense tropical rainforest are compared to the total biomass in the plot. This approach reveals which components of vertical canopy structure are most correlated with total biomass across different successional (e.g., secondary vs. primary forest) and environmental (e.g., edaphic) conditions. In addition, the field-derived vertical canopy profile comparisons serve as a baseline with which to compare lidar-derived vertical canopy profiles. A key question we address is: are metrics from a vertical canopy profile correlated with aboveground biomass over the entire range of conditions encountered in a dense tropical rainforest, or do they saturate in old-growth or "primary" forest areas?

Second, we examine the relationship between vertical canopy profiles derived from both lidar and field techniques. Because of obscuration effects, less lidar energy is available at the bottom of the canopy. Therefore an existing transformation technique (Lefsky et al. 1999b, Harding et al. 2001) is also used on the lidar data for comparison. Metrics from both normal and transformed lidar profiles are then compared with corresponding metrics from field profiles. Next, we examine the relationship between complete profiles from lidar (normal and transformed) and field techniques. This process illustrates the relationship between vertical canopy profiles derived using vastly different techniques (i.e., field vs. lidar remote sensing), and whether transformations of lidar profiles are necessary. The two questions we address here are: 1) are metrics from untransformed or transformed lidar profiles correlated with metrics from field profiles and 2) are lidar- and field-derived vertical canopy profiles from each plot related or are they significantly different?

Finally, we compare the relationships between aboveground biomass and metrics from both field- and lidar-derived vertical canopy profiles. In this section we illustrate how lidar compares with the field techniques for predicting aboveground biomass across different successional and environmental conditions. The primary question in this section is: do metrics from lidar profiles explain the same level of variation in biomass as metrics from field profiles?

Methods

La Selva Biological Station

This study uses field and lidar data acquired at the La Selva Biological Station (McDade et al. 1994), a 1536 ha tropical forest research facility located in northeast Costa Rica (Figure 3.1). La Selva is comprised of a mixture of

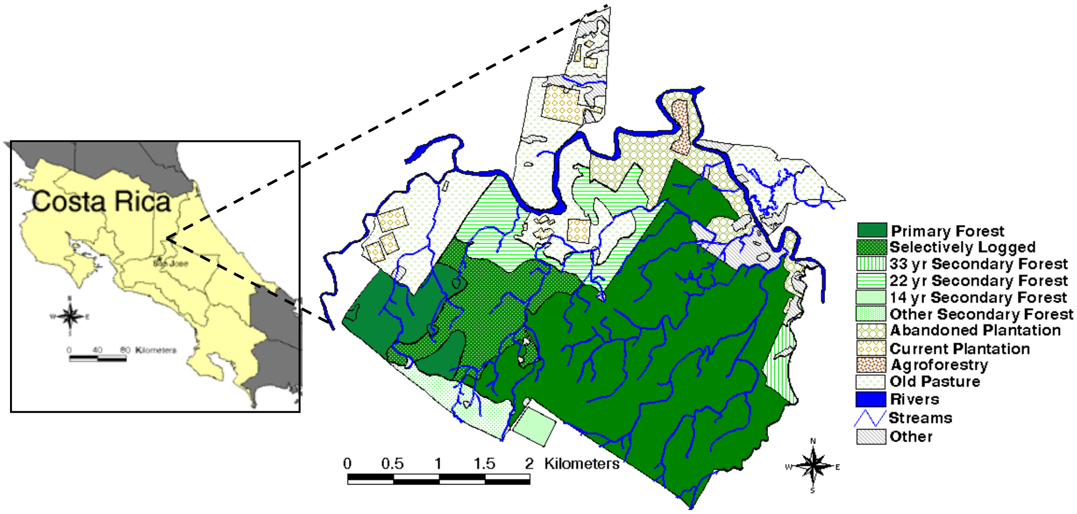

Figure 3.1 Locator map for study site at La Selva Biological Station in northeastern Costa Rica. La Selva is a 1546 ha area comprised of a mixture of primary and secondary tropical rainforest, agroforesty, plantations, and recently abandoned pastures.

lowland primary and secondary tropical rainforest (classified as "tropical wet forest" in (Holdridge et al. 1971), agroforestry and plantation plots, and recently abandoned pastures (McDade et al. 1994, Matlock Jr. and Hartshorn 1999). Within these separate areas there are ongoing studies related to forest carbon dynamics (Clark and Clark 2000), light environments in primary and secondary forests (Nicotra et al. 1999), and the growth of commercially valuable trees in managed agroforestry plots (Menalled et al. 1998), among many others.

Field Data

Field data were collected across a wide range of successional, land-use and environmental conditions at La Selva (Figure 3.1). Data were collected both as a part of the March 1998 prelaunch validation/calibration campaign of the Vegetation Canopy Lidar mission (Dubayah et al. 1997, Dubayah et al. 2000), and as a part of ongoing field studies at La Selva. Data from 3 different landcover types, 18 primary forest, 3 secondary forest and 6 agroforestry plots were used in this study.

The 18 primary forest plots (0.5 ha each) are evenly stratified over three edaphic and topographic conditions: 6 are located in relatively fertile flat inceptisol areas on old alluvial terraces, 6 are in relatively infertile ultisol areas on ridgetops and 6 are in ultisol areas on steep slopes. All of these plot locations were identified in the laboratory using a GIS, and were established in the field without reference to surrounding forest conditions (i.e., their positions are not biased by local structural characteristics). In all primary plots, detailed measurements of stem diameters of all trees greater than 10 cm diameter have been collected annually as a part of ongoing carbon dynamics studies (see Clark and Clark 2000 for more details). Stem diameters were measured either at breast height (1.37 m) or, when necessary, above buttressing.

Data in secondary forests were collected in three different areas that were approximately 14, 22 (Chazdon 1996, Guariguata et al. 1997, Nicotra et al. 1999) and 31 (Pierce 1992) years old respectively as of March 1998. The 14 and 22 year old secondary forest plots are each 0.5 ha. Six, 25 m diameter circular plots were also geolocated to approximately coincide with lidar footprint locations within the 31 year old secondary forest area. Within the 14 and 22 year old secondary forest plots, all stem diameters greater than 5 cm diameter were measured. In the 31 year old plot, all stem diameters greater than 10 cm diameter were measured. Because of the smaller size of the plots in the 31 year old forest area, the field data from these 6 plots were pooled to form plot-level profiles (see below) and a singe biomass estimate for this 31 year old area.

Estimated aboveground biomass (EAGB) values were then calculated for all live stems in each forest plot using Equation 3.1, which was developed for tropical wet forests (Brown 1997). Plot-level EAGB values (in Mg/ha) were calculated by summing the EAGB values for all live stems within the plot.

Equation 3.1 $\mathbf{EAGB_s} = 21.297 - 6.953(\mathbf{D}) + 0.740(\mathbf{D}^2)$ where **D** is stem diameter in cm, and $\mathbf{EAGB_s}$ is the estimated oven-dried aboveground biomass (in Kg) for the stem. Note that this equation relies exclusively on stem diameter and does not include tree height.

Within each plot, measurements related to vertical canopy structure were also collected on a subset of the trees, with a particular emphasis placed on canopy-forming trees (i.e., classified as either dominant or co-dominant). Stem heights and crown depths (i.e., from the top of the tree to the lowest live branch) were measured using a laser rangefinder. A reflector at the base of the tree was used as a target for horizontal distance measurements. Crown diameters were measured using either a laser rangefinder or standard fiberglass measuring tapes. The crown diameters were measured in the direction of the longest branches and, therefore, represent the maximum horizontal crown extent.

Stem diameter measurements were also used to estimate height and crown dimensions for all remaining trees where these measurements were not taken. Allometric relationships were developed to estimate stem height, crown diameter and crown depth using the subset of trees sampled in each area (Table 3.1). Separate equations were developed for plots in secondary forest areas, and for plots located in primary forest areas with different edaphic conditions (inceptisol vs. ultisols). Separate equations compensated for differences in the coefficient of variation of height and crown measurements in each area that may have been the result of different field crews in each respective area.

Finally, published aboveground biomass and crown volume values from 6 (0.12 ha) agroforestry plots at La Selva (Menalled et al. 1998) were also incorporated into this study. The approximate locations of these plots were determined using an ancillary fine-resolution (~33 cm) lidar data set collected

Table 3.1 Regression models developed from stems with measured heights, crown depths and crown diameter. Separate equations were developed for stems found in plots in secondary forests, and in primary forest areas with different soil conditions.

Y	Plots	Equation*	R^2	RMSE (m)
Height	Primary Inceptisol (n= 111)	y = 15.21 Ln(x) - 26.38	0.822	3.6
	Primary Ultisol (n=302)	y = 10.10 7Ln(x) - 12.41	0.483	5.1
	Secondary (n=631)	y = 10.77 Ln(x) - 11.63	0.745	3.9
Crown Depth	Primary Inceptisol (n= 111)	y = 0.306x + 1.24	0.576	4.3
	Primary Ultisol (n=302)	y = 0.16x + 3.76	0.274	3.2
	Secondary (n=631)	y = 0.28x + 2.29	0.495	3.0
Crown Diameter	Primary Inceptisol (n= 111)	y= 0.20x + 4.17	0.706	2.1
	Primary Ultisol (n=302)	y = 0.14x + 4.41	0.276	2.8
	Secondary (n=631)	y = 0.19x + 2.37	0.532	1.9

*For all equations x= stem diameter (cm) over the northern portion of La Selva (M. Roth unpublished, see Blair and Hofton 1999).

Derivation of Field Vertical Canopy Profiles

Vertical canopy profiles were derived from measured and modeled stem heights and crown dimensions in all plots. The field-derived vertical canopy profiles are comprised of a total of 180 30 cm bins (to correspond with the vertical bin size of the lidar waveforms), for a total height of 54 m. The profiles represent the vertical distribution of crown volume, and the methods for deriving them are described next.

First, all crowns are modeled to have a simple cylindrical shape bounded by the crown depth and crown diameter values, and placed at the appropriate height according to the stem height value. Second, the total cross-sectional area of all intersected crowns within each 30 cm vertical bin is then summed. For each plot, this produces a vertical canopy profile based on the distribution of crown volume. This process is illustrated in Figure 3.2.

Quantile metrics are then calculated for each average profile to represent the relative distribution of canopy materials (Figure 3.2). These metrics represent the height below which X% of the total crown volume is located (denoted as FCVX, where X represents the percentage of "FCV" or field-estimated crown volume). For this study FCV01, FCV05, FCV10, FCV25, FCV75, FCV90, FCV95, FCV99 and "HMFCV" (the height of median crown volume, equivalent to FCV50) were calculated. For simplicity, not all metrics are shown in the results section.

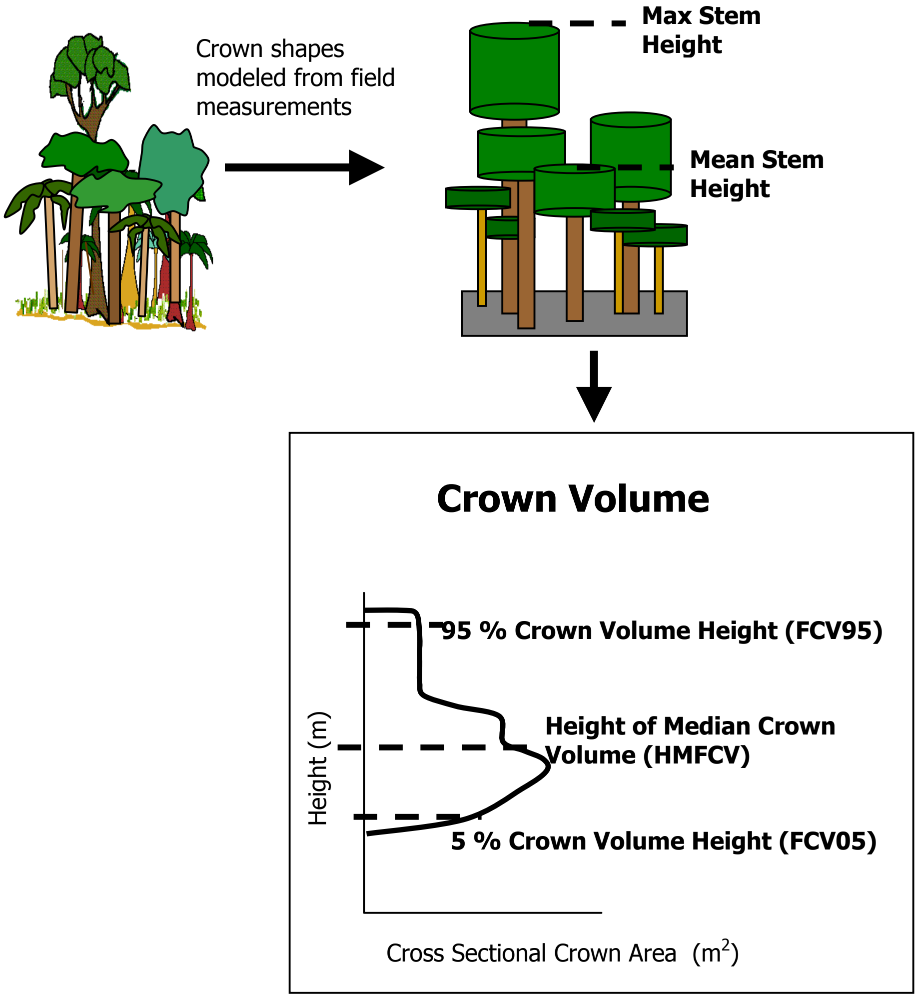

Figure 3.2 Derivation of field vertical canopy profiles. For this study, crown volume distributions were calculated from field measurements in all plots. A simple cylindrical crown shape, bounded by crown depth and crown diameter measurements, was assumed for tree crowns. The cross-sectional area of all crowns intersected is then summed for each 33 cm height interval. Metrics were derived from both the distribution of tree heights (e.g., mean stem height) and from the vertical canopy profiles (e.g., FCV95).

Lidar Data

The lidar data used in this study are from the airborne Laser Vegetation Imaging Sensor (LVIS, Blair et al. 1999). LVIS is a medium-altitude, medium- to large-footprint imaging laser altimeter, designed and developed at NASA's Goddard Space Flight Center. LVIS digitizes the entire return signal, thus providing a waveform relating to the vertical distribution of intercepted canopy and ground surfaces within each footprint (Figure 3.3; and see Blair et al. 1999, Dubayah and Drake 2000, Dubayah et al. 2000 for more details).

In March 1998, LVIS was flown in a NASA C-130 cargo plane over La Selva Biological Station and surrounding regions of northeast Costa Rica. LVIS was flown at an altitude of 8 km above the ground to produce eighty, 25 m diameter footprints separated by ~25 m along- and ~9 m across-track. Only LVIS footprints that were coincident with field study plots were selected for this study. The mean number of LVIS footprints in each plot was approximately 8.

Lidar-Derived Vertical Canopy Profiles

The signal digitized by LVIS is a waveform that relates to the vertical distribution of intercepted canopy and ground surfaces (in 30 cm vertical bins). As such, LVIS waveforms from within each plot were used as one type of vertical canopy profile. In this case, all of the lidar waveforms within a plot were summed to produce a plot-level "average waveform" with which to compare to field-derived vertical canopy profiles from each plot.

Lidar waveforms have also been transformed in previous studies to account for the attenuation of the lidar energy as the laser pulse travels through the canopy (Lefsky 1997, Lefsky et al. 1999a, Lefsky et al. 1999b, Means et al. 1999, Harding et al. 2001). Because some of the laser energy at the top of the canopy is reflected or absorbed, there will be less energy available lower into the canopy. Thus, the MacArthur-Horn technique (MacArthur and Horn 1969, Aber 1979b), which was developed for field studies to produce foliar height profiles from uplooking foliar distance measurements, was modified to transform the waveform into a relative canopy height profile (See Figure 3.3; and Harding et al. 2001 for more details).

Canopy height profiles (CHPs) were then calculated for all shots in each plot based on techniques described in (Harding et al. 2001). In this case, the CHPs were created with 180 30 cm bins. Plot-level CHPs were then derived by summing all individual CHPs within each plot.

Quantile metrics were then calculated for each average lidar profile similar to the technique described above for field profiles (Figure 3.3). The metrics represent the height below which X% of: (a) the total energy of the waveform (including the canopy and ground returns), or, (b) the canopy height profile are located. In this case the denotations are: "HENGX" for the height of X% the waveform energy, and "CHPX " for the height at which X% of the CHP is located below. For this study, the 1, 5, 10, 25, 50, 75, 90,95 and 99 quantile metrics were calculated for each type of lidar profile. The only exception to the above naming scheme is for the height of 50% of the waveform energy, which is referred to as the height of median energy (HOME) to correspond to a previous study (Drake et al. In press). Again, for simplicity, not all metrics are shown in the results section.

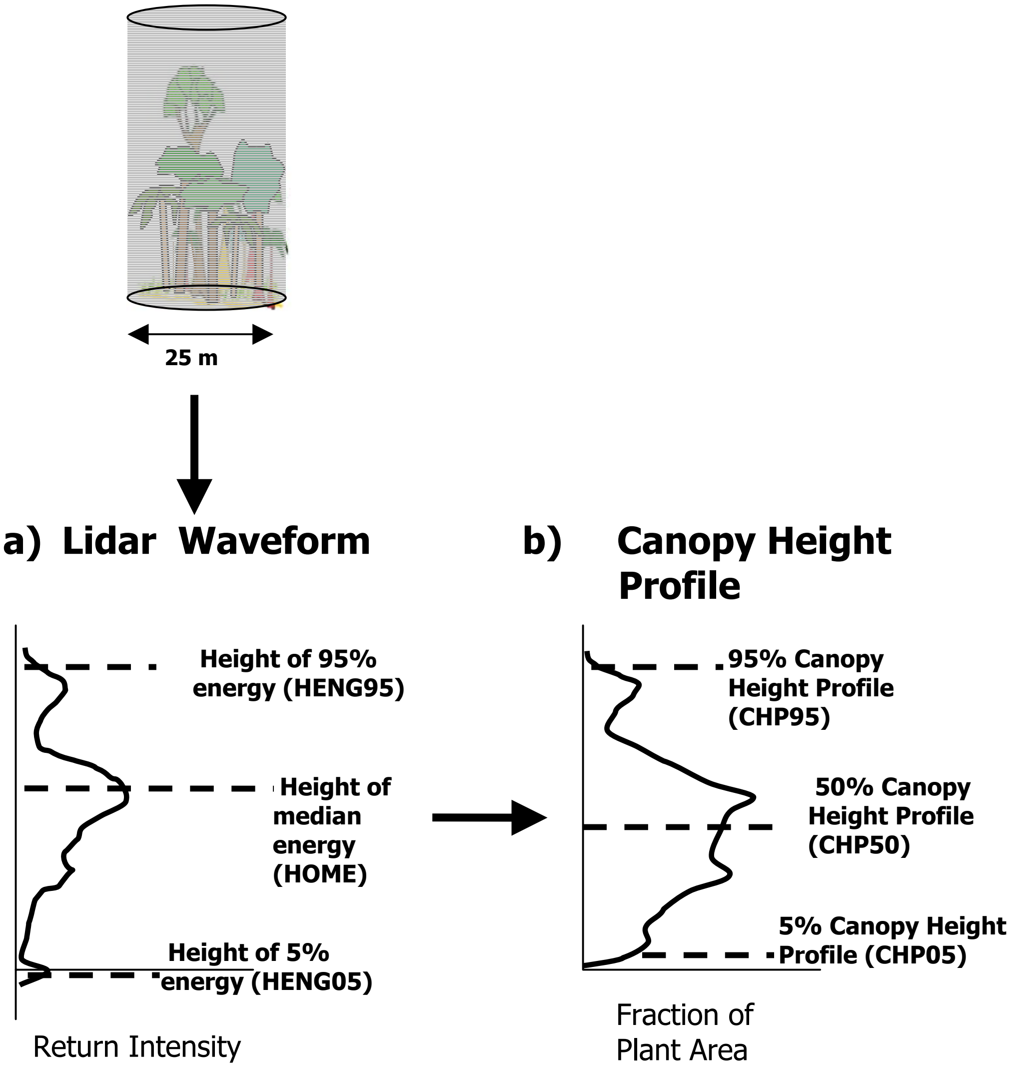

Figure 3.3 Derivation of vertical canopy profiles from lidar data. Coincident footprints from each plot were used both as: a) waveforms directly from the LVIS instrument and b) canopy height profiles that are derived using a exponential transformation of return energy in the waveform as described in Harding et al. (2001). Quantiles (e.g., HOME, CHP50) were calculated from both lidar vertical canopy profile formats.

Analysis

We first examined the relationship between metrics from field-derived vertical canopy profiles and the estimated aboveground biomass (EAGB). Profile metrics, along with the mean and maximum stem heights, for each plot were incorporated into a stepwise regression procedure to predict EAGB. The best single and multiple-term relationships were identified. These relationships were also used as a baseline for comparisons against the lidar-EAGB relationships.

To compare field- and lidar-derived vertical canopy profiles we first examined the relationships between quantile metrics from field- and lidar-derived vertical canopy profiles. Initially, complimentary metrics from both lidar and field profiles were compared. For example the correlation of the 75% metric for both lidar (CHP75 and HENG75) and field (FCV75) was examined using the metrics from all plots. Next the mean difference for each metric was analyzed. This was calculated for each metric by subtracting the lidar metric (e.g., HENG25) from the corresponding field metric (FCV25), and then taking the mean of the differences for all plots. For example, if the mean of all FCV75-HENG75 values was a positive number then the lidar metric is "lower on average" than the corresponding field metric.

Next, we analyzed the relationship between the entire lidar- and field-derived vertical canopy profiles. The correlation of individual lidar and field profiles was examined for each plot. To do this, the untransformed lidar waveforms were also converted into 180 (30 cm) bin profiles. Because the raw waveform bin size is 30 cm, this simply involved cutting the waveform at ground level, and at 54 m (bin 180) above ground level. In addition, all untransformed lidar and field profiles were normalized to compensate for differences in units (i.e., crown area and digitizer counts). We initially examined the correlation of complete average lidar profiles and corresponding field profiles. However, whereas field profiles are only from the top of the highest canopy to the bottom of the lowest crown, lidar profiles are continuous from the canopy top to the ground. We therefore, cut the portion of the lidar profile that was below the field-measured lowest live branch and reexamined the correlation between lidar and field profiles. Quantile metrics were not, however, recalculated for the cut lidar profiles.

As a final comparison of field and lidar profiles, we performed a goodness-of-fit analysis between lidar and field-based vertical canopy profiles. We measured the goodness-of-fit as the fraction of area shared by two types of normalized average profiles for each plot. The area overlap index (AOI) was calculated from the area of both average profiles that overlaps divided by the total area of both profiles. Statistical significance of differences between lidar and field profiles was then assessed by randomization of subplot-level profiles (e.g., individual lidar footprints or crown volume distributions from 25 m diameter circular subsets within each plot). The normalized subplot-level profiles from lidar and field methods were first pooled together. Then AOI between the observed average vertical profiles were compared with AOI of average profiles from 999 pairs of subsets, composed of random partitions of subplot lidar and field data from within the same larger plot. If the “actual” AOI (i.e., between average lidar- and field-derived profiles) was less than all but 49 or fewer AOI from the randomization procedure then the average profiles were considered significantly different (α=0.05)

Lastly, we identified the best linear combination of lidar profile metrics for predicting EAGB. Metrics from lidar profiles in all plots were used in a stepwise regression procedure to predict EAGB, and the best single and multiple-term relationships were identified. We then compared these relationships with corresponding relationships between EAGB and metrics from field profiles.

Results

Field-derived Vertical Canopy Profiles

Nearly all of the metrics listed in Table 3.2 from field-derived vertical canopy profiles and the maximum and mean stem height increase from agroforestry to secondary forest, and from secondary to primary forest. The notable exception is for FCV05, which is higher in agroforestry plots than in secondary plots, but is still highest in primary forest plots. These trends are apparent in Figure 3.4 where the narrow distribution of crown volume in the uniform agroforestry plots is all higher aboveground than the lower portion of canopy materials in the secondary (and in some cases primary) forest plots.

Field-derived Vertical Canopy Profile Metrics vs. EAGB

The increase in most field profile metrics parallels an increase in EAGB from agroforestry to primary forest plots (Table 3.2). The range of EAGB varies greatly within secondary and primary forest plots. Within secondary plots large, remnant stems (i.e., those not cleared when the area was originally deforested)

Table 3.2 Field characteristics by landcover type. For field-derived vertical canopy profile metrics and field estimated aboveground biomass (EAGB) the first value is the median, and the values in parentheses are the range of values from all plots within each type.

Field Variable	**Agroforestry**	**Secondary**	**Primary**
Number of plots	6	3	18
Max Stem Height (m)	10.4 (10.4- 11.9)	34.6 (32.5- 42.4)	40.0 (31.7- 47.0)
Mean Stem Height (m)	9.4 (9.2- 11.4)	14.3 (11.6- 21.0)	16.9 (15.8- 19.1)
FCV05* (m)	7.0 (6.7- 9.0)	6.0 (5.3- 9.3)	8.0 (7.0- 9.3)
FCV25* (m)	7.6 (7.3- 9.7)	12.0 (8.7- 14.7)	12.3 (11.0- 15.7)
HMFCV* (m)	8.4 (8.0- 10.3)	16.7 (12.0- 20.0)	16.9 (14.3- 22.0)
FCV75* (m)	9.2 (9.0- 11.0)	20.7 (18.0- 26.3)	22.7 (19.0- 29.3)
FCV95* (m)	9.7 (9.5- 11.7)	25.0 (24.0- 34.3)	31.7 (25.0- 38.3)
EAGB (Mg/ha)	29 (28- 48)	124 (70- 193)	173 (113- 206)

* Quantiles from field-estimated crown volume distribution (see Figure 3.2 and text for details).

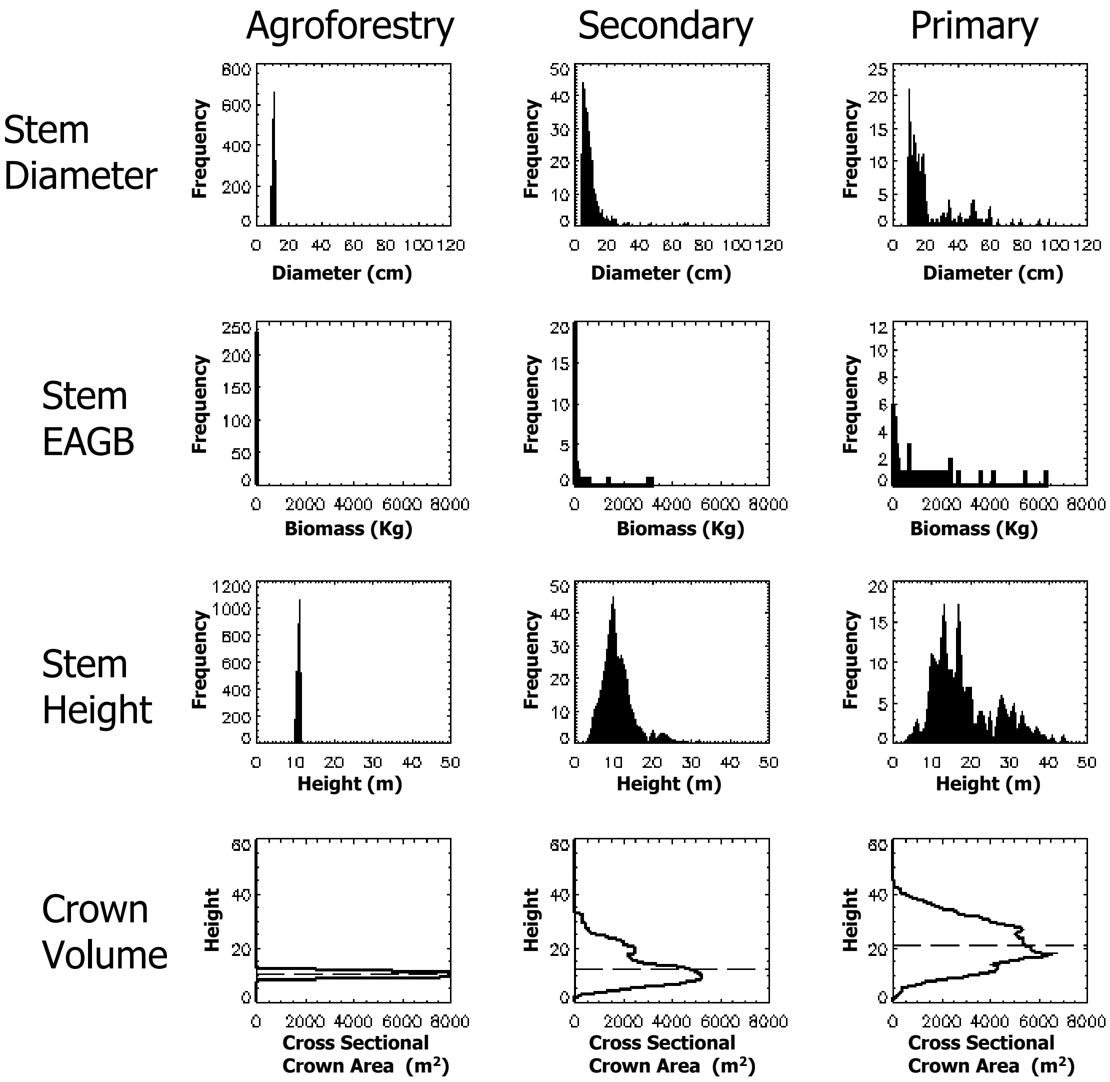

Figure 3.4 Histograms of stem diameters, estimated stem biomass and stem height, and crown volume distributions from an example plot within three different landcover types. For crown volume distributions, the height of median crown volume (HMFCV) is represented by the dotted line.

may comprise over 15% of the basal area in secondary forest areas (Guariguata et al. 1997), and therefore contribute a large proportion to the overall plot-level aboveground biomass. These remnant stems also increase both height metrics (e.g., maximum height) and upper profile metrics (e.g., FCV95).

As a result the best single predictor of EAGB (R^2=0.88) across this wide range of conditions is a metric from the upper portion of the profiles, FCV95 (Table 3.3, equation 1). The relationship between this field metric and EAGB is non-asymptotic across all land-use, successional and environmental conditions sampled at La Selva (Figure 3.5). The standard error (RMSE) for this single-term relationship is 21.65 Mg/ha.

If two or more metrics were used in a multiple regression to predict differences in EAGB across all plots, the R^2 values increased further. With 4 metrics from the field vertical canopy profile, approximately 94% of the variation in EAGB was explained. In addition, the RMSE dropped to approximately 16 Mg/ha, which is approximately 10% of the mean EAGB value for primary forest plots at La Selva. For the multi-term equations, the metrics that were the best predictors of EAGB (Table 3.3.) were from both the upper and lower portions of the field profile (e.g., FCV90 and FCV10). Thus, differences in both the upper and lower portions of canopy profiles are highly related to variation in aboveground biomass in this Neotropical landscape.

Table 3.3 Regression equations for field-estimated vertical canopy profile metrics vs. estimated aboveground biomass (EAGB). Data is from all plots (n=26) sampled at La Selva Biological Station.

Equation	**R^2**	**RMSE (Mg/ha)**
(1) $Y = 6.2*FCV95 - 28.5$	0.88	21.7
(2) $Y = 3.9*FCV99 + 15.9*FCV10 - 126.6$	0.92	18.0
(3) $Y = 7.7*FCV99 + 20.2*FCV10 - 5.71*FCV90 - 141.7$	0.93	17.3
(4) $Y = 7.6*FCV99 + 46.0*FCV10 - 7.2*FCV90 - 24.6*FCV05 - 144.7$	0.943	16.0

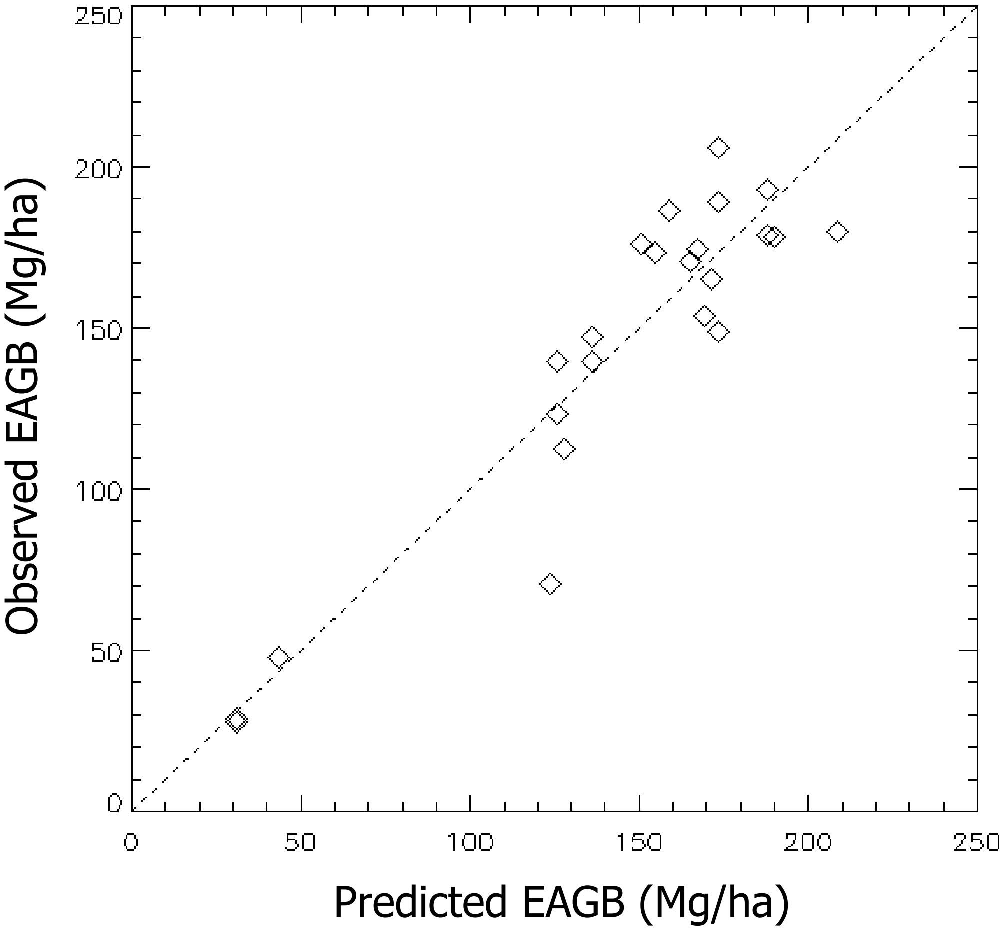

Figure 3.5 Predicted vs. field estimated aboveground biomass (EAGB) from all plots at La Selva. The predicted EAGB values are from a single-term regression (Table 3.3, equation 1) using the FCV95 metric from field-derived vertical canopy profiles.

Lidar-derived Vertical Canopy Profiles

In general, metrics from lidar vertical canopy profiles (waveforms and CHPs) also increase from agroforestry to secondary forest, and from secondary to primary forest (Table 3.4). As is the case for the field metric FCV05, the exception in this trend is the transformed lidar metric CHP05, which is higher in agroforestry and primary forest plots than in secondary plots. In contrast, the corresponding untransformed waveform metric, HENG05, does increase from agroforestry to primary forest. HENG05 is negative in several plots, because the waveform is the entire lidar signal, including the ground return. In many cases (particularly in agroforestry plots) a large portion of the overall energy is in the lower portion of the last gaussian pulse (i.e., below the ground reference level which is the peak of the last gaussian pulse). These trends can be seen in Figure 3.6 where there is an increase in the height of lidar profile metrics from agroforestry to primary forest plots.

Lidar- vs. Field-derived Vertical Canopy Profile Metrics

The values for most of the lidar vertical canopy profile metrics (Table 3.4) increase from agroforestry to primary forest plots, and therefore follow a similar trend to the corresponding field metrics (Table 3.2). The values for upper metrics from both waveforms and CHPs closely mirror equivalent metrics in the field crown volume distributions (e.g., FCV95 vs CHP95). In contrast the differences between the lower field and lidar quantiles (e.g., FCV05 vs. CHP05) are greater.

Table 3.4 Lidar vertical canopy profile metrics by landcover type. The first value is the median, and the values in parentheses are the range of values from all plots within each landcover type.

Profile Metric	Agroforestry	Secondary	Primary
HENG05* (m)	-1.7 (-3.0 – (-1.3))	0.3 (-1.8- 1.3)	3.4 (-1.2- 7.1)
HENG25* (m)	0.5 (-1.5- 3.8)	11.5 (4.7- 11.7)	16.6 (9.9- 21.2)
HOME* (m)	4.8 (0.3- 7.4)	16.2 (9.0- 17.6)	21.6 (12.0- 28.4)
HENG75* (m)	7.8 (2.1- 9.7)	18.2 (14.0- 25.5)	23.9 (19.6- 33.7)
HENG95* (m)	10.2 (5.7- 12.8)	22.8 (20.6- 34.5)	27.4 (24.6- 37.5)
CHP05 (m)**	3.9 (3.0- 4.4)	3.3 (3.1- 3.9)	3.9 (2.5- 6.1)
CHP25 (m)**	6.7 (4.3- 8.0)	8.3 (7.3- 8.5)	11.1 (8.2- 14.1)
CHP50 (m)**	8.5 (5.3- 10.4)	13.0 (11.1- 14.0)	18.6 (13.7- 23.9)
CHP75 (m)**	10.0 (6.7- 12.3)	17.9 (15.4- 22.1)	23.4 (18.3 –31.1)
CHP95 (m)**	11.5 (8.0- 13.1)	21.2 (21.0- 28.5)	23.4 (18.3-37.1)

*Quantiles from untransformed waveforms (see Figure 3 and text for details).

** Quantiles from “canopy height profile” transformation of waveforms (see Figure 3 and text for details).

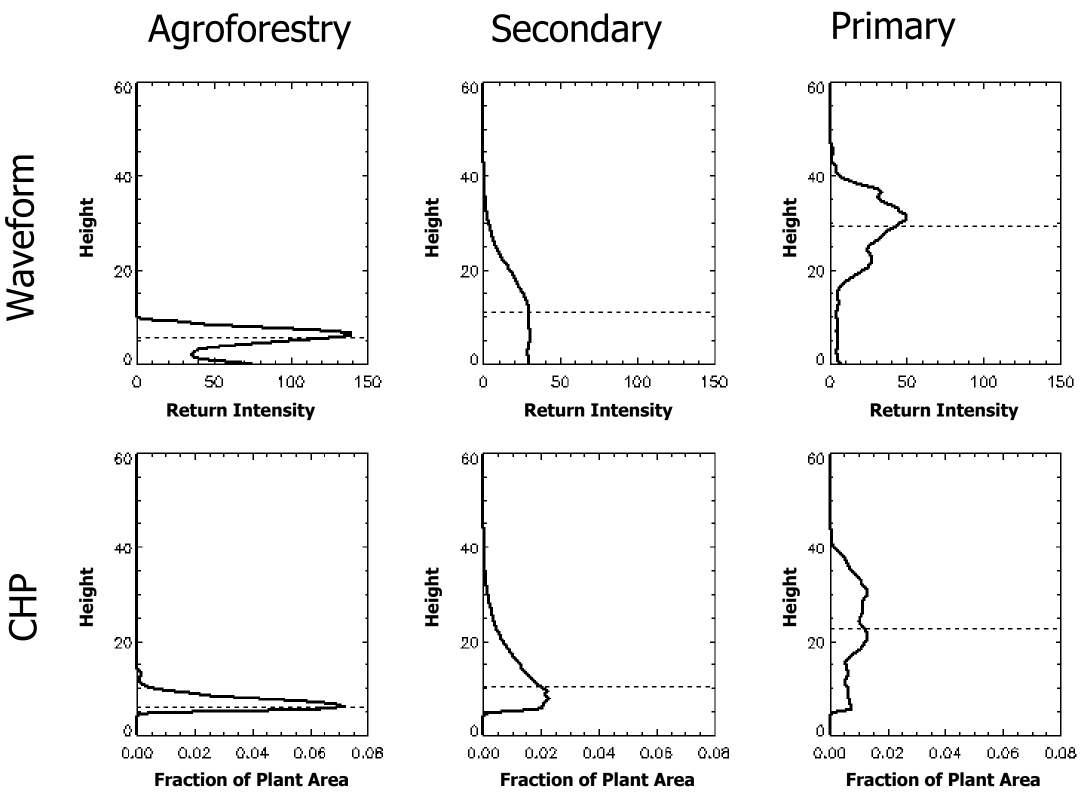

Figure 3.6 Lidar-derived vertical canopy profiles (waveforms and CHPs) from an example plot within three different landcover types. The median or 50% height for both the waveforms (HOME) and the CHP (CHP50) is represented by the dotted line.

To further examine the relationship between corresponding lidar and field profile metrics, a simple linear regression analysis was performed. The regression results (Figure 3.7 and Table 3.5) illustrate that metrics from both lidar and field profiles are all highly correlated, except for the lower metrics (e.g., FCV05 vs CHP05). In all but one case, the R^2 and RMSE values show the untransformed waveform metrics are more similar to the field profile metrics than the CHP metrics (Table 3.5 A., Figure 3.7). In most cases the RMSE values on the waveform metric equations are less than 12% of the median value of the corresponding field metric, and are less than 14% of the median value in the CHP metric equations.

In most cases, the mean of differences between lidar and field metrics is less than 2 m (Table 3.5 B.). Again the exception is for the lowest profile metric where the mean difference is approximately 6 m for the waveform metric (FCV05-HENG05) and 4 m for the CHP metric (FCV05-CHP05). This illustrates that the bottom portion of the lidar profiles are typically lower than the field profiles. The most likely explanation for this is that whereas the crown volume distributions start with the lowest branch on a measured tree (e.g., a tree over 10 cm dbh in primary plots), lidar profiles are continuous from the top of the canopy to the ground (and below for waveforms as mentioned above). As a result this difference is to be expected.

Lidar- vs. Field-derived Vertical Canopy Profiles

There is a fairly good qualitative agreement between lidar- and field-derived vertical canopy profiles. Both average waveforms and average CHPs

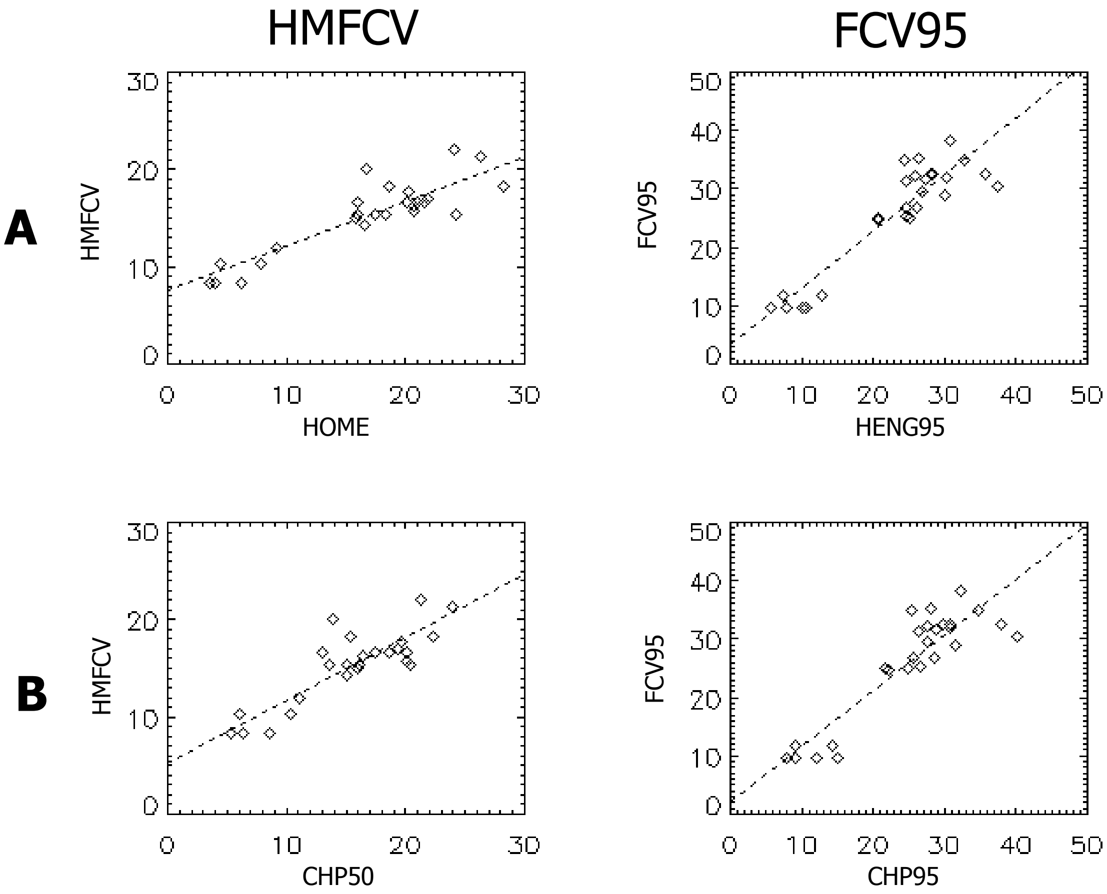

Figure 3.7 Relationships between corresponding metrics derived from field (y-axis) and lidar (X-axis) vertical canopy profiles. A) Relationships between two metrics from lidar waveforms (HOME, HENG95) and the corresponding field profile metrics (HMFCV, FCV95) B) Relationships between two metrics from lidar CHPs (CHP50, CHP95) and the corresponding field profile metrics (HMFCV, FCV95). For all plots, the dotted line represents the regression line. See Table 3.5 for R^2, RMSE and mean difference values.

Table 3.5 Comparison of corresponding metrics from field- and lidar-derived vertical canopy profiles. A) Regression results from field and associated lidar metrics (e.g., FCV25 vs. HENG25 or CHP25). R^2 and RMSE (parentheses) values are listed. B) Mean difference values (field minus lidar) for each metric.

A

Lidar Profile	FCV05	FCV25	HMFCV	FCV75	FCV95
Waveform	0.22 (0.94 m)	0.78 (1.06 m)	0.81 (1.78 m)	0.79 (2.84 m)	0.83 (3.93 m)
CHP	0.01 (1.06 m)	0.53 (1.59 m)	0.74 (2.07 m)	0.80 (2.82 m)	0.80 (4.23 m)

B

Lidar Profile	FCV05	FCV25	HMFCV	FCV75	FCV95
Waveform	6.07 m	-0.33 m	-1.12 m	-0.21 m	1.62 m
CHP	4.10 m	1.81 m	-0.15 m	-0.20 m	0.95 m

tend to follow a similar overall pattern as the field-derived vertical canopy profiles. With the exception of untransformed average waveforms in primary forest areas, lidar and field vertical canopy profiles tend to have their largest peaks at approximately the same height. In addition, the canopy heights (i.e., the top of the profile) from both lidar and field techniques are also closely related in all landcover types.

Lidar and field profiles in most plots are also highly correlated (Table 3.6). Waveforms and field profiles from secondary forest plots are the most highly correlated, followed by primary forest and agroforestry plots. In contrast, CHPs and field profiles from primary forest plots are the most highly correlated, followed by secondary forest and agroforestry plots.

In both agroforestry and primary plots, CHPs are more highly correlated than waveforms with field-derived vertical canopy profiles. In secondary forest plots, however, untransformed waveforms were more highly correlated than CHPs with field profiles. This same general trend can be seen in Figure 3.8, where removal of the ground return in agroforestry plots, and where transformation of the lower portion of the profile in primary forest plots allows the CHP to more closely resemble the field profiles. Similarly, because the field vertical canopy profiles are from the top of the canopy to the bottom of the lowest live crown for trees over 10 cm stem diameter (in primary plots), when the correlation analyses are only performed on the portion of both profiles within this range for each plot, there is a slight improvement in the correlations (Table 3.6 B).

Table 3.6 Correlation between lidar and field-based vertical canopy profiles. A) Correlation of lidar waveforms or CHP vs. crown volume distributions. B) Correlation using portion of lidar profiles that are above the lowest live crown measured in each plot. For all comparisons, median correlation coefficients between lidar and field data for plots within each landcover type are listed first, followed by the observed range of coefficients in that type.

		Agroforestry	**Secondary**	**Primary**
A	**Waveform**	0.27 (0.06-0.70)	0.88 (0.79-0.93)	0.60 (0.02-0.85)
	CHP	0.46 (0.01-0.78)	0.74 (0.57-0.90)	0.78 (0.45-0.93)
B	**Waveform (Cut)**	0.45 (0.05-0.86)	0.89 (0.83-0.93)	0.59 (0.07-0.87)
	CHP (Cut)	0.62 (0.24-0.86)	0.74 (0.57-0.90)	0.80 (0.53-0.93)

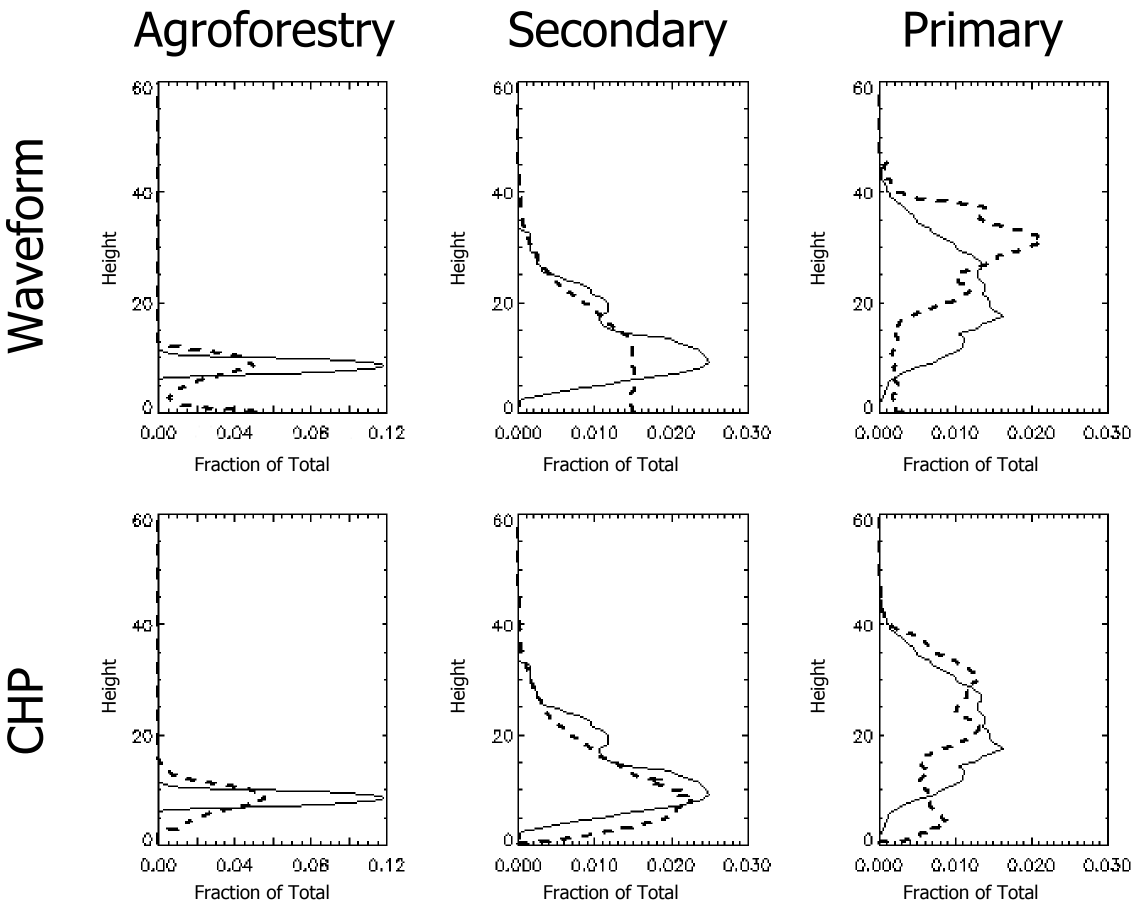

Figure 3.8 Field (solid) and lidar (dashed line) vertical canopy profiles from an example plot within three different landcover types. All profiles have been normalized as a fraction of their total value (e.g., fraction of total crown volume).

The results from goodness-of-fit analysis of lidar and field profiles follow similar trends (Table 3.7). The area of overlap between average waveform and field profiles (as characterized by the area overlap index, AOI) is highest in secondary forests, followed by primary forests and agroforestry areas. The AOI between the average CHP and field profiles was greatest in primary forest plots, followed by secondary forest and agroforestry plots.

Although both correlation coefficients (Table 3.6) and AOI (Table 3.7) between lidar and field profiles are generally quite high, in most cases the average profiles are significantly different (Table 3.7). In other words, the AOI between average lidar and field profiles for a given plot are typically smaller than the AOI from all 999 pairs of subsets composed of random partitions of sub-plot level field and lidar profiles. For example, in the agroforestry areas, lidar and field profiles in five out of six plots were significantly different. Similarly, average lidar profiles were significantly different from field profiles in 17 out of 18 primary forest plots. However, average waveforms were significantly different from field profiles in only one out of three secondary plots, whereas average CHPs were all significantly different from field profiles in secondary forest areas.

In summary, in many cases there are significant differences between profiles derived using lidar and field techniques. Nonetheless, the upper quantile metrics from lidar (e.g., HENG95 or CHP95) and field (e.g., FCV95) techniques are highly correlated. In addition, the mean differences between many of the upper metrics are less than 2 m. As such lidar data can resolve

Table 3.7 Goodness-of-fit between lidar and field-based vertical canopy profiles, measured as the fraction of area shared by two types of normalized average profiles for each plot. The area overlap index (AOI) was calculated from the area of both average profiles that overlaps divided by the total area of both profiles. Statistical significance of differences between lidar and field profiles was assessed by randomization. Subplot data from field and lidar methods were pooled. Then AOI between the observed average vertical profiles were compared with AOI of average profiles from 999 pairs of subsets, composed of random partitions of subplot lidar and field data from within the same larger plot (see text). For all comparisons, mean AOI between lidar and field data for plots within each landcover type are listed first, followed by the observed range of AOI values in that type.

	Agroforestry	**Secondary**	**Primary**
Waveform	0.27* (0.07-0.42)	0.82** (0.77-0.86)	0.64**** (0.40-0.80)
CHP	0.38* (0.20-0.48)	0.73*** (0.63-0.83)	0.75**** (0.59-0.86)

*Average profiles from 1 out of 6 plots were not significantly different ($p < 0.05$)
**Average profiles from 2 out of 3 plots were not significantly different ($p < 0.05$)
***Average profiles for all plots were significantly different ($p < 0.05$)
****Average profiles from 1 out of 18 plots were not significantly different ($p < 0.05$)

differences in canopy structure across this Neotropical landscape, without equivalence to field profiles.

Lidar-derived Vertical Canopy Profile Metrics vs. EAGB

Metrics from lidar vertical canopy profiles follow a similar trend to metrics from field profiles: all lidar metrics except CHP05 (Table 3.4) are greater in plots with greater biomass (Table 3.2). As a result, lidar metrics are highly correlated with EAGB across all of the plots sampled (Table 3.8). The best single predictor of EAGB was the height of median energy (HOME) metric with an R^2 value of 0.87 and an RMSE of approximately 23 Mg/ha (Table 3.8, equation 1). Although this quantile metric differs from the best single predictor of EAGB from field profiles (FCV95), the level of variation that is explained by both metrics is approximately equal (88% vs. 87%, Tables 3.3 and 3.8). The relationship is also non-asymptotic across all land-use, successional and environmental conditions at La Selva (Figure 3.9).

When two or more metrics are used in a multiple linear regression, the R^2 values increase (Table 3.8, equations 2-4), as with multiple regression results from field metrics. For example with 4 metrics from the lidar profiles, the R^2 values are approximately 0.94, and the RMSE is approximately 16 Mg/ha (again, approximately 10% of the mean EAGB value for primary forest plots at La Selva). Another similarity with field equations is that the metrics that were the best predictors of EAGB were from both the upper and lower portions of the canopy (e.g., HENG10 and HENG90). However, one key difference between field and lidar equations is that the median metric (HOME) was in every lidar

Table 3.8 Regression equations for lidar vertical canopy profile metrics vs. estimated aboveground biomass (EAGB). Data is from all plots (n=26) sampled at La Selva Biological Station.

Equation	**R^2**	**RMSE (Mg/ha)**
(1) Y = 6.6*HOME- 24.8	0.87	22.6
Y = 6.2*HOME-0.75*HENG10+26.5	0.88	21.3
Y = 8.0*HOME+ 8.4*HENG10-9.8*HENG25+ 64.4	0.92	18.2
Y = 5.2*HOME+ 10.5*HENG10-12.5*HENG25 –3.6*HENG90+49.8	0.94	16.1

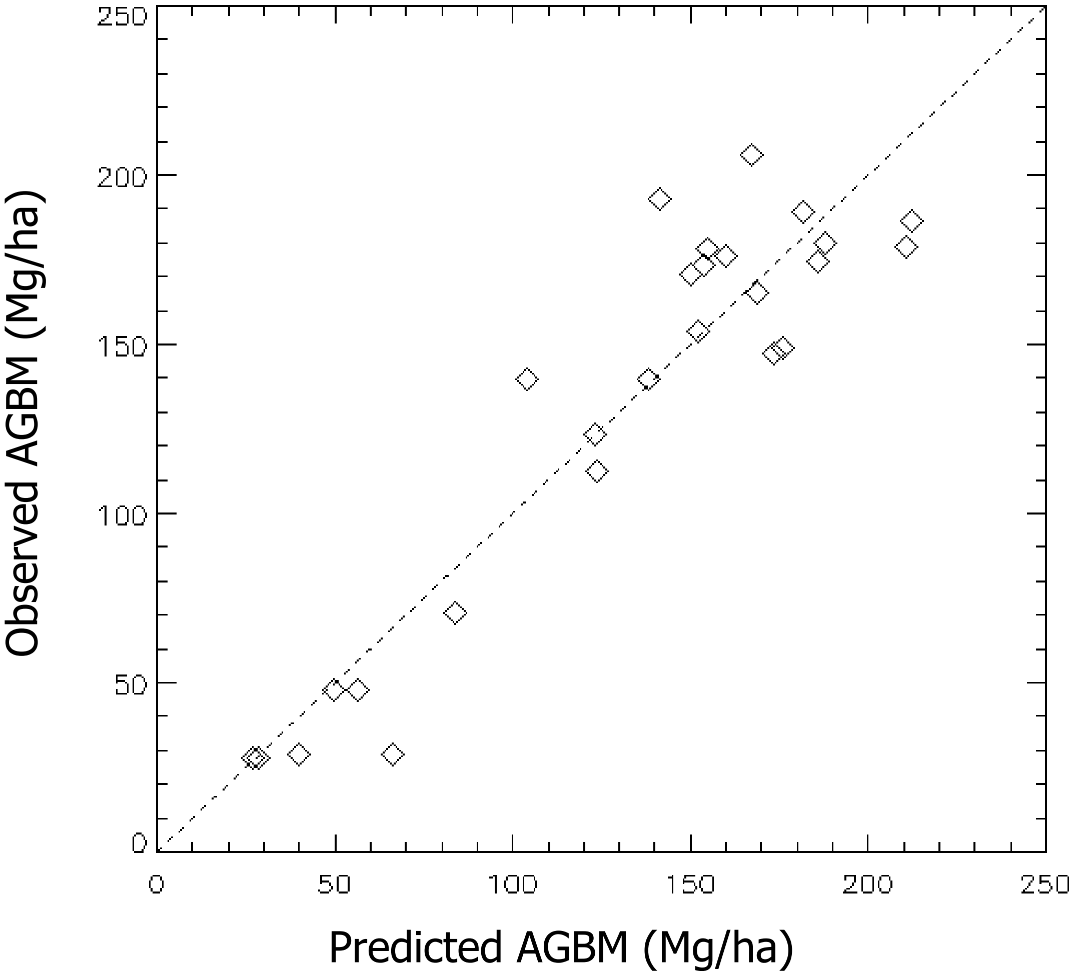

Figure 3.9 Predicted vs. field estimated aboveground biomass (EAGB) from all plots at La Selva. The predicted EAGB values are from a single-term regression (Table 3.8, Equation 1) using the HOME metric from lidar-derived vertical canopy profiles.

equation. Another important result is that for all equations, metrics from the untransformed waveforms were chosen over CHP metrics through the stepwise multiple regression analysis.

Discussion

Relationship between Field-derived Vertical Canopy Profiles and Biomass

The first portion of this research focused on the correlation between metrics from field-derived vertical canopy profiles and the total aboveground biomass. The strong relationship between single (e.g., FCV95) or multiple metrics from the field profiles and EAGB illustrates the value of quantifying variation in vertical canopy structure. The differences in the relative distribution of crown volume are strongly correlated with different EAGB levels across a wide variety of landcover types at La Selva Biological Station, including old-growth forest areas.

Some of the potential reasons that vertical canopy profiles are highly correlated with EAGB are illustrated in Figure 3.4. Although the density of stems in agroforestry and secondary forest plots are much higher than in primary forest plots, it is the relatively few, very large canopy-forming individuals in primary forest plots that contribute heavily to the total aboveground biomass in each plot. In addition, these large individual stems constitute the bulk of the upper portion of the vertical canopy profiles in primary forest plots. In contrast, the relatively few remnant stems in secondary forest areas create only a small upper mode in both the vertical canopy profile and the distribution of stem heights (Figure 3.4).

Similarly, within primary forest plots, the death of individual trees, and poor micro-environmental conditions can lead to lower-stature canopies (e.g., the low end of the range for FCV95 in Table 3.2), with lower total EAGB (e.g., one primary forest plot had an EAGB of only 113 Mg/ha, Table 3.2). As a result, upper quantile metrics (e.g. FCV95) from the field-derived vertical canopy profiles are highly correlated with overall EAGB across this landscape.

The relationship between metrics from field-derived vertical canopy profiles and aboveground biomass is important because it illustrates that height and canopy structure are important indicators of current ecosystem state. More importantly, metrics that relate to differences in the relative vertical distribution of canopy structure are responsive to variation in total aboveground biomass across the entire range of conditions sampled. It is reasonable that vertical canopy structure should be correlated to aboveground biomass in forest ecosystems, however the relationship between canopy metrics (e.g., crown volume metrics) and aboveground biomass is not well established for most forests. Most field studies have instead focused on the relationship between the height and biomass of individual stems, and not the relationship between vertical canopy structure and biomass at a plot (e.g., 0.5 ha) level. Because lidar instruments are sensitive to variation in canopy structure in temperate forests (Lefsky et al. 1999a, Harding et al. 2001), there is a need to examine the relationships between canopy structure and aboveground biomass from a field perspective as well. Our results suggest that differences in the relative vertical distribution of canopy structure provide an important means to characterize the current state of Neotropical ecosystems.

Relationship between Complete Field- and Lidar-derived Vertical Canopy Profiles

We have demonstrated that metrics from field-derived canopy profiles are correlated with EAGB at La Selva. Next we examined the sensitivity of lidar data to differences in canopy structure across different landcover types (e.g., agroforestry, secondary and primary forest). Although field and lidar profiles are correlated and have high AOI (Tables 3.6 and 3.7 respectively) in many cases there are significant differences between field and lidar profiles on a plot-to-plot basis (Table 3.7, Figure 3.8). Similarly, Harding et al. (2001) also found that lidar CHPs and field profiles (derived from ground-based sightings to plant intercepts) had qualitative similarities but were statistically different.

To a certain degree, the differences between entire profiles from lidar and field techniques found in this study should be expected. The effects of modeling stem heights and crown dimensions (Table 3.1) for many stems, as well as the assumption that crowns are filled cylinders are simplifications. In reality, crowns are highly irregular in shape, and crown materials are often clumped. Whether these model assumptions lead to biases in the field profiles in relation to the true distribution of crown volume is uncertain, however they will certainly contribute to differences between field and lidar profiles.

Even if the forest structure in each plot were destructively sampled to provide an actual crown volume distribution, there would still likely be differences between these profiles and lidar profiles. First, lidar instruments sample the entire distribution of canopy materials from the highest crown to the ground, whereas the field profiles developed in this study are only from the highest crown to the base of the lowest crown sampled. Second, trees that were used to create the crown volume distribution were only a portion of the plants that are found in each plot. Trees that were under 10 cm diameter (5 cm in secondary plots) were not included. As a result the field profiles do not include many of the smaller trees that also contribute to the lidar profiles.

A third cause for differences between lidar and field profiles is that the lidar signal is affected by the decreasing total amount of energy as the pulse travels lower into the canopy. For example in Figure 3.8, the upper portion of the lidar waveform is higher than the corresponding field-derived profile in a primary forest plot. Although a modified MacArthur-Horn transformation of the signal may make intuitive sense to compensate for this problem, there are still important assumptions (e.g., horizontal homogeneity or no clumping of canopy materials) that may create other biases (Lefsky et al. 1999a, Means et al. 1999, Harding et al. 2001). In this case, the transformation of the waveforms into CHPs did increase the correlation and goodness-of-fit values (Tables 3.6 and 3.7) with field profiles in primary forest and agroforestry areas compared with the untransformed waveforms, but there were still the same number of significant differences between field and lidar profiles. The correlation and goodness-of-fit of CHP and field profiles in secondary forest areas were lower than the untransformed waveform values. Further, all of the secondary forest plots had significant differences after the transformation, whereas the average waveform and field profiles from two of the three secondary forest plot areas were not significantly different. Thus, it is unclear if the modified MacArthur-Horn transformation of the lidar signal improves representation of canopy structure in this Neotropical landscape.

Although significant differences exist between lidar and field profiles, there are also important qualitative similarities (Figure 3.8). For example, both lidar and field profiles from different landcover types are distinct. (To test if lidar data are sensitive to differences in canopy structure between different landcover types we performed an additional goodness-of-fit analysis where we compared "type-level" average waveforms or CHPs produced from all individual waveforms or CHPs in one landcover type (e.g., primary forest) with the corresponding type-level profile from another landcover type (e.g., secondary forest). To test for significance we compared the AOI from these type level comparisons with the AOI from 999 pairs of subsets where all individual profiles (i.e., CHP or waveforms) from both landcover types were first pooled and then were randomly partitioned to create new "synthetic type-level" profiles.) In all cases, the lidar profiles from each landcover type were significantly different ($p < 0.005$) from all other landcover types. This shows that large-footprint lidar instruments are sensitive to important differences in vertical canopy structure in this Neotropical forest, and can thus be used to differentiate landcover types.

Relationship between Metrics from Field- and Lidar-derived Vertical Canopy Profiles

Although significant differences exist between the complete normalized vertical canopy profiles from lidar and field techniques, metrics from both field and lidar profiles are highly correlated (Table 3.5), and the mean differences between corresponding upper quantile metrics (e.g., FCV95 vs. HENG95) are all small (< 2m). This demonstrates that lidar is sensitive to important differences in canopy structure both within and across landcover types.

Comparisons of the quantile metrics derived from lidar and field profiles are not as strongly influenced by subtle differences in the overall spread of the profiles as are goodness-of-fit comparisons of the complete profiles. As such although there are obvious differences in the bottom-most metrics (e.g., FCV05 vs. HENG05, Table 3.5), the upper metrics from both lidar and field profiles are closely related. This is important because upper quantile metrics from the field profiles (FCV95) were the best predictors of EAGB in this Neotropical landscape.

Comparison of the Relationships between Field- and Lidar-derived Vertical Canopy Profiles and Biomass

We found that metrics from lidar vertical canopy profiles are approximately as correlated with EAGB (Table 3.8) at La Selva as field profile metrics (Table 3.3). This shows that large-footprint lidar instruments are sensitive to variation in EAGB, despite the significant differences between some lidar and field profiles.

In a related study (Drake et al. In press) we found that mean canopy height and the height of median energy from lidar waveforms were highly correlated with EAGB at La Selva. This extension of that earlier work provides a more thorough examination of the relationship between the complete lidar profile and EAGB, and also allows for a comparison with similar field techniques.

Although the best single predictor of EAGB from field (FCV95) and lidar (HOME) profiles differs, if the corresponding lidar metric is used instead (i.e., HENG95) the relationship is still quite strong (R^2=0.83). The HOME metric may be more strongly influenced by the amount of lidar energy that penetrates to the ground, and therefore will be much lower in areas with more open canopy conditions. For example in the agroforestry areas HOME is much lower than than HENG95 (Table 3.4 and Figure 3.6) caused primarily by the presence of strong ground returns. This may help to explain why metrics from untransformed waveforms were selected over CHP metrics in a stepwise multiple regression analysis (Table 3.8). Because the ground return is redistributed to the canopy return during the modified MacArthur-Horn technique (Harding et al. 2001), these metrics may not be sensitive to differences in both canopy structure and openness in different landcover types. In any case, waveform transformation did not improve estimates of biomass.

Conclusions

Although past research has examined changes in field-derived vertical canopy profiles (e.g., foliar height profiles) through different stages of forest succession (Aber 1979b, a, Brown and Parker 1994, Pare and Bergeron 1995), the relationship between metrics from field profiles and biomass has generally not been examined, primarily because vertical canopy profiles are difficult to construct. Because large-footprint lidar instruments can rapidly record vertical canopy profiles over large forested areas in contrast to labor-intensive field methods, they represent a breakthrough in the remote sensing of forest canopy structure with great potential for large-scale land surface characterization.

In this study we found that lidar data are sensitive to important differences in canopy structure over a wide range of conditions (i.e., from young secondary forests to primary tropical rainforests). We also showed that lidar profiles (even with a MacArthur-Horn transformation) are not equivalent to field profiles of the vertical distribution of crown volume. Nonetheless, metrics from untransformed lidar profiles are as good as metrics derived from field profiles for biomass estimation. Because changes in canopy structure are highly correlated with changes in aboveground biomass through time, lidar provides a new method for estimating carbon stocks in dense tropical forests.

The remaining challenge is to explore the generality of the relationships between vertical canopy profiles and aboveground biomass in different forest ecosystems. For example, will the relationships developed at La Selva Biological Station, a tropical wet forest (Holdridge et al., 1971) also apply to tropical moist forests in the Amazon that may receive half of the La Selva rainfall totals? Our future work will test the generality of these relationships in other tropical regions and will develop new relationships in areas with different environmental conditions if necessary. This process will set the stage for using global lidar observations from future spaceborne lidar instruments, such as the Vegetation Canopy Lidar (Dubayah et al. 1997), to estimate biomass in terrestrial ecosystems globally.

Chapter 4. Aboveground biomass estimation in closed canopy Neotropical forests using lidar remote sensing: Factors affecting generality of relationships

Abstract

Estimates of aboveground biomass provide critical information for modeling carbon dynamics in terrestrial ecosystems. Lidar remote sensing is an efficient method for estimating forest structural characteristics, such as aboveground biomass, because vertical forest structure is sampled. Previous studies have shown that canopy metrics from lidar data are highly correlated with aboveground biomass in a variety of closed-canopy forests, however the generality of these site-specific relationships has remained untested. In this study, we compare relationships between lidar canopy metrics and forest structural summaries such as aboveground biomass from (1) a tropical wet forest site (4200mm rain/yr) in Costa Rica and (2) across a series of tropical moist forest field sites spanning a rainfall gradient (2000-3000 mm rain/yr) in Panama.

We found that in both regions lidar metrics were strongly correlated (R^2: 0.65-0.92) with forest structural summaries including mean stem diameter, basal area and aboveground biomass. We also showed that the relationships differed between these regions unless deciduousness of canopy trees in Panama was considered. Adjusting for leaf-drop removed statistically significant differences between the two regions in the relationships between a lidar metric and both mean stem diameter and basal area. The relationships between lidar

metrics and aboveground biomass, however, remained significantly different between the two study areas. This was primarily due to the different general allometric relationships used to estimate aboveground biomass in tropical wet forests and tropical moist forests. Future efforts should continue to examine climatic factors that may influence the generality of the relationships between lidar metrics and forest structural characteristics, and address the dearth of allometric data on the very large trees that can dominate the biomass of primary tropical forests.

Introduction

Aboveground biomass is the total amount of biological material (usually oven-dried to remove water) present above the soil surface in a specified area. Because plant biomass is approximately 50% carbon, estimates of the total aboveground biomass in forest ecosystems are critical for carbon dynamics studies at multiple scales. These estimates provide initial conditions for ecosystem and biogeochemical models (e.g., Foley et al. 1996, Friend et al. 1997, Hurtt et al. 1998, Potter 1999) that simulate the exchange of carbon and energy between the atmosphere and forest canopies through time. Also estimates of carbon fluxes from deforestation, land cover change, and other disturbances depend on knowing the forest carbon stocks before disturbance (e.g., Houghton 1991).

Forest canopy structure is highly dynamic both temporally and spatially. As forests recover from past disturbance events, there are typically changes in the horizontal (e.g., increases in basal area) and vertical (e.g., an increase in stand height) distribution of forest structure that accompany an overall increase in aboveground biomass (Aber 1979a, Bormann and Likens 1979, Oliver and Larson 1990, Richards 1996). Additionally, variability in climatic (e.g., temperature, precipitation), edaphic, and other environmental factors (e.g., exogenous disturbances) result in differences in the spatial distribution of aboveground biomass and vertical canopy structure (e.g., Lieberman et al. 1996, Yamakura et al. 1996, Laurance et al. 1999, Clark and Clark 2000). For example, in nutrient poor areas, forests typically are lower-stature and contain less aboveground biomass than in nutrient rich areas (Oliver and Larson 1990, Kimmins 1997). Furthermore, there is usually a connection between differences in vertical canopy structure and differences in biomass both through plant succession and across areas with contrasting environmental conditions.

The interconnection of vertical structure and aboveground biomass creates an opportunity to estimate aboveground biomass using lidar (**li**ght **d**etecting **a**nd **r**anging) remote sensing. Lidar remote sensing has proven to be an efficient tool in the study of forest structure in a variety of forest environments (Nelson et al. 1988a, Magnussen et al. 1999, Means et al. 1999, Drake et al. In press). Because lidar instruments sample the vertical distribution of canopy (e.g., leaves and branches) and ground surfaces (Blair and Hofton 1999, Dubayah and Drake 2000, Dubayah et al. 2000, Harding et al. 2001) and because of ecological and biomechanical links between biomass and vertical structure (King and Loucks 1978, Oohata and Shinozaki 1979, O'Neill and DeAngelis 1981, Givnish 1986, Franco and Kelly 1998), several studies have found a strong correlation between lidar metrics and aboveground biomass

(Nelson et al. 1988a, Lefsky et al. 1999b, Means et al. 1999, Drake et al. In press).

In a recent study, Drake et al. (in press) found a strong, non-asymptotic linear relationship between canopy height metrics from lidar data and aboveground biomass in a dense, closed-canopy tropical forest. These results are encouraging because the broad scale estimation of aboveground biomass in tropical forests has been a difficult task. Previous remote sensing studies have shown that although passive optical and active radar sensors are sensitive to differences in aboveground biomass in young (0-15 years old) secondary forests, they are not as sensitive to differences in biomass in older, high-biomass primary forest areas (e.g., Luckman et al. 1997, Nelson et al. 2000, Steininger 2000).

The relationships that have been developed between lidar metrics and aboveground biomass (e.g., Means et al. 1999, Drake et al. In press) are site specific and there have been no attempts to compare relationships developed in areas with different environmental conditions. It is necessary to examine the generality of these relationships in different regions and biomes so that global terrestrial biomass estimates can be made using data from future airborne and spaceborne lidar instruments such as the Vegetation Canopy Lidar (Dubayah et al. 1997) and the Ice, Cloud, and Land Elevation Satellite (Schutz 1998).

Our primary goal in this study is to examine the relationship between lidar metrics and aboveground biomass in closed-canopy Neotropical forest areas with different annual precipitation amounts. We focus on a tropical wet forest (sensu Holdridge et al. 1971) area in Costa Rica, and on a tropical moist forest area in Panama that receives 50-75% less rainfall on average. Our first question is: do the relationships between lidar metrics and allometrically estimated aboveground biomass differ between the two study areas? Although biomass must be estimated from allometric relationships, basal area and mean stem diameter are precise, directly measured structural properties that are themselves often used to predict forest biomass (Brown 1997). Our second question therefore is: do relationships between lidar metrics and these directly measured forest structural characteristics (e.g., basal area) differ between the two study areas? We also are interested in looking for additional factors (e.g., environmental characteristics) that could help explain any differences in the relationships.

Methods

Study Areas

This study concentrates on field and lidar data collected in two areas of Central America. The first study area is the La Selva Biological Station in the Atlantic lowlands of northeastern Costa Rica (McDade et al. 1994). La Selva is a 1540 ha research facility that is comprised of a mixture of primary and secondary tropical forest, agroforestry, and current or abandoned pasture areas (Figure 4.1). This area receives approximately 4200 mm rainfall per year (Sanford Jr. et al. 1994, OTS 2001) and is classified as “tropical wet forest” according to the Holdridge classification method (Holdridge et al. 1971). In this study we report data from several primary and secondary forest and agroforestry sites (Table 4.1).

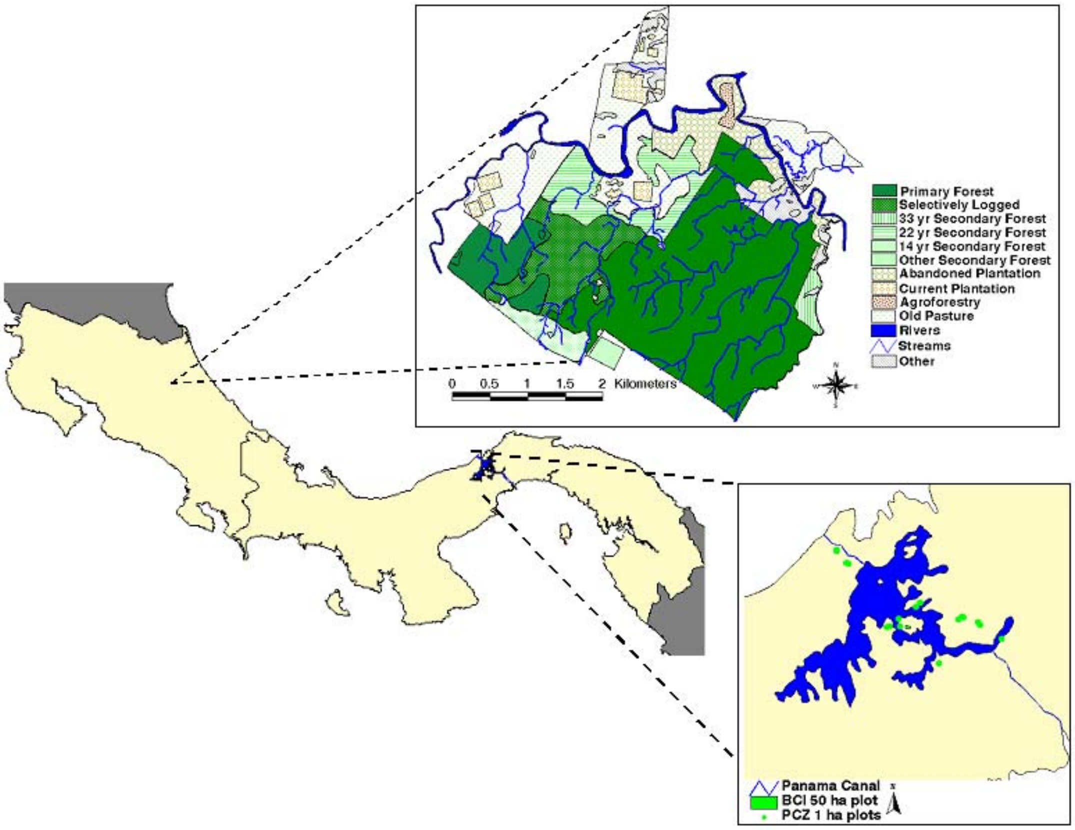

Figure 4.1 Locator maps for two study areas. The first study area was La Selva Biological Station in Northeastern Costa Rica. La Selva is a 1540 ha research facility comprised of pasture, agroforestry, secondary and primary tropical wet forest areas. The second study area was around the former Canal Zone in Panama. A series of 19 1 ha primary and secondary forest plots were included, as well as data from the 50 ha plot on Barro Colorado Island. The plots in Panama span a rainfall gradient from approximately 2000-3000 mm rainfall per year and are considered tropical moist forests.

Table 4.1 Forest structural summaries for all field data used in this study.

Study Site	**Land Cover Type**	**Number of Sites**	**Plot Size (ha)**	**Mean Quadratic Mean Stem Diameter (cm)**	**Mean Basal Area (m^2 ha^{-1})**	**Mean Estimated AGBM (Mg ha^{-1})**	**Related Study**
Barro Colorado Island, Panama	Primary Forest	25	1.0	28.16	26.27	286.77* (338.87)**	Condit (1998)
Panama Canal Zone Plots	Primary Forest	15	1.0	26.69	25.23	257.73* (295.46)**	Condit et al. (2000)
	Secondary Forest	4	1.0	24.35	26.89	277.91*	Condit et al. (2000)
La Selva Biological Station, Costa Rica	Primary Forest	18	0.5	20.76	23.6	160.5***	Clark and Clark (2000)
	31 yr Secondary Forest	1	0.3	22.24	26.71	147.7***	VCL****
	22 yr Secondary Forest	1	0.25	12.85	22.05	129.4***	Nicotra et al. 1999
	14 yr Secondary Forest	1	0.25	10.46	14.28	78.5***	Nicotra et al. 1999
	Agroforesty	6	0.12	9.03	14.48	34.3	Menalled et al. 1998

* Estimated aboveground biomass (Mg/ha) using general equation for tropical moist forests in Brown (1997)
** Including plots with trees whose diameters are greater than the largest tree used to develop the regression in Brown (1997)
*** Estimated aboveground biomass (Mg/ha) using general equation for tropical wet forests in Brown (1997)
**** Data collected as part of 1998 pre-launch VCL field campaign at La Selva

The second study area is centered on the Isthmus of Panama along the Panama Canal (Figure 4.1). This area spans a precipitation gradient ranging from approximately 2000 mm rainfall per year on the Pacific coast of Panama to 3000 mm rainfall per year on the Atlantic side (Condit et al. 2000, Pyke et al. In press) and is classified as lowland “tropical moist forest” (Holdridge et al. 1971). Within this broad area, we focus on a series of 1 ha plots distributed throughout this precipitation gradient (Pyke et al. In press), and on the 50 ha research site on Barro Colorado Island (Condit 1998).

Field data

Field data collected as a part of different ongoing field studies at each study area was used in this work (Table 4.1). In the Costa Rica study area, field data were collected in 18 0.5 ha primary forest plots (Clark and Clark 2000), and 3 secondary forest areas of 14, 22 (Guariguata et al. 1997, Nicotra et al. 1999) and 31 (Pierce 1992) years since abandonment as of March 1998. In addition, published data for 6 agroforestry plots (Menalled et al. 1998) were included among the Costa Rica study sites to correspond to an earlier study (Drake et al. In press).

At the Panama study area, field data were collected in the 1 ha research plots near the Panama Canal (the “Panama Canal plots” in Table 4.1, Pyke et al. In press). There were a total of 19 of these 1 ha plots that were sampled with the lidar instrument. Four of these sites are mature secondary forests, and the rest are primary forest (Table 4.1). The remaining field data in Panama were from the 50 ha plot on Barro Colorado Island (BCI, Condit 1998). In this case, the 50 ha plot was first divided into 50 1 ha square plots. Next, the spatial correlation length of the lidar metrics used in this study (metrics discussed below) was determined to be approximately 90-100 m (Figure 4.2) so every other 1 ha plot was discarded to maintain relative independence of the independent variable in the regression analysis. This left a total of 25 1 ha plots from BCI in a checkerboard pattern.

Within each of these primary and secondary forest plots at both study areas, stem diameters were measured in a marked location either at breast height or, when necessary, above buttressing (see methods in Condit 1998, Clark and Clark 2000). In the present study only stems with diameters greater than or equal to 10 cm were included, except for the 14 and 22 year old secondary plots at La Selva where all stems greater than 5 cm diameter were also included to correspond with an earlier study (Drake et al. In press).

Stem diameter measurements were used to estimate aboveground biomass values for each measured tree using general allometric equations (Brown 1997) for tropical wet forests (Equation 4.1) at the Costa Rica study area, and for tropical moist forests (Equation 4.2) at the Panama study area. Stem diameters were also used to calculate quadratic stem diameter (QMSD, Equation 4.3) and basal area (Equation 4.4) for each plot.

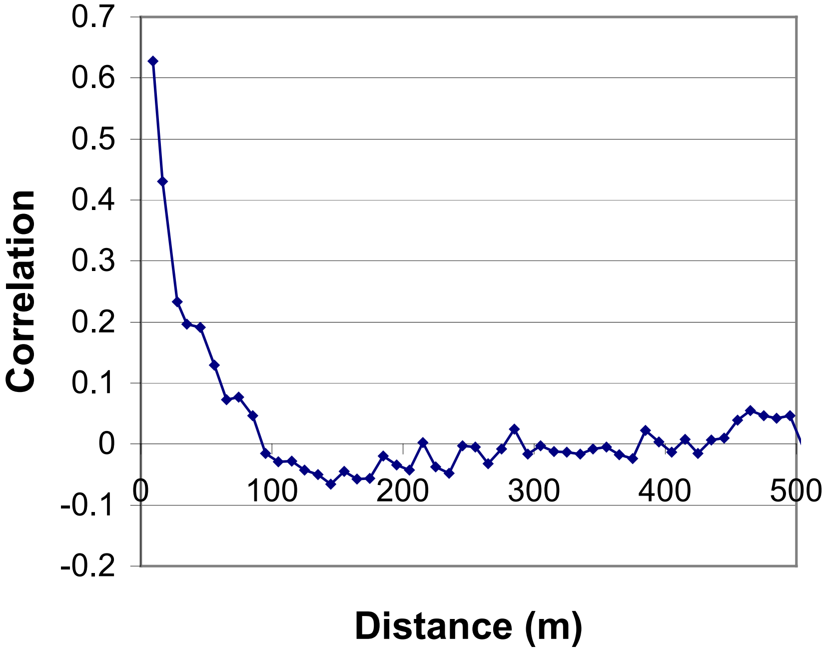

Figure 4.2 The correlation length of the lidar height of median energy metric at Barro Colorado was determined to be approximately 90-100 m.

Equation 4.1 $\mathbf{AGBM_s} = 21.297 - 6.953(\mathbf{D}) + 0.740(\mathbf{D}^2)$ where **D** is the stem diameter in cm, and **AGBMs** is the estimated oven-dried aboveground biomass for the stem in kg

Equation 4.2 $\mathbf{AGBM_s} = \exp(-2.134 + 2.530 * \ln(\mathbf{D}))$ where **D** is the stem diameter in cm, and **AGBMs** is the estimated oven-dried AGBM for the stem in kg, and "exp" means "*e* raised to the power of"

Equation 4.3 $\mathbf{QMSD} = \mathrm{sqrt}\ (\ (\Sigma\ (\mathbf{D}^2)/\mathbf{n})$ where **D** is the stem diameter in cm, n is the number of stems in the plot and **QMSD** is the quadratic mean stem diameter in cm

Equation 4.4. $\mathbf{BA} = \Sigma\ (\pi\ (\mathbf{D}/2)^2)$ where **D** is the stem diameter in *meters* and BA is the basal area (m^2) measured at breast height

Plot-level values of estimated aboveground biomass were then calculated by summing all estimated stem-level aboveground biomass values and converting to standard units (Mg/ha). Sixteen plots at the Panama study area contained stems whose diameters were larger than the maximum diameter used to develop the original allometric equation (Equation 4.2), therefore, only plots that contained stems within this regression range (<150 cm) were used in the regression analysis comparing lidar metrics with EAGB. However all plots were used in the regression analysis involving lidar metrics and QMSD or basal area.

Lidar data

Lidar data were collected over both study areas in March 1998 by the Laser Vegetation Imaging Sensor (LVIS, Blair et al. 1999, Dubayah et al. 2000). LVIS is an airborne scanning laser altimeter (Figure 4.3) designed and developed at NASA's Goddard Space Flight Center. LVIS measures the roundtrip time for pulses of near-infrared laser energy to travel to the surface and back. The incident energy pulse interacts with canopy (e.g., leaves and branches) and ground features and is reflected back to a telescope on the instrument. Unlike most other laser altimeters, LVIS digitizes the entire time-varying amplitude of the backscattered energy (in 30 cm vertical bins). This yields a "waveform" or profile related to the vertical distribution of intercepted surfaces from the top of canopy to the ground (see Figure 4.3 and Blair et al. 1999, Dubayah and Drake 2000, Dubayah et al. 2000).

In this study, a footprint size of approximately 25 m in diameter was used. This exceeds the average crown diameter of large emergent trees in closed-canopy tropical forests (King 1996, Richards 1996) and thereby consistently allows lidar energy to reach the ground through inter-crown gaps (Dubayah et al. 1997). LVIS scanned across a swath of approximately 1 km with a 50% overlap of footprints across swath, and contiguous along-track footprint spacing (Figure 4.3). LVIS footprints can be geolocated to within 2 meters (Blair and Hofton 1999). At both study areas, only LVIS footprints that were entirely coincident with field plots were included.

For the LVIS observations that fell within each field plot some were eliminated according to two different filtering rules. First, if the total energy

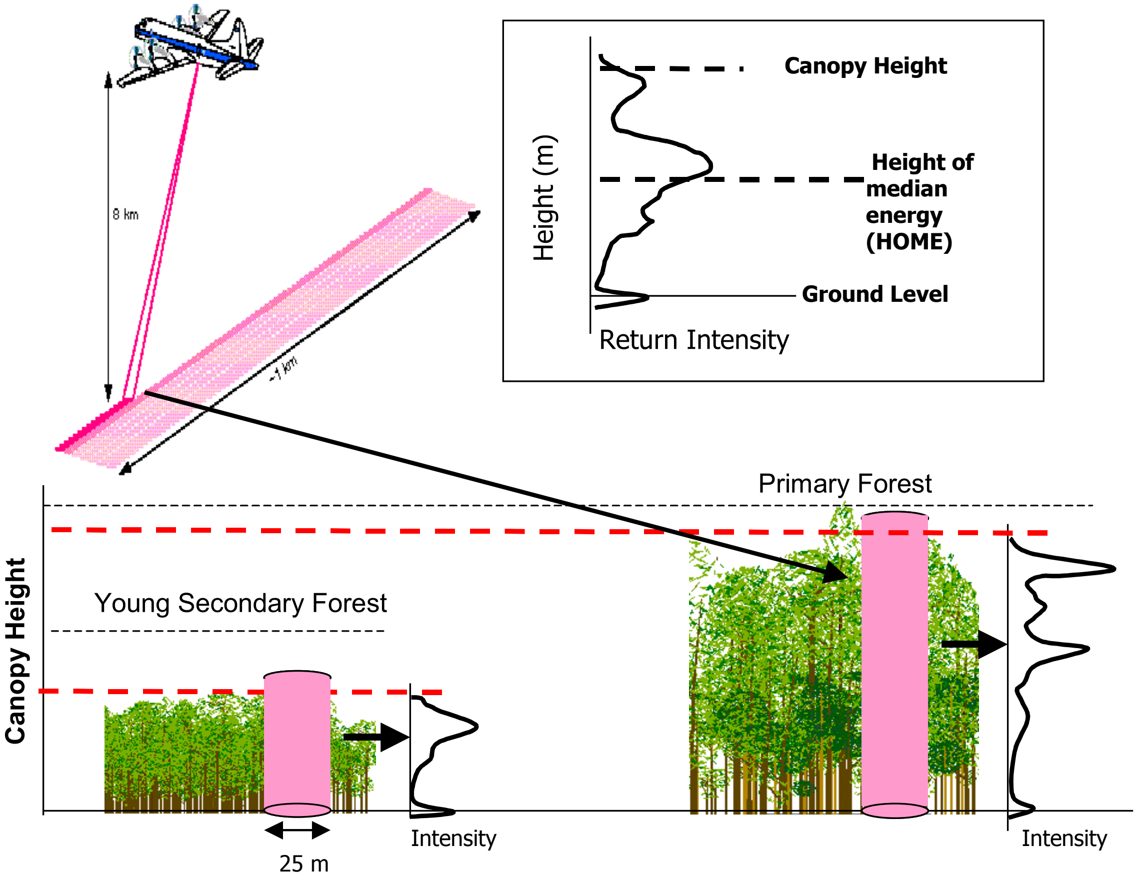

Figure 4.3 The scanning airborne Laser Vegetation Imaging Sensor (LVIS) was flown over both study areas. LVIS digitizes waveforms related to the vertical distribution of canopy and ground surfaces within each 25 m diameter footprint. Canopy height and the height of median energy (HOME) metrics were calculated for all LVIS shots.

received at the instrument was less than 10% of the mean total energy for all shots, and the shot elevation was greater than 200 m higher than the lowest elevation for the plot then the shot was eliminated. This filter was used to remove only shots that were reflected off of clouds. Second, if the last portion of the waveform did not return to the background noise level for the shot (plus one standard deviation) the shot was eliminated. This eliminated shots whose ground returns were obviously not recorded. Together these filters removed approximately 30% of all LVIS shots.

Two metrics were derived from the LVIS waveforms. First, canopy height was calculated by identifying the location within the waveform where the signal initially increases above the mean background noise level (the canopy top). Next the ground return is identified as the center of the last gaussian pulse. The canopy height is then the distance between these two locations.

The other lidar metric, height of median energy (HOME), is calculated by first identifying the location of the median of the entire signal (i.e. above the noise level), including the energy from both canopy and ground surfaces (Drake et al. In press). This location is then referenced to the ground to derive a height. The HOME metric is therefore influenced by both the vertical distribution of canopy elements (Drake et al. In review) and the canopy cover because in more open canopies a greater proportion of the lidar energy is reflected from the ground thus lowering the HOME metric. Plot-level means for canopy height and HOME were then calculated for all shots that fell within each plot.

Adjustment of Lidar HOME for Deciduousness in Panama

The Costa Rica study area receives approximately 4200 mm rain/year and is in the tropical wet forest life zone (Holdridge et al. 1971). The leaf loss from canopy trees at La Selva was minimal when the lidar flights occurred in mid-March 1998. In contrast, the Panama study area spans a rainfall gradient from approximately 2000-3000 mm rain/year. When the lidar flights occurred in late March 1998, this area was at the end of its dry season and leaf loss from canopy-forming trees was extensive in some areas. As a result, more of the lidar energy was able to penetrate through the upper canopy, thereby reducing the lidar HOME metric relative to the Costa Rica study area. To compensate for this effect, a proportional adjustment to the HOME metric was made based on the estimated fraction of crown area that was deciduous (FCAD). The first step was to linearly interpolate between data points for precipitation and the fraction of crown area deciduous as listed in Condit et al. (2000). The relationship (Equation 4.5) was then used to interpolate FCAD from average precipitation values for all Panama field plots. Lidar HOME was then proportionally adjusted in these Panama plots by the fraction of crown area deciduous using the relationship in Equation 4.6.

Equation 4.5 **FCAD**= -0.02 ***Rainfall** + 60.27 where **Rainfall**=mm/yr and **FCAD**= fraction of crown area deciduous (developed from Condit et al. 2000)

Equation 4.6 **HOME′** = **HOME**/(1-**FCAD**) where HOME= lidar height of median energy (m) and **FCAD**= fraction of crown area deciduous

Data Analysis

A linear regression analysis was used to develop relationships between plot-level averages of lidar metrics and field-derived QMSD, basal area and EAGB for each study area. The lidar metric that was the best single predictor was then identified. For each forest structural characteristic (e.g., QMSD), an analysis of covariance (ANCOVA) was then performed to test for significant differences in the slope and intercept of the relationships (Zar 1996) developed for each site. This process was used for both the normal and deciduous adjusted HOME metrics.

Results

General Site Characteristics

Primary and secondary forest sites in Panama have a larger quadratic mean stem diameter (QMSD), basal area and estimated aboveground biomass on average than the corresponding primary and secondary field sites in Costa Rica (Table 4.1). Of these forest structural characteristics, the difference in mean basal area between the two sites is the least, at approximately 10% for primary forest plots, followed by an approximately 30% larger QMSD in the plots at the Panama study area. The largest difference is for estimated aboveground biomass, which is approximately 70% larger in the Panama plots that fall within the range of the general allometric equation (Equation 4.2), and 95% larger for all the Panama plots (including those outside the range) than primary forest plots in the Costa Rica study area. The mean estimated aboveground biomass value for BCI that we calculated using Equation 4.2 (287 Mg/ha) corresponds well with a mean of 290 Mg/ha reported in Chave et al. (In preparation) using an equation that includes stem diameter, height and wood density.

The difference between lidar metrics from both study areas (Table 4.2) was not as large. Lidar canopy heights were on average approximately 5% larger in primary forest plots in Panama compared to the Costa Rican plots. The differences between lidar height of median energy (HOME) values were on average less than 2%, as both were approximately 20 m.

Relationship between lidar HOME and allometrically estimated aboveground biomass

The lidar metric HOME is highly correlated with estimated aboveground biomass (EAGB) in both study areas (Figure 4.4). In the Panama study area, the R^2 value is 0.66 for plots whose tree diameters are all within the range of the general allometric equation (Equation 4.2), and 0.82 for all Panama plots, with RMSE values of 31.52 Mg/ha and 39.10 Mg/ha respectively. For the Costa Rica relationship, the R^2 value is 0.89 and the RMSE is 22.54 Mg/ha.

Although the R^2 value is greater for the Costa Rica relationship, the “relative regression error” (RMSE divided by mean) is slightly lower for the Panama relationship compared to the Costa Rica relationship (11.5% and 14.06% respectively, Table 4.3). Thus, both the Panama and Costa Rica regression relationships are similar in terms of proportional errors in aboveground biomass estimates. In addition, the relative regression errors for

Table 4.2 Summaries for all lidar data used in this study.

Study Site	Land Cover Type	Number of Sites	Plot Size (ha)	Mean Number of Shots per Plot	Mean Lidar Height (m)	Mean Height of Median Energy (HOME) (m)
Barro Colorado Island, Panama	Primary Forest	25	1.0	29	34.93	20.29
Panama Canal Zone Plots	Primary Forest	15	1.0	13	31.28	19.16
	Secondary Forest	4	1.0	12	29.77	18.41
La Selva Biological Station, Costa Rica	Primary Forest	18	0.5	9	31.33	20.14
	31 yr Secondary Forest	1	0.3	8	25.48	16.65
	22 yr Secondary Forest	1	0.5	6	17.68	11.32
	14 yr Secondary Forest	1	0.5	7	23.67	9.21
	Agroforesty	6	0.12	3	9.47	1.68

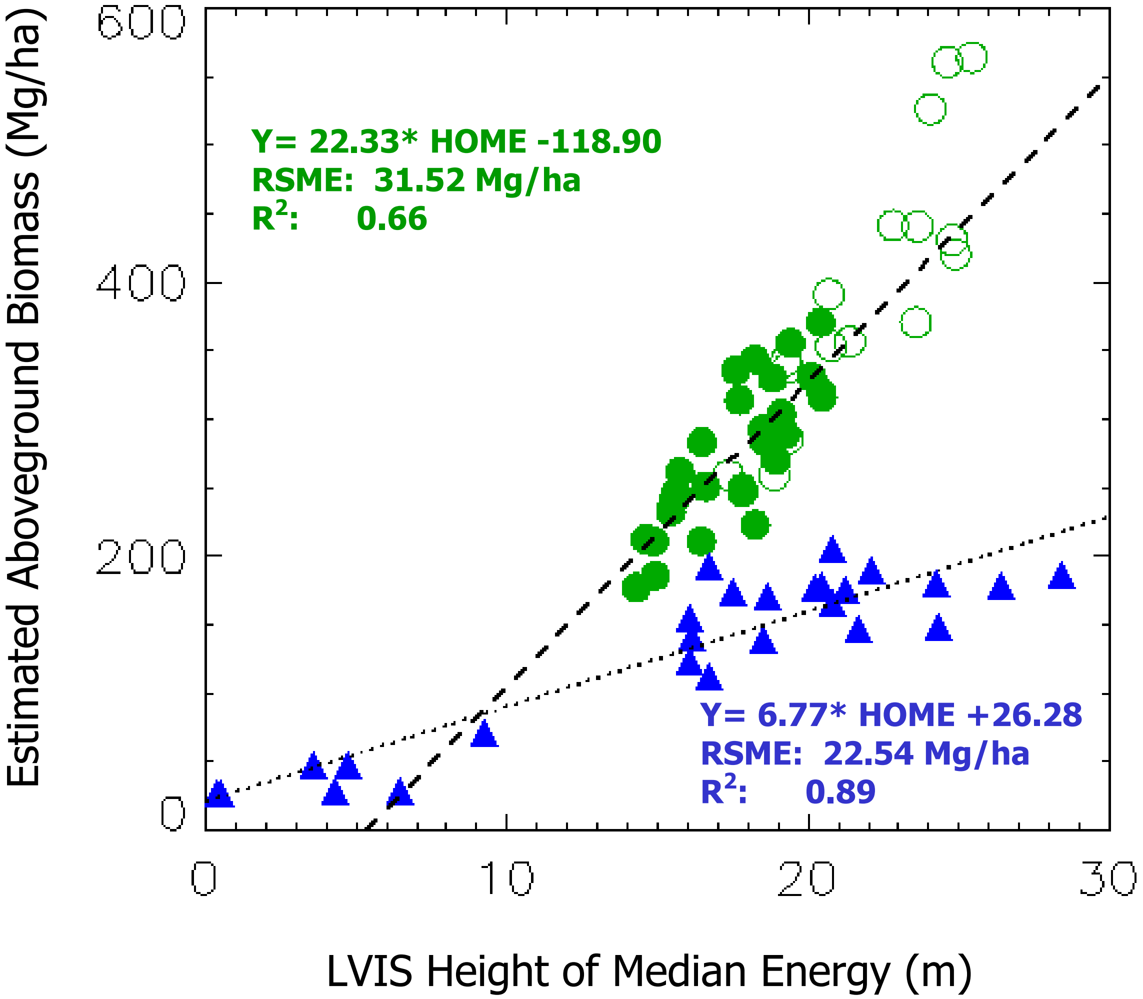

Figure 4.4 Regression analysis for lidar height of median energy (m) vs. plot-level allometrically estimated aboveground biomass (Mg/ha) for study areas in Panama (circles, dashed line, upper left equation) and Costa Rica (triangles, dotted line, lower left equation). The open circles in the Panama regression relationship indicate plots that contain stems whose diameters are larger than the original distribution sampled to develop the allometric equation (equation 4.2) and were not included in the regression analysis.

Table 4.3 Coefficients of variation in forest structural characteristics and the relative regression errors from lidar equations for study sites in Panama and Costa Rica

Forest Structural Characteristic	Panama CV	Panama Relative Regression Error*	La Selva CV	La Selva Relative Regression Error*
Quadratic Mean Stem Diameter	11.83	6.94 (6.59**)	9.60	8.77
Basal Area	16.44	8.95 (9.89**)	11.94	12.87
Estimated Aboveground Biomass	19.25 (28.94**)	11.50 (12.27***) (11.36**)	14.01	14.06

*Relative regression error = RMSE/ mean

**With leafdrop-modified lidar height of median energy.

*** Including plots with trees whose diameters are greater than the largest tree used to develop the regression in Brown (1997) both relationships are at or below the coefficient of variation (CV) for EAGB (Table 4.3).

In other regards however, there is a great deal of divergence between the relationships for the two study areas (Figure 4.4). The slope is much greater in the Panama relationship (22.33) compared to the Costa Rica relationship (6.33). The Panama regression equation also has a negative intercept, probably the result of only sampling within relatively high biomass areas. An analysis of covariance (ANCOVA) shows that the slopes and intercepts of these two equations are significantly different ($p<0.01$).

The regression lines from Figure 4.4 show that there is a great deal more EAGB in the Panama study area for any lidar HOME above 9 m. To some degree this is expected because although mean EAGB is approximately 70% higher in Panama primary forest plots, the lidar HOME is essentially the same (Tables 4.1 and 4.2). However, the differences in mean QMSD and basal area between the two study areas are smaller than the differences between mean aboveground biomass. Although aboveground biomass must be estimated using allometric relationships, both QMSD and basal area are directly measured, relatively precise quantities. This raises the next question that we address: do relationships between lidar metrics and forest structural summaries that are not allometrically estimated also differ between the two study areas?

Relationship between Lidar HOME and Directly Measured Structural Summaries

Lidar HOME is strongly correlated with quadratic mean stem diameter (QMSD) in both study areas (Figure 4.5). The level of variation in QMSD explained by the HOME metric (i.e., the R^2 value) is approximately 92% in the Costa Rica study area compared to 66% in the Panama study area. However, the RMSE in Panama (1.89 cm) is somewhat lower than the value from the Costa Rica relationship (2.09 cm). In addition, the relative regression errors for both relationships are smaller than the CV in QMSD for the respective sites (Table 4.3)

HOME is also strongly correlated with basal area in both areas (Figure 4.6). In this case the level of variation explained is approximately equal for both areas (~70%). The relative regression error (Table 4.3) from the Panama relationship (9%) is smaller than in the Costa Rica relationship (12.9%). In this case the relative regression error from the Panama relationship is smaller than the CV for basal area (16.4%), however the relative regression error from the Costa Rica relationship is slightly larger than the CV for basal area (11.9%).

The relationships between lidar HOME and QMSD (Figure 4.5) and between HOME and basal area (Figure 4.6) are not as divergent at the two study areas as were the relationships between HOME and EAGB (Figure 4.4). The slopes of the relationships between HOME and QMSD are similar at both sites, and were not found to be significantly different ($p=0.55$) in an ANCOVA analysis. Intercepts for the HOME-QMSD relationships, however, were found to be significantly different ($p<0.01$), indicating that the relationships are not

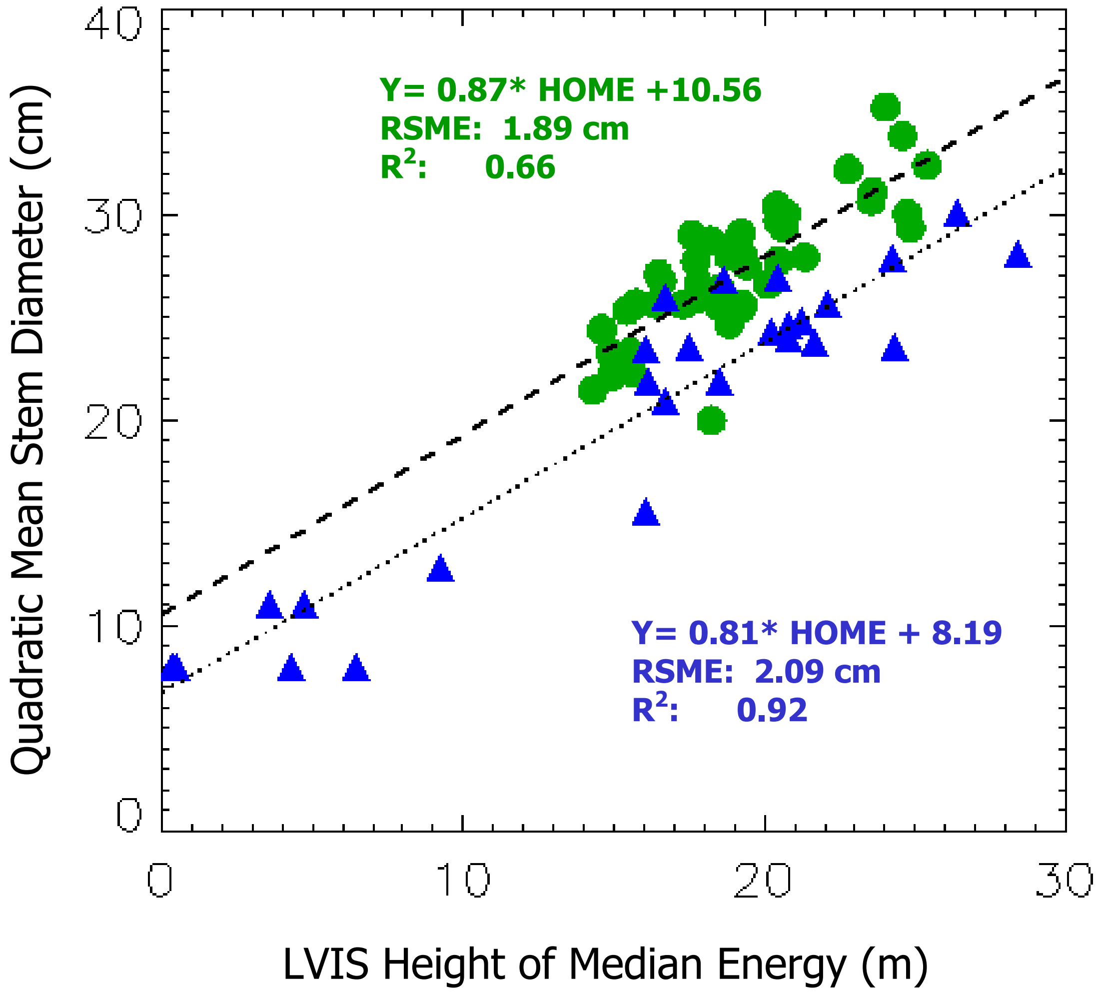

Figure 4.5 Regression analysis for lidar height of median energy (m) vs. plot-level quadratic mean stem diameter (cm) for study areas in Panama (circles, dashed line, upper left equation) and Costa Rica (triangles, dotted line, lower left equation).

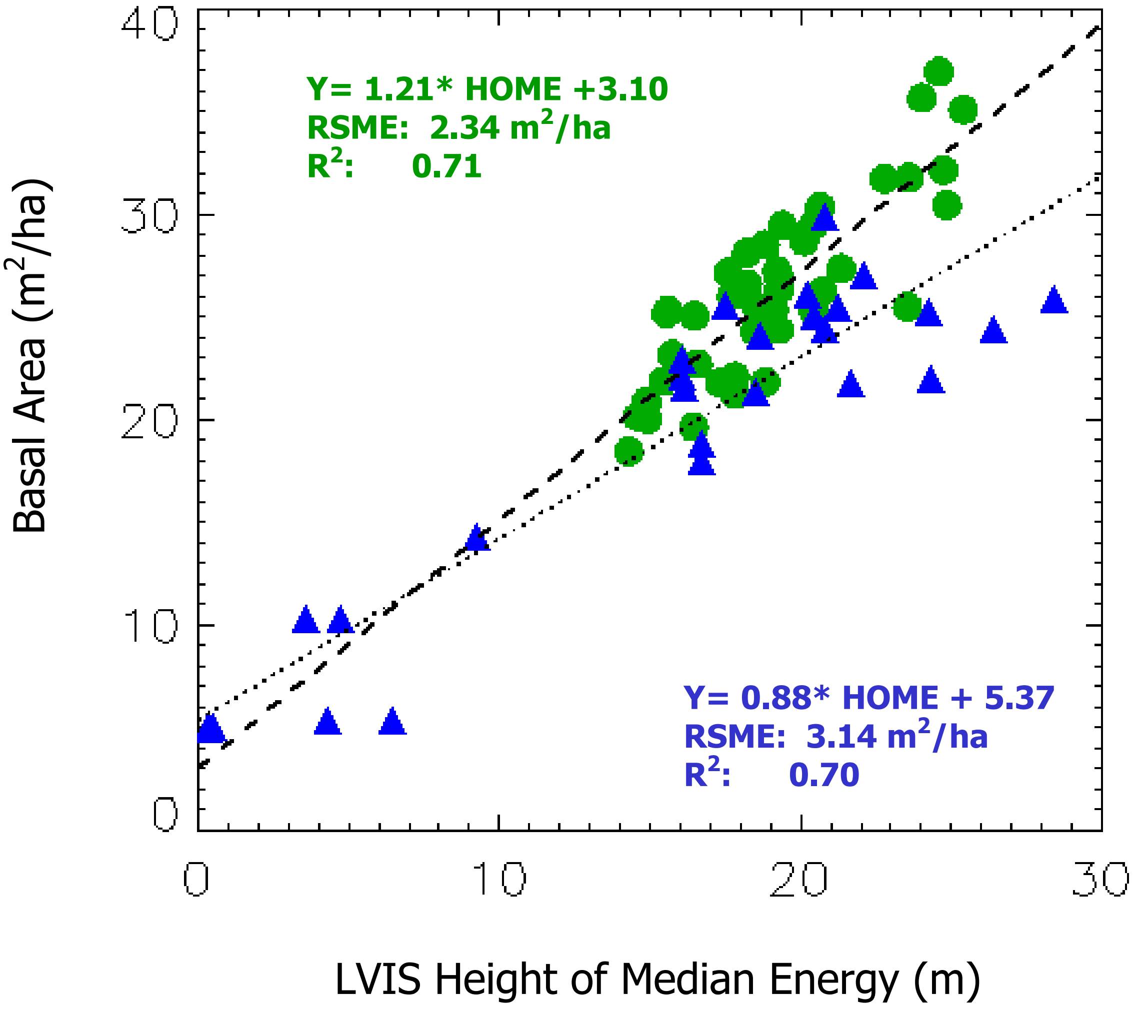

Figure 4.6 Regression analysis for lidar height of median energy (m) vs. plot-level basal area (m^2/ha) for study areas in Panama (circles, dashed line, upper left equation) and Costa Rica (triangles, dotted line, lower left equation).

equivalent between study sites. Similarly, both the slopes and the intercepts of the HOME-basal area relationships were found to be significantly different between the two study areas, however it should be noted that the y-intercept term in the Panama linear regression relationship was not significantly different from zero (p=0.19).

The differences in these relationships show that the Panama plots have a greater QMSD and more basal area for the same median height (lidar HOME). Again, from the field and lidar summary statistics (Tables 4.1 and 4.2) this is anticipated because although the mean basal area and QMSD are higher in the Panama plots, the lidar HOME is approximately the same.

There are two possible reasons for differences in the lidar HOME- basal area and HOME-QMSD relationships between study areas. First, tree diameters could be larger for a given tree height on average at Panama. An analysis of the relationship between stem diameter and stem height from both Panama (based on allometry from BCI in Bohlman et al. In review*)* and La Selva supports this trend (Figure 4.7). It is possible that this individual-level relationship could influence the plot-level relationships between lidar HOME and either basal area or QMSD. A second possible explanation is that the drier conditions at Panama resulted in more leaf loss, which in turn lowered lidar HOME values. The HOME metric is determined by the vertical distribution of canopy elements (e.g., leaves and branches), therefore a reduction in leaf abundance of canopy-forming trees in drought-deciduous areas (Condit et al. 2000) would allow more energy to penetrate further into the canopy, thereby

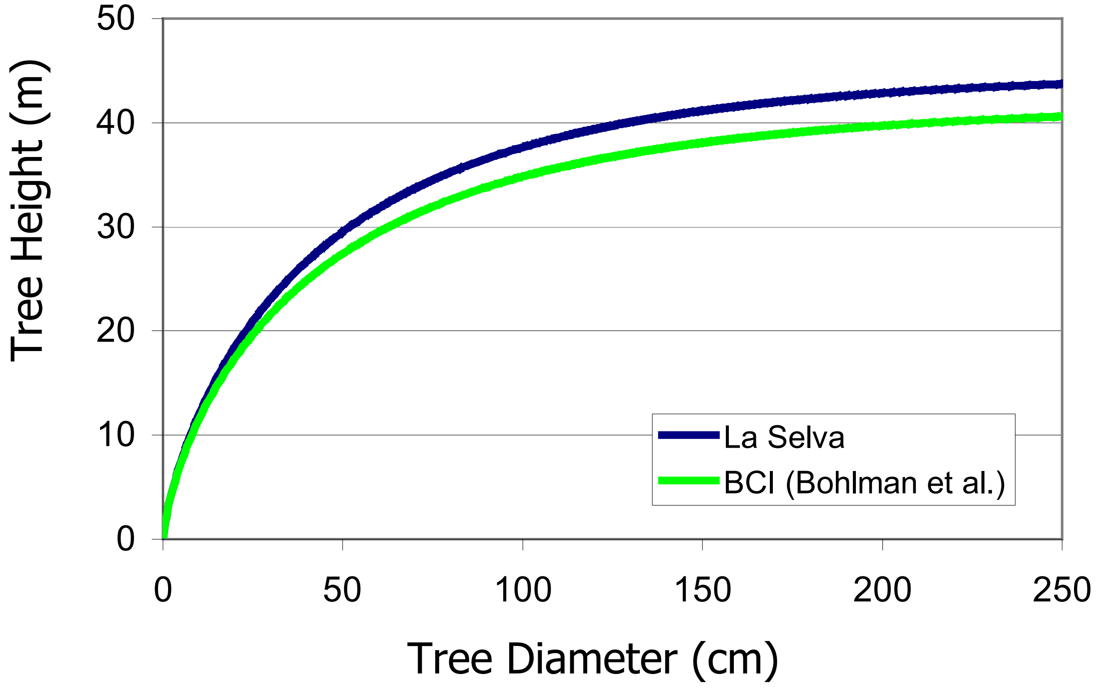

Figure 4.7 Relationship between tree stem diameter and height at La Selva Biological Station, Costa Rica (dark line) and at Barro Colorado Island, Panama (light line). The relationship at Barro Colorado Island is from Bohlman et al. (in review). The relationship at La Selva is from the primary forest plots (Clark and Clark 2000) and is adapted from Drake et al. (in review).

lowering the HOME value. We therefore next examine the effect of this deciduousness on the relationship between HOME and forest structural summaries.

Relationship between Deciduous-adjusted Lidar HOME and Directly Measured Structural Characteristics

The proportional adjustment of HOME for the effect of leaf loss of canopy trees preserved the strength of the relationships between HOME and QMSD (Figure 4.8) and between HOME and basal area (Figure 4.9). The level of variation in basal area that is explained with HOME decreased slightly (from 70% to 65%), whereas the R^2 value for the HOME-QMSD relationship increased slightly (from 0.66 to 0.7). More importantly, after adjustment the relationships are much more similar between the two study areas.

The differences between the slope and the intercept from both HOME′-QMSD relationships are not significantly different using an ANCOVA test ($p=0.85$ and 0.21 respectively). Similarly, the difference in slope from the HOME′-basal area relationships in the two study areas is smaller and not significantly different ($p=0.06$). The intercepts in the HOME′-basal area relationships were found to be significantly different ($p<0.01$). Nonetheless, where the data cover the same range of HOME′ and basal areas, the two point clouds now overlap more completely and appear similar (Figure 4.9).

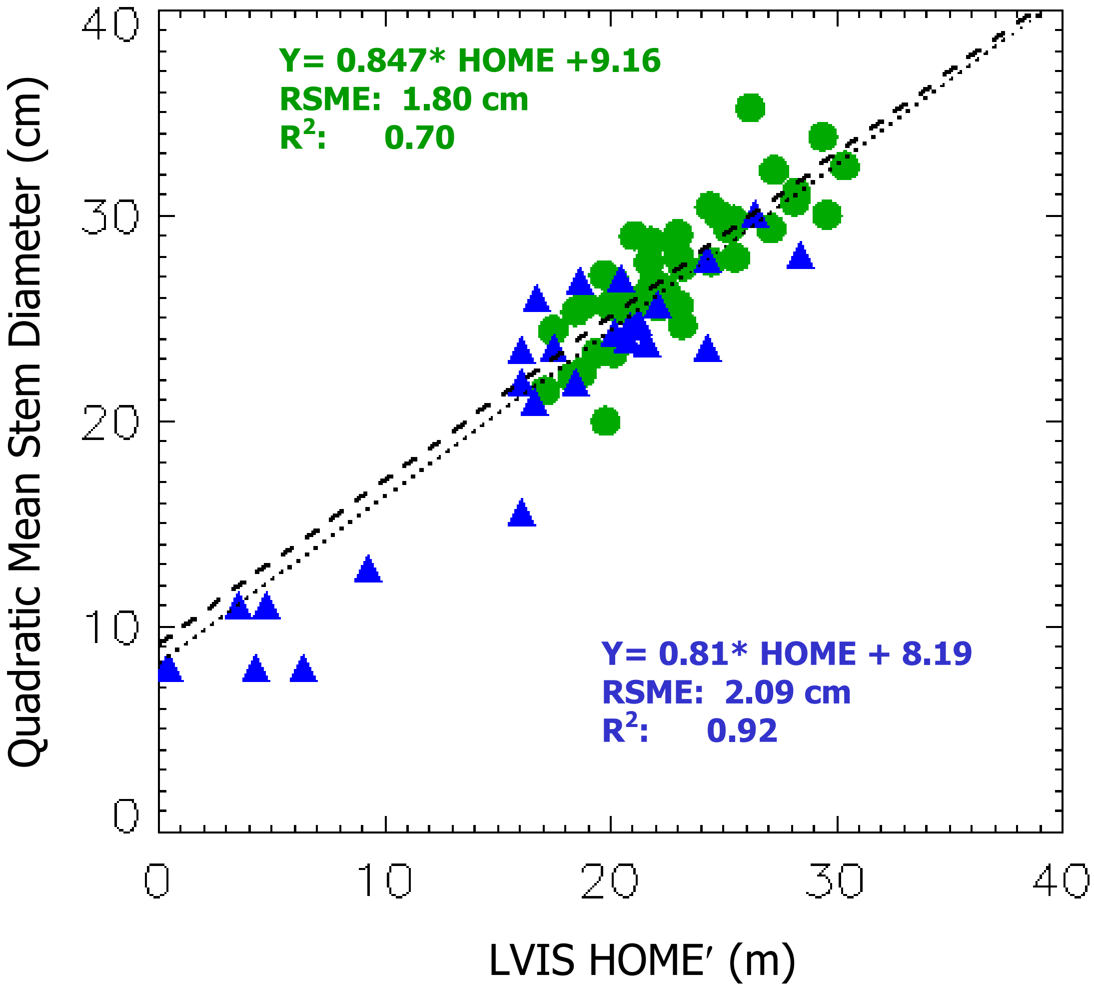

Figure 4.8 Regression analysis for deciduous-adjusted lidar height of median energy (m) vs. plot-level quadratic mean stem diameter (cm) for study areas in Panama (circles, dashed line, upper left equation) and Costa Rica (triangles, dotted line, lower left equation).

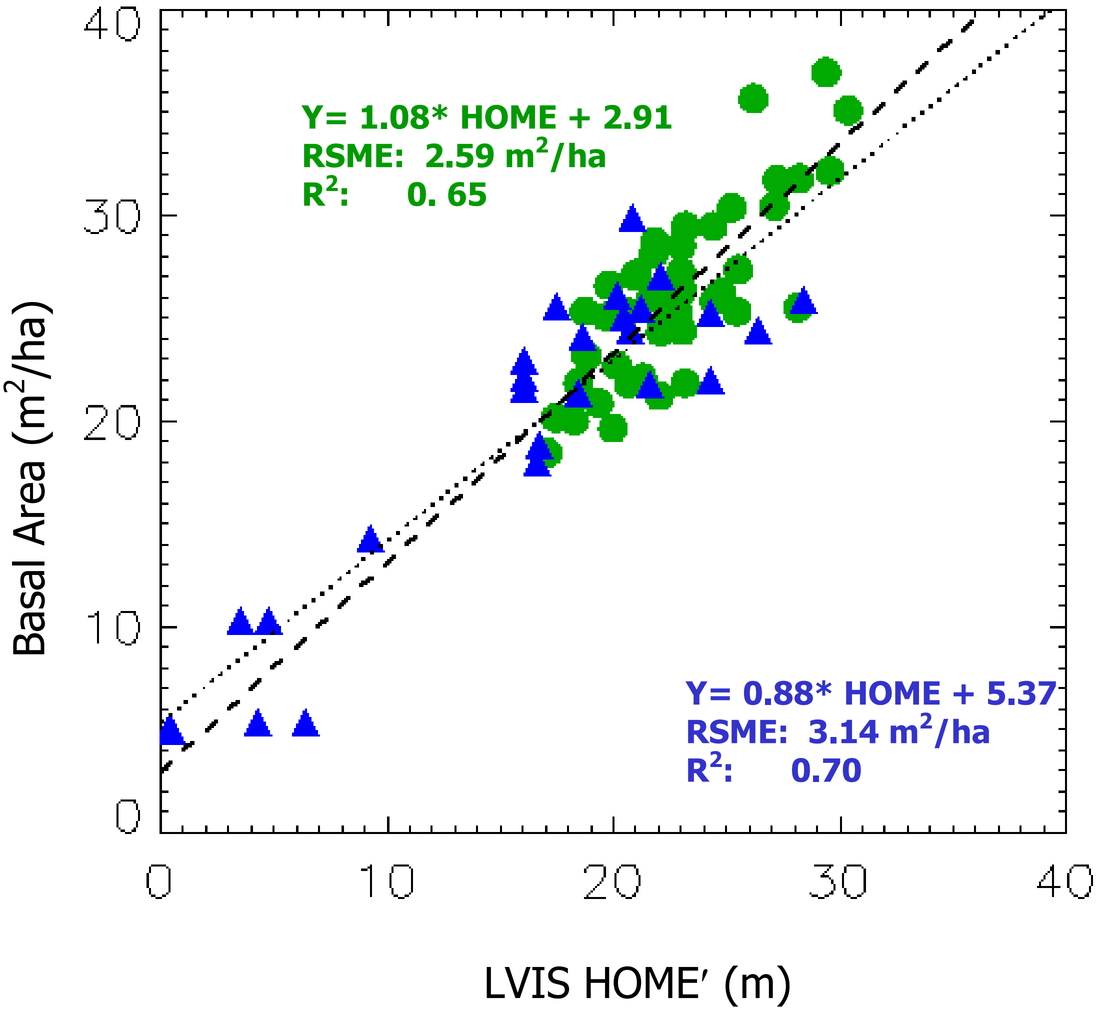

Figure 4.9 Regression analysis for deciduous-adjusted lidar height of median energy (m) vs. plot-level basal area (m^2/ha) for study areas in Panama (circles, dashed line, upper left equation) and Costa Rica (triangles, dotted line, lower left equation).

Thus, proportional adjustment of lidar HOME metrics by simple fraction of crown area deciduous values eliminated much of the difference between HOME-basal area and HOME-QMSD relationships at both Costa Rica and Panama plots. The minor remaining differences may be the result of small differences in diameter vs. height relationships in both study areas (Figure 4.7) or a difference in the ranges of conditions studied combined with a modest nonlinearity in the underlying causal relationship. In either case, leaf loss in canopy trees at the end of the dry season in Panama was responsible for much of the difference between relationships in these two tropical regions that we found with unadjusted lidar data.

Relationship between Deciduous-adjusted Lidar HOME and Allometrically Estimated Aboveground Biomass

As with the directly measured variables, the adjustment in HOME also did not greatly affect the strength of the relationship between HOME and EAGB at the Panama study area (Figure 4.10). The R^2 and the RMSE stayed approximately the same (66% and ~31Mg/ha respectively) after HOME values were adjusted. In contrast, although the adjustment did slightly reduce the slope of the Panama relationship (from 22.33 to 21.46), the relationships from the two study areas were still significantly different in both slope and the intercept ($p<0.01$, from ANCOVA).

The differences in relationships between HOME′ and EAGB for the two study areas can be linked to two factors. First, the individual-level diameter vs. height allometric relationships are slightly different for the two study areas.

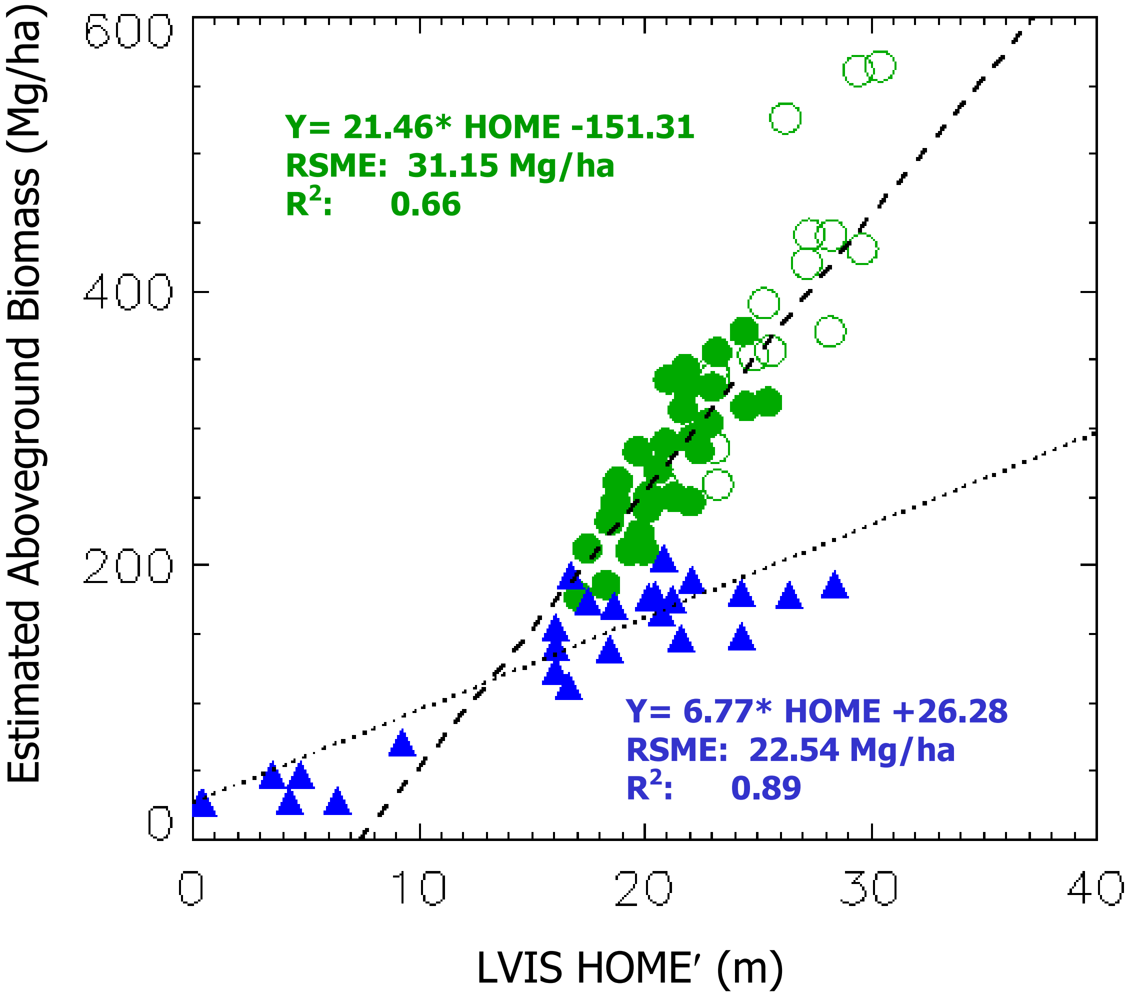

Figure 4.10 Regression analysis for deciduous-adjusted lidar height of median energy (m) vs. plot-level allometrically-estimated aboveground biomass (Mg/ha) for study areas in Panama (circles, dashed line, upper left equation) and Costa Rica (triangles, dotted line, lower left equation). The open circles in the Panama regression relationship indicate plots that contain stems whose diameters are larger than the original distribution sampled to develop the allometric equation (Equation 4.2) and were not included in the regression analysis.

As mentioned earlier, the result of this effect is that for a given tree height, trees in Panama are predicted to have a slightly greater diameter on average than trees in the Costa Rica study area (Figure 4.7). The second, and more important, cause for differences between the two study areas is the effect of using different allometric equations to estimate aboveground biomass from stem diameter. At the same total basal area, Panama sites are calculated to have much larger biomass than nearly all similar sites in Costa Rica (Figure 4.11). This is despite having only minor differences in HOME-QMSD (Figure 4.8) and HOME-basal area (Figure 4.9) relationships after adjustment for leaf loss. As a result, sites at Panama and Costa Rica with nearly identical basal areas and HOME′ values may have very different EAGB values.

Discussion

Lidar remote sensing has shown promise for the estimation of aboveground biomass in a variety of temperate and tropical forests (e.g., Means et al. 1999, Drake et al. In press). In these studies, different metrics from large-footprint lidar waveforms (normal or transformed to account for attenuation and absorption of lidar energy through the canopy) have been used to predict aboveground biomass. However, the generality of relationships between lidar metrics and aboveground biomass remained untested. This study provides an initial assessment of the generality of the relationships between lidar metrics and aboveground biomass in closed-canopy Neotropical forests.

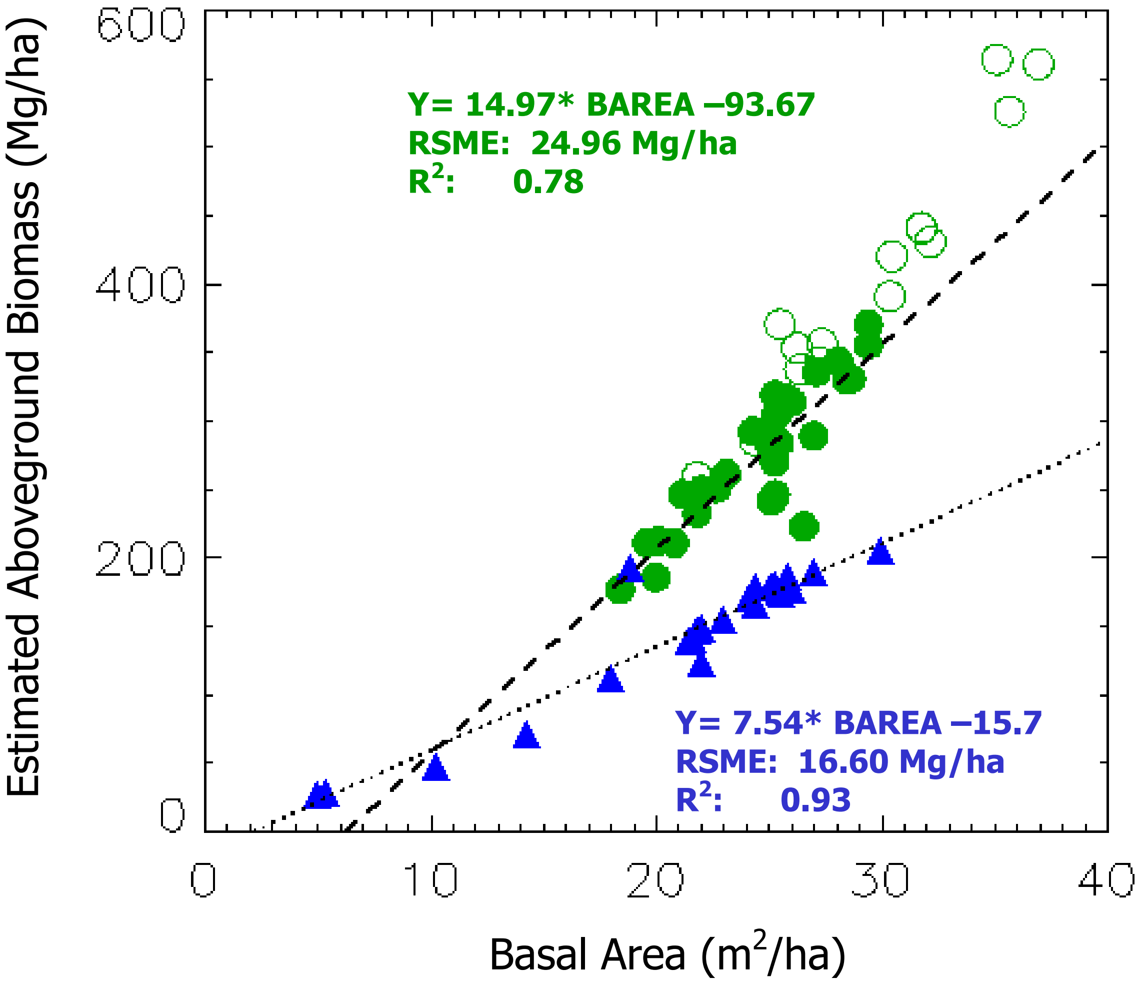

Figure 4.11 Regression analysis for plot-level basal area (m^2/ha) vs. plot-level allometrically estimated aboveground biomass (Mg/ha) for study areas in Panama (circles, dashed line, upper left equation) and Costa Rica (triangles, dotted line, lower left equation). The open circles in the Panama regression relationship indicate plots that contain stems whose diameters are larger than the original distribution sampled to develop the allometric equation (Equation 4.2) and were not included in the regression analysis.

Our results show that relationships between a simple lidar metric (height of median energy) and directly measured forest structural characteristics, such as basal area and QMSD, are nearly identical at both Costa Rica and Panama study areas after accounting for the extensive leaf loss of canopy-forming trees in Panama during the study period (Figures 4.8 and 4.9). There is still a subtle difference in the HOME′-basal area relationships from the two study areas that could be attributable to differences in the individual-level diameter vs. height allometric relationships for the two sites. Nevertheless, these results illustrate that the same lidar metric, HOME, is strongly correlated with basal area and QMSD. In addition, the relationships appear to be general across both tropical wet and tropical moist forest life zones.

The relationships between lidar metrics and allometrically estimated aboveground biomass are significantly different, however, for these two study areas. Although adjustment for leaf loss slightly improved the agreement between the two site-specific relationships, the two different allometric equations (Equations 4.1 and 4.2) used to estimate aboveground biomass lead to significant differences at both study areas. If instead the same allometric equation (e.g., the tropical wet forest equation; Equation 4.1) is applied in both study areas the relationships between HOME′ and EAGB are no longer distinct (Figure 4.12). Estimated aboveground biomass values for the Panama plots fall entirely within the data envelope of the relationship between HOME′-EAGB for the Costa Rica plots. This demonstrates that the differences in the lidar-biomass relationships at the two study areas are primarily the result of the two allometric relationships used to estimate aboveground biomass.

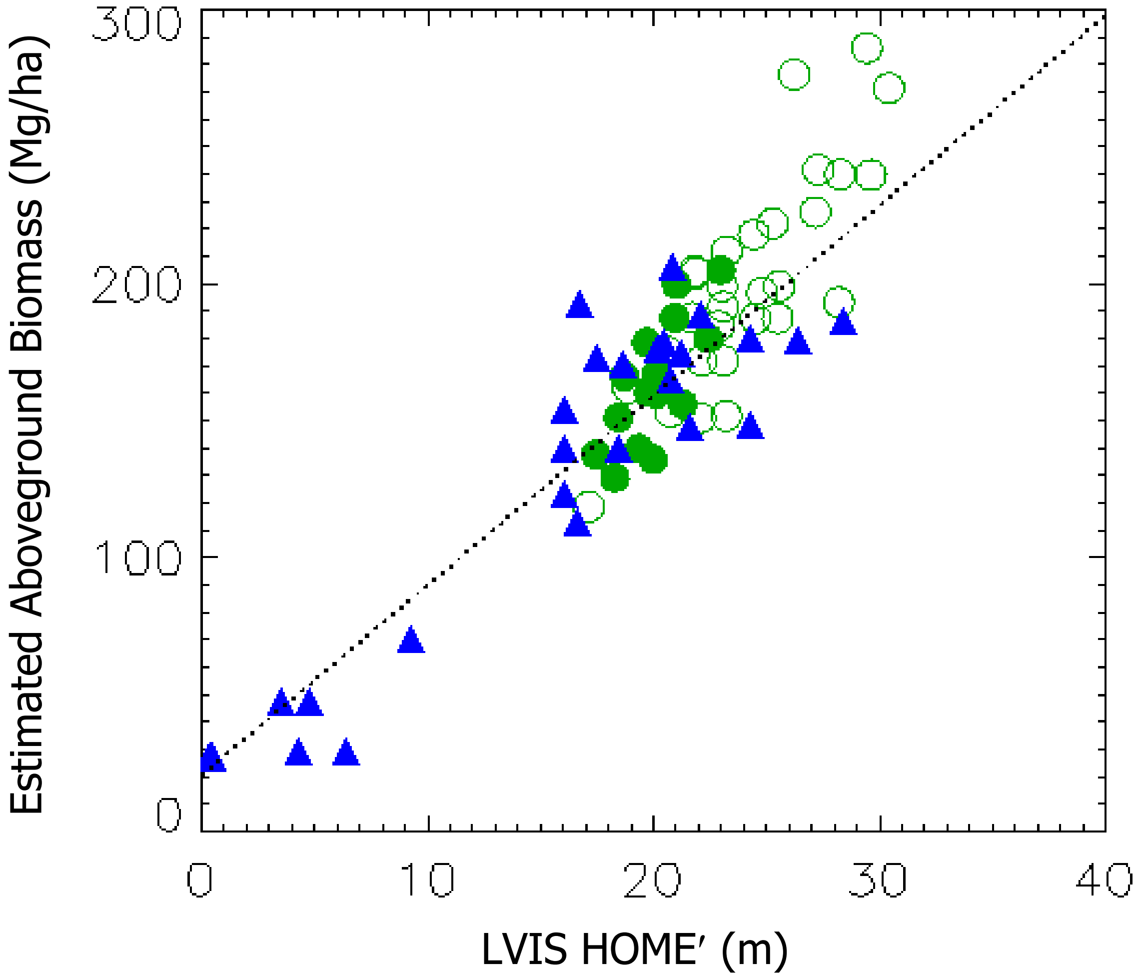

Figure 4.12 Deciduous-adjusted lidar height of median energy vs. plot-level aboveground biomass estimated using only the tropical wet forest allometric equation (Equation 4.1) for study areas in Panama (circles) and Costa Rica (triangles). The open circles indicate plots in the Panama study area that contain stems whose diameters are larger than the original distribution sampled to develop the allometric equation (Equation 4.2).

This effect of using contrasting allometric equations is also illustrated in the relationships between field-measured basal area and EAGB for the two study areas (Figure 4.11), where primary forest plots of the same basal area (approximately 20-30 m^2/ha) are estimated to contain approximately 50-70% more aboveground biomass in the Panama tropical moist forests plots than in the Costa Rica tropical wet forest plots. Because some sites in these two study areas have approximately the same basal area and median height (or HOME′), as evidenced in Figure 4.9, one of the only remaining variables that could contribute to such a large difference in aboveground biomass at the two study areas is wood density. The question remains: are stems in tropical moist forest areas actually 50-70% denser on average than those in tropical wet forest areas? In other words, for the same basal area and lidar height of median energy do tropical moist forests contain 50-70% more carbon than tropical wet forests?

Because remotely sensed estimates of biomass (and carbon) are ultimately dependent on allometric relationships, an assessment of the applicability of these general allometric equations vs. locally-derived allometric equations (cf. Keller et al. In Press) would be beneficial. The general allometric equations (Equations 4.1 and 4.2) for each respective life zone were developed from approximately 170 destructively sampled trees in different areas (Brown 1997). Although the divergence between tree biomass estimates from each life zone is much greater for large trees (Brown 1997), the number of these large, high-biomass trees that have been sampled is low. For the tropical wet forest equation (Equation 4.1) 26 trees with stem diameters greater than 70 cm were sampled, and for the tropical moist equation (Equation 4.2) only 5 trees greater than 70 cm diameter were sampled (Brown 1997). Further, the largest tree sampled to develop the tropical moist forest equation had a stem diameter of 148 cm, whereas the largest tree diameter sampled in the Panama study area was 220 cm. We therefore join with other authors (Brown et al. 1995, Clark and Clark 2000) who have called for more destructive sampling, especially of large trees, in different tropical life zones to more rigorously assess the robustness of general allometric equations. Ultimately, this will allow for better broad-scale, remotely sensed aboveground biomass estimates.

Assuming that the general allometric equations used in this study are reasonably accurate, these results have significant implications for how global observations from future spaceborne lidar instruments (e.g., VCL) should be used to produce global estimates of terrestrial aboveground biomass. Our results show that it will likely be necessary to develop a series of relationships between lidar metrics and aboveground biomass in different bioclimatic life zones. For example, lidar observations from tropical wet forests could be used in an equation such as the relationship developed for the Costa Rica study area, whereas in other tropical moist forests the Panama relationships may be applicable. Future research will test the applicability of these new relationships at other study areas within the same bioclimatic life zone.

These results also illustrate the importance of climatic variables for developing general algorithms for the estimation of aboveground biomass in different tropical areas using lidar data. For example, average rainfall data can be used to estimate leaf loss in canopy-forming trees during the dry season, which, as we have shown, will affect the generality of the relationship between lidar metrics and tropical forest aboveground biomass. At a minimum, if leaf phenology data and models are unavailable, biomass estimates would need to be developed from lidar data collected while the canopy is fully leafed out.

This study only begins the exploration of the generality of the relationships between lidar metrics and aboveground biomass in closed-canopy Neotropical forests, however it illustrates that this research area holds great potential. The strong correlation of lidar metrics with aboveground biomass in a variety of tropical forests is an improvement over many existing remote sensing techniques which are currently not able to reliably estimate biomass in older secondary and primary forests (Luckman et al. 1997, Steininger 2000, Nelson et al. 2000). Although relationships between lidar metrics and biomass may differ, the geographic regions where these differences occur appear to be distinct and may be predicted using climatic variables such as temperature and rainfall.

Future work in other tropical and extra-tropical forest environments may reveal that it is possible to develop a relatively simple algorithm or model to estimate terrestrial aboveground biomass globally from a suite of lidar and climatic metrics. In more open tropical woodlands, it is likely that additional lidar metrics such as canopy top height and a canopy cover index will be necessary to estimate aboveground biomass accurately. We also expect that the fusion of lidar data with high spatial and temporal satellite imagery will further extend the utility of these data.

Chapter 5. Summary and Conclusions

This research has shown that large-footprint lidar instruments are effective tools for aboveground biomass estimation in dense, closed-canopy tropical forests. The analysis in chapter 2 illustrated that metrics from lidar waveforms are highly correlated with aboveground biomass, as well as basal area and mean stem diameter at a tropical wet forest. Furthermore, the relationships were not asymptotic through the entire range of conditions sampled. This is important because this tropical forest has a canopy cover that is among the highest found in closed-canopy tropical forests.

The nature of the relationship between lidar metrics and aboveground biomass was further explored in chapter 3. Lidar waveform metrics are strongly correlated with metrics from field-derived crown volume distributions. In other words, lidar data are sensitive to important differences in the vertical distribution of canopy structure in different land cover types. This is an important component of the strong relationship between lidar metrics and aboveground biomass in tropical forests because metrics from field crown volume distributions were also strong predictors of aboveground biomass. This relationship is the result of the ecological and biomechanical links between vertical structure and aboveground biomass (King and Loucks 1978, Oohata and Shinozaki 1979, O'Neill and DeAngelis 1981, Givnish 1986, Franco and Kelly 1998).

It is also likely that lidar waveform metrics such as height of median energy (HOME) are strongly influenced by the degree of canopy cover. In open canopies, more lidar energy passes through the canopy and is reflected from the ground. This creates a large ground peak and thereby will result in a relatively low HOME value. This trend was observed in the differences in HOME values from agroforestry and primary forest areas in chapter 4 (Table 4.2), and is illustrated in Figure 5.1. As a result, areas that are more open due to anthropogenic (e.g., selective logging) or natural (e.g., treefall) disturbances will have lower AGBM and HOME values compared to dense undisturbed primary forest areas. This trend can be observed in the landscape-level image of lidar-estimated AGBM (Figure 2.10) where selectively logged areas in the western portion of La Selva have lower predicted AGBM densities than undisturbed (but environmentally similar) areas in the eastern portion of La Selva.

The trends discussed above illustrate why lidar metrics such as HOME are good predictors of AGBM at the tropical wet forest study areas from chapters 2 and 3. However, there still remained a question as to how generally applicable these relationships are in tropical areas with environmental conditions different from La Selva. The results in chapter 4 show that environmental variables such as total annual precipitation are pertinent in at least two ways to the exploration of the generality of relationships between lidar metrics and forest structural characteristics.

First, these variables can explain differences in leaf phenology that will affect lidar data collected during periods of canopy deciduousness. If leaf phenology data or models are unavailable, then estimates of aboveground biomass could still be developed from lidar data collected while the canopy is fully leafed out. Second, environmental variables may also be used to delineate

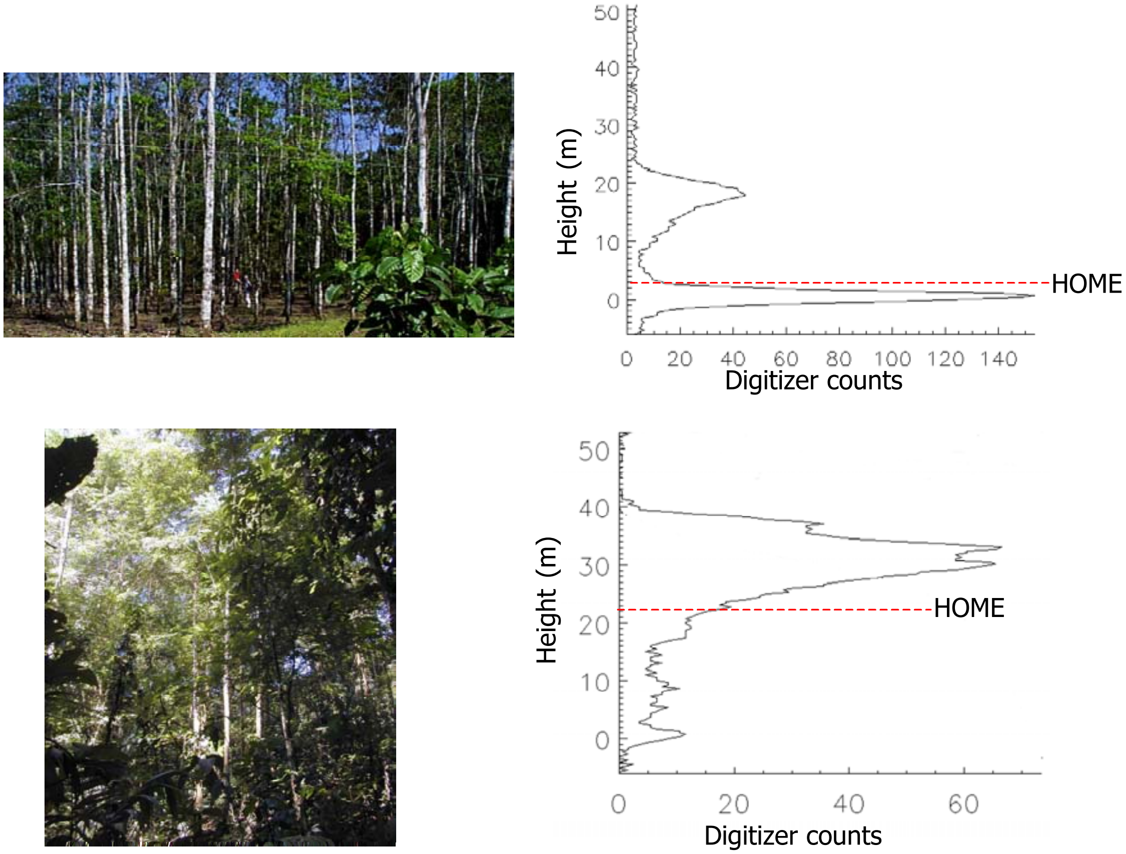

Figure 5.1 The lidar height of median energy (HOME) metric is sensitive to differences in the vertical distribution of canopy elements, as well as the canopy cover. In low canopy cover conditions found in agroforestry areas at La Selva Biological Station (upper portion), much of the lidar energy is reflected from the ground, thus lowering HOME. In contrast, most of the energy is reflected from the canopy elements in primary forest areas (lower portion), thus increasing HOME.

regions where appropriate relationships between lidar metrics and aboveground biomass should be applied based on underlying field-developed allometric relationships. For example, in areas that are designated as tropical wet forest the HOME- EAGB relationship from La Selva (Table 2.4, equation 4) may be appropriate, whereas in tropical moist forests the relationship from Panama (Figure 4.10) could be used. It should be noted, however, that further research into both the generality of lidar and field allometric relationships is necessary.

Perhaps the most important finding of this research is that lidar metrics are highly correlated with estimated aboveground biomass in a variety of conditions found in closed canopy Neotropical forests. This represents a great improvement over previous attempts to estimate aboveground biomass using passive optical (Nelson et al. 2000, Steininger 2000) and synthetic aperture radar or SAR (Luckman et al. 1997). Figure 5.2 is a visualization of the estimated improvement of large-footprint lidar for AGBM estimation at La Selva over the published saturation limits of passive optical and SAR in closed-canopy Neotropical forests. Non-gray areas represent information that is gained through the use of large-footprint lidar for aboveground biomass estimation.

This represents an important breakthrough in the remote sensing of land surface characteristics. The sensitivity of lidar to differences in aboveground biomass within primary and older secondary forests in tropical wet (chapter 2 and 3) and tropical moist forests (chapter 4) will be invaluable to global biogeochemical models that estimate carbon fluxes between vegetation and the atmosphere.

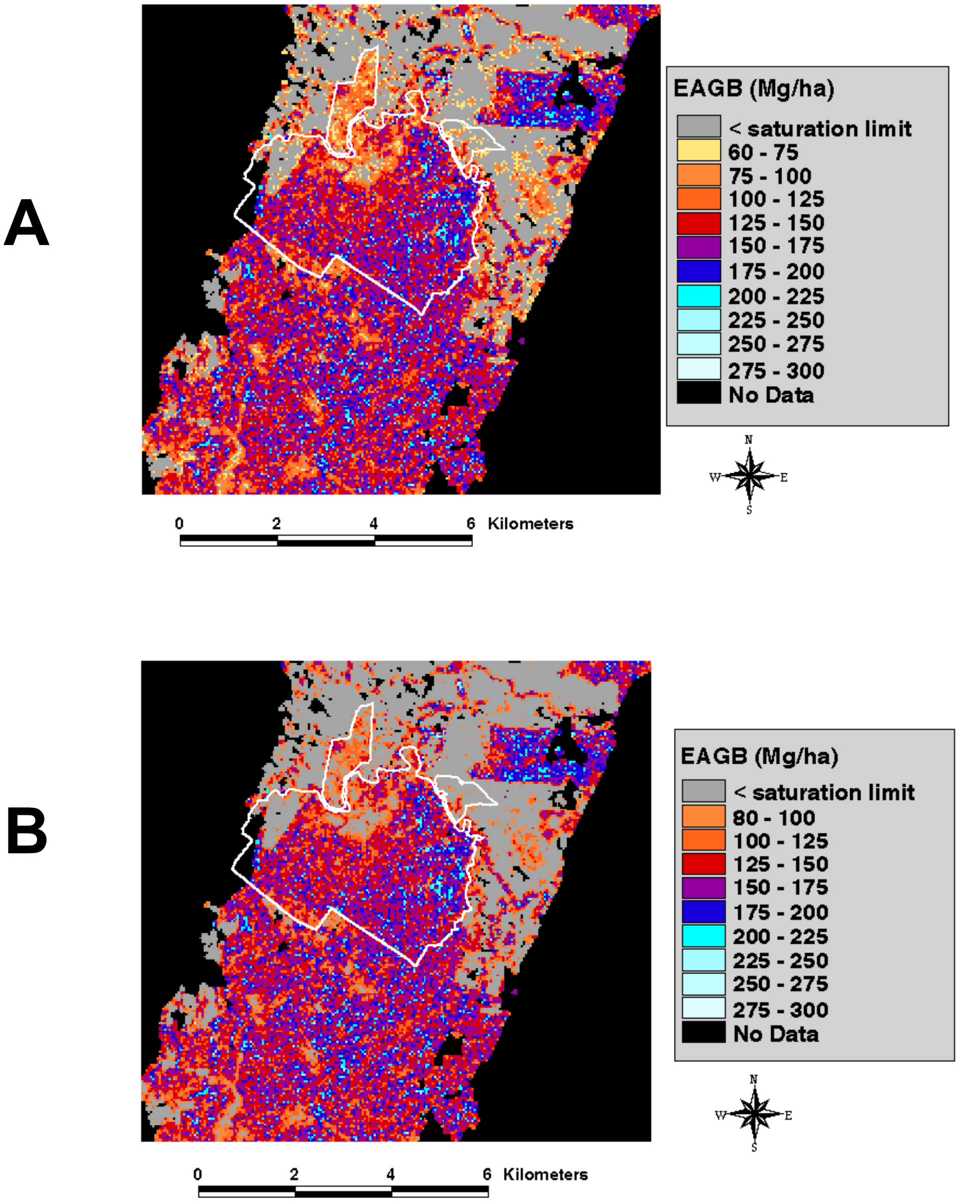

Figure 5.2 Visualization of aboveground biomass information gained through the use of large-footprint lidar vs. (A) synthetic aperture radar and (B) passive optical remote sensing techniques Saturation limits are adapted from published values for L-band SAR (Luckman et al. 1997) and Landsat TM (Steininger 2000)

The Road Ahead

The research in this dissertation is only a first step towards developing global biomass estimates in terrestrial vegetation using large-footprint lidar. There are several areas that future lidar research should focus on to achieve that goal. Several of these areas are discussed below.

First, the relationships between lidar metrics and directly measured forest structural characteristics must be examined in other areas. These structural characteristics, such as canopy height metrics, basal area and mean stem diameter, can be quantified in a relatively precise manner. As a result they represent a better “target” to assess the accuracy of lidar (e.g., Peterson 2000 for accuracy of canopy heights). In addition, the examination of the generality of the relationships between lidar metrics and directly measurable characteristics is relatively straightforward because they are not dependent on field-estimated allometric equations.

Second, future studies should test the applicability of these new linear relationships between lidar metrics (e.g., HOME) and allometrically estimated aboveground biomass in other study areas within the same tropical life zone. For example, will the relationship from the Panama study area (Figure 4.10) also apply to tropical moist forests in the Amazon basin? Further, will either relationship apply to Paleotropical forests such as the tall Dipterocarp forests in Southeast Asia? Although no lidar data are presently available from this region, the preliminary analysis presented in chapter 1 reveals that the relationship between field-collected stand height and biomass is fairly robust throughout the tropics (Figure 1.4).

Third, future studies should also begin to explore other lidar metrics that can be used to improve the generality of aboveground biomass estimation techniques. For example, the incorporation of a lidar derived canopy cover index, such as the ratio of energy in the ground return (chapter 2), along with the canopy height metric may help extend relationships into open woodlands.

Fourth, when several of the research areas above have been more fully investigated then it should be possible to develop a general algorithm for global biomass estimation. This kind of approach could identify areas where the appropriate relationship between lidar metrics and estimated aboveground biomass should be used. For example, if relationships are valid within fairly broad bioclimatic life zones (Holdridge et al. 1971) then these areas could be identified, along with other important climatic variables that may directly affect the relationships (e.g., drought deciduousness). This research would allow for relatively straightforward global terrestrial biomass estimates using future spaceborne large-footprint lidar instruments.

Fifth, future research should also focus on the fusion of lidar data with other remotely sensed data and products from other remote sensing instruments. High temporal resolution data (e.g., from the **MOD**erate resolution **I**maging **S**ensor) could provide information related to seasonal and long-term vegetation dynamics that would be missed by relatively short-term spaceborne lidar missions such as the Vegetation Canopy Lidar (Dubayah et al. 1997). Additionally, data products from these sensors such as land cover distributions could be helpful for efforts to extrapolate outside of areas that are sampled with spaceborne lidar instruments (see Dubayah et al. 2000). High spatial resolution data (e.g., from IKONOS) could also benefit landscape to regional scale carbon flux estimation efforts, as well as to aid efforts to scale-up to broader spatial scales. Hyperspectral instruments (e.g., Hyperion on the Earth Observing-1 satellite) may provide data related to leaf phenology that could be of direct use in adjusting lidar metrics (similar to chapter 4). In addition, future radar data sets may be complementary to spaceborne lidar data, especially in areas that are frequently cloud covered.

Finally, future research should also begin to connect lidar data with biogeochemical models. In particular, new height-structured terrestrial ecosystem models such as the Ecosystem Demography (ED) model (Hurtt et al. 1998, Moorcroft et al. In press) can be readily initialized with lidar data to predict carbon fluxes over policy relevant time scales. Upcoming research will focus on using airborne large-footprint lidar data to initialize the ED model at a variety of temperate and tropical sites. These efforts can then one day be extended to initialize ED with land surface information from spaceborne lidar to produce estimates of global carbon fluxes.

REFERENCES

Aber, J. D. 1979a. Foliage-height profiles and succession in Northern hardwood forests. Ecology **60**:18-23.

Aber, J. D. 1979b. A method for estimating foliage-height profiles in broad-leaved forests. Journal of Ecology **67**:35-40.

Anderson, G. L., J. D. Hanson, and R. H. Haas. 1993. Evaluating Landsat thematic mapper derived vegetation indexes for estimating aboveground biomass on semiarid rangelands. Remote Sensing of Environment **45**:165-175.

Baker, J. R., P. L. Mitchell, R. A. Cordey, G. B. Groom, J. J. Settle, and M. R. Stileman. 1994. Relationships between physical characteristics and polarimetric radar backscatter for Corsican pine stands in Thetford Forest, UK. International Journal of Remote Sensing **15**:2827-2849.

Baldocchi, D., and S. Collineau. 1994. The physical nature of solar radiation in heterogeneous canopies: Spatial and temporal attributes. Pages 21-71 *in* M. M. Caldwell and R. W. Pearcy, editors. Exploitation of Environmental Heterogeneity by Plants. Academic Press, New York.

Battle, M., M. L. Bender, P. P. Tans, J. W. C. White, J. T. Ellis, T. Conway, and R. J. Francey. 2000. Global carbon sinks and their variability inferred from atmospheric O-2 and delta C-13. Science **287**:2467-2470.

Birdsey, R. A., R. Mickler, D. Sandberg, R. Tinus, J. Zerbe, and K. O'Brien, editors. 1997. USDA Forest Service global change research program highlights: 1991-1995. General Technical Report NE-237. USDA Forest Service Northeastern Forest Experiment Station, Radnor, PA.

Blair, J. B., D. B. Coyle, J. Bufton, and D. J. Harding. 1994. Optimization of an airborne laser altimeter for remote sensing of vegetation and tree canopies. Pages 939-941 *in* IGARSS-'94- Surface and Atmospheric Remote Sensing: Technologies Data Analysis and Interpretation. IEEE, Pasadena, CA.

Blair, J. B., and M. A. Hofton. 1999. Modeling laser altimeter return waveforms over complex vegetation using high-resolution elevation data. Geophysical Research Letters **26**:2509-2512.

Blair, J. B., D. L. Rabine, and M. A. Hofton. 1999. The Laser Vegetation Imaging Sensor (LVIS): A medium-altitude, digitization-only, airborne laser altimeter for mapping vegetation and topography. ISPRS Journal of Photogrammetry and Remote Sensing **54**:115-122.

Bohlman, S. A., R. Condit, S. T. O'Brien, R. B. Foster, and S. P. Hubbell. In review. Using species-specific allometric equations to predict canopy structure on Barro Colorado Island, Panama.

Bormann, B. T., and G. E. Likens. 1979. Pattern and Process in a Forested Ecosystem. Springer-Verlag, New York.

Boyd, D. S., G. M. Foody, and P. J. Curran. 1999. The relationship between the biomass of Cameroonian tropical forests and radiation reflected in middle infrared wavelengths (3.0-5.0 um). International Journal of Remote Sensing **20**:1017-1023.

Brown, I. F., L. A. Martinelli, W. W. Thomas, M. Z. Moreira, C. A. C. Ferreira, and R. A. Victoria. 1995. Uncertainty in the biomass of Amazonian forests: An example from Rondonia, Brazil. Forest Ecology and Management **75**:175-189.

Brown, M. J., and G. G. Parker. 1994. Canopy light transmittance in a chronosequence of mixed-species deciduous forests. Canadian Journal of Forest Research-Revue Canadienne De Recherche Forestiere **24**:1694-1703.

Brown, S. 1997. Estimating biomass and biomass change of tropical forests: A primer. UN-FAO Forestry Paper 134, Rome, Italy.

Brown, S., and A. E. Lugo. 1990. Tropical secondary forests. Journal of Tropical Ecology **6**:1-32.

Brown, S., and A. E. Lugo. 1992. Aboveground biomass estimates for tropical moist forests of the Brazilian Amazon. Interciencia **17**:8-18.

Cannell, M. G. R. 1982. World Forest Biomass and Primary Production. Academic Press, London, UK.

Cannell, M. G. R. 1984. Woody biomass of forest stands. Forest Ecology and Management **8**:299-312.

Chave, J., R. Condit, T. Guynup, S. Lao, J. P. Caspersen, J. P. Megonigal, R. B. Foster, and S. P. Hubbell. In preparation. Spatial and temporal variation in biomass of a tropical rain forest: Results from a large census plot in Panama. Journal of Ecology.

Chazdon, R. L. 1996. Spatial heterogeneity in tropical forest structure: Canopy palms as landscape mosaics. Trends in Ecology & Evolution **11**:8-9.

Clark, D. A., S. Brown, D. W. Kicklighter, J. Q. Chambers, J. R. Thomlinson, and J. Ni. 2001. Measuring net primary production in forests: Concepts and field methods. Ecological Applications **11**:356-370.

Clark, D. B. 1990. La Selva Biological Station: A blueprint for stimulating tropical research. Pages 9-27 *in* A. H. Gentry, editor. Four Neotropical Rainforests. Yale University Press, New Haven, CT.

Clark, D. B., and D. A. Clark. 2000. Landscape-scale variation in forest structure and biomass in a tropical rain forest. Forest Ecology and Management **137**:185-198.

Clark, D. B., D. A. Clark, and J. M. Read. 1998. Edaphic variation and the mesoscale distribution of tree species in a neotropical rain forest. Journal of Ecology **86**:101-112.

Clark, D. B., D. A. Clark, P. M. Rich, S. Weiss, and S. F. Oberbauer. 1996. Landscape scale evaluation of understory light and canopy structure: Methods and application in a neotropical lowland rain forest. Canadian Journal of Forest Research **26**:747-757.

Condit, R. 1998. Tropical Forest Census Plots. Springer-Verlag, Berlin, Germany.

Condit, R., K. Watts, S. A. Bohlman, R. Perez, R. B. Foster, and S. P. Hubbell. 2000. Quantifying the deciduousness of tropical forest canopies under varying climates. Journal of Vegetation Science **11**:649-658.

Cressie, N. A. 1991. Statistics for Spatial Data. John Wiley and Sons, New York.

Curran, P. J., G. M. Foody, R. M. Lucas, M. Honzak, and J. Grace. 1997. The carbon balance of tropical forests: From the local to the regional scale. Pages 201-227 *in* P. R. van Gardingen, G. M. Foody, and P. J. Curran, editors. Scaling-up from Cell to Landscape. Cambridge University Press, Cambridge.

Danson, F. M., and P. J. Curran. 1993. Factors affecting the remotely sensed response of coniferous forest plantations. Remote Sensing of Environment **43**:55-65.

DeFries, R., M. Hansen, and J. Townshend. 1995. Global discrimination of land cover types from metrics derived from AVHRR pathfinder data. Remote Sensing of Environment **54**:209-222.

Denslow, J. S., and G. S. Hartshorn. 1994. Tree-fall gap environments and forest dynamic processes. Pages 120-127 *in* L. A. McDade, K. S. Bawa, H. A. Hespenheide, and G. S. Hartshorn, editors. La Selva: Ecology and Natural History of a Neotropical Rain Forest. University of Chicago Press, Chicago.

Dixon, R. K., S. Brown, R. A. Houghton, A. M. Solomon, M. C. Trexler, and J. Wisniewski. 1994. Carbon pools and flux of global forest ecosystems. Science **263**:185-190.

Dobson, M. C. 2000. Forest information from synthetic aperture radar. Journal of Forestry **98**:41-43.

Dobson, M. C., F. T. Ulaby, T. Letoan, A. Beaudoin, E. S. Kasischke, and N. Christensen. 1992. Dependence of radar backscatter on coniferous forest biomass. IEEE Transactions on Geoscience and Remote Sensing **30**:412-415.

Dobson, M. C., F. T. Ulaby, and L. E. Pierce. 1995a. Land-cover classification and estimation of terrain attributes using synthetic aperture radar. Remote Sensing of Environment **51**:199-214.

Dobson, M. C., F. T. Ulaby, L. E. Pierce, T. L. Sharik, K. M. Bergen, J. Kellndorfer, J. R. Kendra, E. Li, Y. C. Lin, A. Nashashibi, K. Sarabandi, and P. Siqueira. 1995b. Estimation of forest biophysical characteristics in Northern Michigan with Sir-C/X-Sar. IEEE Transactions on Geoscience and Remote Sensing **33**:877-895.

Drake, J. B., R. Dubayah, R. Knox, and D. Clark. In review. Relationship between vertical canopy profiles and biomass in a Neotropical rainforest. Remote Sensing of Environment.

Drake, J. B., R. O. Dubayah, D. B. Clark, R. G. Knox, J. B. Blair, M. A. Hofton, R. L. Chazdon, J. F. Weishampel, and S. Prince. In press. Estimation of tropical forest structural characteristics using large-footprint lidar. Remote Sensing of Environment.

Drake, J. B., and J. F. Weishampel. 2000. Multifractal analysis of canopy height measures in a longleaf pine savanna. Forest Ecology and Management **128**:121-127.

Dubayah, R., J. B. Blair, J. L. Bufton, D. B. Clark, J. JaJa, R. G. Knox, S. B. Luthcke, S. Prince, and J. F. Weishampel. 1997. The Vegetation Canopy Lidar mission. Pages 100-112 *in* Land Satellite Information in the Next Decade II: Sources and Applications. American Society for Photogrammetry and Remote Sensing, Bethesda, MD.

Dubayah, R. O., and J. B. Drake. 2000. Lidar remote sensing for forestry. Journal of Forestry **98**:44-46.

Dubayah, R. O., R. G. Knox, M. A. Hofton, J. B. Blair, and J. B. Drake. 2000. Land surface characterization using lidar remote sensing. Pages 25-38 *in* M. J. Hill and R. J. Aspinall, editors. Spatial Information for Land Use Management. Gordon and Breach Science Publishers, Australia.

Falkowski, P., R. J. Scholes, E. Boyle, J. Canadell, D. Canfield, J. Elser, N. Gruber, K. Hibbard, P. Hogberg, S. Linder, F. T. Mackenzie, B. Moore, T. Pedersen, Y. Rosenthal, S. Seitzinger, V. Smetacek, and W. Steffen. 2000. The global carbon cycle: A test of our knowledge of earth as a system. Science **290**:291-296.

Fan, S., M. Gloor, J. Mahlman, S. Pacala, J. Sarmiento, T. Takahashi, and P. Tans. 1998. A large terrestrial carbon sink in North America implied by atmospheric and oceanic carbon dioxide data and models. Science **282**:442-446.

FAO. 1995. Forest resources assessment 1990: Global synthesis. Food and Agriculture Organization, Rome, Italy.

Ferrazzoli, P., and L. Guerriero. 1996. Passive microwave remote sensing of forests: A model investigation. IEEE Transactions on Geoscience and Remote Sensing **34**:433-443.

Ferrazzoli, P., S. Paloscia, P. Pampaloni, G. Schiavon, D. Solimini, and P. Coppo. 1992. Sensitivity of microwave measurements to vegetation biomass and soil-moisture content - A case-study. IEEE Transactions on Geoscience and Remote Sensing **30**:750-756.

Fetcher, N., S. F. Oberbauer, and R. L. Chazdon. 1994. Physiological ecology of plants. Pages 128-141 *in* L. A. McDade, K. S. Bawa, H. A. Hespenheide, and G. S. Hartshorn, editors. La Selva: Ecology and Natural History of a Neotropical Rain Forest. University of Chicago Press, Chicago.

Foley, J. A., I. C. Prentice, N. Ramankutty, S. Levis, D. Pollard, S. Sitch, and A. Haxeltine. 1996. An integrated biosphere model of land surface processes, terrestrial carbon balance, and vegetation dynamics. Global Biogeochemical Cycles **10**:603-628.

Foody, G. M., and P. J. Curran. 1994. Estimation of tropical forest extent and regenerative stage using remotely-sensed data. Journal of Biogeography **21**:223-244.

Foody, G. M., G. Palubinskas, R. M. Lucas, P. J. Curran, and M. Honzak. 1996. Identifying terrestrial carbon sinks: Classification of successional stages in regenerating tropical forest from Landsat TM data. Remote Sensing of Environment **55**:205-216.

Franco, M., and C. K. Kelly. 1998. The interspecific mass-density relationship and plant geometry. Proceedings of the National Academy of Sciences, USA **95**:7830-7835.

Franklin, J. F., D. R. Berg, D. A. Thornburgh, and J. C. Tappeiner. 1997. Alternative sivicultural approaches to timber harvesting: Variable retention harvest systems. Pages 111-139 *in* K. A. Kohm and J. F. Franklin, editors. Creating a Forestry for the 21st Century. Island Press, Washington DC.

Fransson, J. E. S., F. Walter, and L. M. H. Ulander. 2000. Estimation of forest parameters using CARABAS-II VHF SAR data. IEEE Transactions on Geoscience and Remote Sensing **38**:720-727.

Friend, A. D., A. K. Stevens, R. G. Knox, and M. G. R. Cannell. 1997. A process-based, terrestrial biosphere model of ecosystem dynamics (Hybrid v3.0). Ecological Modelling **95**:249-287.

Gaston, G., S. Brown, M. Lorenzini, and K. D. Singh. 1998. State and change in carbon pools in the forests of tropical Africa. Global Change Biology **4**:97-114.

Gifford, R. M. 1994. The global carbon-cycle: A viewpoint on the missing sink. Australian Journal of Plant Physiology **21**:1-15.

Givnish, T. J. 1986. Biomechanical constraints on self-thinning in plant populations. Journal of Theoretical Biology **119**:139-146.

Goetz, S. J., S. D. Prince, S. N. Goward, M. M. Thawley, and J. Small. 1999. Satellite remote sensing of primary production: an improved production efficiency modeling approach. Ecological Modelling **122**:239-255.

Green, R. M., N. S. Lucas, P. J. Curran, and G. M. Foody. 1996. Coupling remotely sensed data to an ecosystem simulation model - An example involving a coniferous plantation in upland Wales. Global Ecology and Biogeography Letters **5**:192-205.

Guariguata, M. R., R. L. Chazdon, J. S. Denslow, J. M. Dupuy, and L. Anderson. 1997. Structure and floristics of secondary and old-growth forest stands in lowland Costa Rica. Plant Ecology **132**:107-120.

Hall, F. G., Y. E. Shimabukuro, and K. F. Huemmrich. 1995. Remote sensing of forest biophysical structure using mixture decomposition and geometric reflectance models. Ecological Applications **5**:993-1013.

Harding, D. J., M. A. Lefsky, G. G. Parker, and J. B. Blair. 2001. Laser altimeter canopy height profiles: Methods and validation for closed-canopy, broadleaf forests. Remote Sensing of Environment **76**:283-297.

Hardisky, M. A., F. C. Daiber, C. T. Roman, and V. Klemas. 1984. Remote sensing of biomass and annual net aerial primary productivity of a salt marsh. Remote Sensing of Environment **16**:91-106.

Harrell, P. A., E. S. Kasischke, L. L. BourgeauChavez, E. M. Haney, and N. L. Christensen. 1997. Evaluation of approaches to estimating aboveground biomass in southern pine forests using SIR-C data. Remote Sensing of Environment **59**:223-233.

Hofton, M. A., J. B. Blair, J. B. Minster, J. R. Ridgeway, N. P. Williams, J. L. Bufton, and D. L. Rabine. 2000a. An airborne scanning laser altimetry survey of Long Valley, California. International Journal of Remote Sensing **21**:2413-2437.

Hofton, M. A., J. B. Minster, and J. B. Blair. 2000b. Decomposition of laser altimeter waveforms. IEEE Transactions on Geoscience and Remote Sensing **38**:1989-1996.

Holdridge, L. R., W. C. Grenke, W. H. Hatheway, T. Liang, and J. J. A. Tosi. 1971. Forest Environments in Tropical Life Zones: A Pilot Study, First edition. Pergamon Press, New York, NY.

Holland, E. A., and S. Brown. 1999. Technical Comments: North American carbon sink. Science **283**:1815.

Houghton, R. A. 1991. Tropical deforestation and atmospheric carbon dioxide. Climatic Change **19**:99-118.

Houghton, R. A. 1996. Converting terrestrial ecosystems from sources to sinks of carbon. Ambio **25**:267-272.

Hurtt, G. C., P. R. Moorcroft, S. W. Pacala, and S. A. Levin. 1998. Terrestrial models and global change: challenges for the future. Global Change Biology **4**:581-590.

Husch, B., C. I. Miller, and T. W. Beers. 1982. Forest Mensuration, Third edition. John Wiley & Sons, New York.

Hyyppa, J., J. Pulliainen, M. Hallikainen, and A. Saatsi. 1997. Radar-derived standwise forest inventory. IEEE Transactions on Geoscience and Remote Sensing **35**:392-404.

Imhoff, M. L. 1995. Radar backscatter and biomass saturation - Ramifications for global biomass inventory. IEEE Transactions on Geoscience and Remote Sensing **33**:511-518.

Jin, Y. Q., and C. Liu. 1997. Biomass retrieval from high-dimensional active/passive remote sensing data by using artificial neural networks. International Journal of Remote Sensing **18**:971-979.

Kaiser, J. 1998. Climate change - Possibly vast greenhouse gas sponge ignites controversy. Science **282**:386-387.

Kasischke, E. S., N. L. Christensen, and L. L. Bourgeauchavez. 1995. Correlating radar backscatter with components of biomass in loblolly-pine forests. IEEE Transactions on Geoscience and Remote Sensing **33**:643-659.

Kasischke, E. S., J. M. Melack, and M. C. Dobson. 1997. The use of imaging radars for ecological applications - A review. Remote Sensing of Environment **59**:141-156.

Keller, M., M. Palace, and G. C. Hurtt. In Press. Biomass estimation in the Tapajos National Forest, Brazil: Examination of sampling and allometric uncertainties. Forest Ecology and Management.

Kimes, D. S., R. F. Nelson, D. L. Skole, and W. A. Salas. 1998. Accuracies in mapping secondary tropical forest age from sequential satellite imagery. Remote Sensing of Environment **65**:112-120.

Kimmins, J. P. 1997. Forest Ecology: A Foundation for Sustainable Management, 2nd edition. Prentice-Hall, Inc., Upper Saddle River, NJ.

King, D., and O. L. Loucks. 1978. The theory of tree bole and branch form. Radiation and Environmental Biophysics **15**:141-165.

King, D. A. 1996. Allometry and life history of tropical trees. Journal of Tropical Ecology **12**:25-44.

Kolchugina, T. P., and T. S. Vinson. 1995. Role of Russian Forests in the Global Carbon Balance. Ambio **24**:258-264.

Laurance, W. F., P. M. Fearnside, S. G. Laurance, P. Delamonica, T. E. Lovejoy, J. Rankin-de Merona, J. Q. Chambers, and C. Gascon. 1999. Relationship between soils and Amazon forest biomass: A landscape-scale study. Forest Ecology and Management **118**:127-138.

Lefsky, M. A. 1997. Application of lidar remote sensing to the estimation of forest canopy and stand structure. Ph.D. dissertation. Department of Environmental Sciences, University of Virginia, Charlottesville.

Lefsky, M. A., W. B. Cohen, S. A. Acker, G. G. Parker, T. A. Spies, and D. Harding. 1999a. Lidar remote sensing of the canopy structure and biophysical properties of Douglas-fir western hemlock forests. Remote Sensing of Environment **70**:339-361.

Lefsky, M. A., D. Harding, W. B. Cohen, G. Parker, and H. H. Shugart. 1999b. Surface lidar remote sensing of basal area and biomass in deciduous forests of eastern Maryland, USA. Remote Sensing of Environment **67**:83-98.

LeToan, T., A. Beaudoin, J. Riom, and D. Guyon. 1992. Relating forest biomass to SAR data. IEEE Transactions on Geoscience and Remote Sensing **30**:403-411.

Li, X. W., A. H. Strahler, and C. E. Woodcock. 1995. A hybrid geometric optical-radiative transfer approach for modeling albedo and directional reflectance of discontinuous canopies. IEEE Transactions on Geoscience and Remote Sensing **33**:466-480.

Lieberman, D., M. Lieberman, R. Peralta, and G. S. Hartshorn. 1996. Tropical forest structure and composition on a large-scale altitudinal gradient in Costa Rica. Journal of Ecology **84**:137-152.

Lieberman, M., D. Lieberman, and R. Peralta. 1989. Forests are not just swiss cheese: Canopy stereogeometry of non-gaps in tropical forests. Ecology **70**:550-552.

Lin, Y. C., and K. Sarabandi. 1999a. A Monte Carlo coherent scattering model for forest canopies using fractal-generated trees. IEEE Transactions on Geoscience and Remote Sensing **37**:440-451.

Lin, Y. C., and K. Sarabandi. 1999b. Retrieval of forest parameters using a fractal-based coherent scattering model and a genetic algorithm. IEEE Transactions on Geoscience and Remote Sensing **37**:1415-1424.

Luckman, A., J. Baker, T. M. Kuplich, C. D. F. Yanasse, and A. C. Frery. 1997. A study of the relationship between radar backscatter and regenerating tropical forest biomass for spaceborne SAR instruments. Remote Sensing of Environment **60**:1-13.

MacArthur, R. H., and H. S. Horn. 1969. Foliage profile by vertical measurements. Ecology **50**:802-804.

MacDicken, K. G., Winrock International. 1997. A guide to monitoring carbon storage in forestry and agroforestry projects. Available at: http://www.winrock.org

Maclean, G. A., and W. B. Krabill. 1986. Gross-merchantable timber volume estimation using an airborne lidar system. Canadian Journal of Remote Sensing **12**:7-18.

Magnussen, S., and P. Boudewyn. 1998. Derivations of stand heights from airborne laser scanner data with canopy-based quantile estimators. Canadian Journal of Forest Research **28**:1016-1031.

Magnussen, S., P. Eggermont, and V. N. LaRiccia. 1999. Recovering tree heights from airborne laser scanner data. Forest Science **45**:407-422.

Matlock Jr., R. B., and G. S. Hartshorn. 1999. Organization for Tropical Studies: La Selva Biological Station. Bulletin of the Ecological Society of America **80**:188-193.

McDade, L. A., K. S. Bawa, H. A. Hespenheide, and G. S. Hartshorn, editors. 1994. La Selva: Ecology and Natural History of a Neotropical Rain Forest. University of Chicago Press, Chicago.

Means, J. E., S. A. Acker, D. J. Harding, J. B. Blair, M. A. Lefsky, W. B. Cohen, M. E. Harmon, and W. A. McKee. 1999. Use of large-footprint scanning airborne lidar to estimate forest stand characteristics in the Western Cascades of Oregon. Remote Sensing of Environment **67**:298-308.

Menalled, F. D., M. J. Kelty, and J. J. Ewel. 1998. Canopy development in tropical tree plantations: A comparison of species mixtures and monocultures. Forest Ecology and Management **104**:249-263.

Moorcroft, P., G. C. Hurtt, and S. Pacala. In press. Scaling rules for vegetation dynamics: A new terrestrial biosphere model for global change studies. Ecological Monographs.

Moran, E. F., E. Brondizio, P. Mausel, and Y. Wu. 1994. Integrating Amazonian vegetation, land-Use, and satellite data. BioScience **44**:329-338.

Myneni, R. B. 1991. Modeling radiative transfer and photosynthesis in three-dimensional vegetation canopies. Agricultural and Forest Meterology **55**:323-344.

Naesset, E. 1997a. Determination of mean tree height of forest stands using airborne laser scanner data. ISPRS Journal of Photogrammetry and Remote Sensing **52**:49-56.

Naesset, E. 1997b. Estimating timber volume of forest stands using airborne laser scanner data. Remote Sensing of Environment **61**:246-253.

Nelson, R. 1997. Modeling forest canopy heights: The effects of canopy shape. Remote Sensing of Environment **60**:327-334.

Nelson, R., D. Kimes, W. A. Salas, and M. Routhier. 2000. Secondary forest age and tropical forest biomass estimation using thematic mapper imagery. BioScience **50**:419-431.

Nelson, R., W. Krabill, and J. Tonelli. 1988a. Estimating forest biomass and volume using airborne laser data. Remote Sensing of Environment **24**:247-267.

Nelson, R., R. Oderwald, and T. G. Gregoire. 1997. Separating the ground and airborne laser sampling phases to estimate tropical forest basal area, volume, and biomass. Remote Sensing of Environment **60**:311-326.

Nelson, R., R. Swift, and W. Krabill. 1988b. Using airborne lasers to estimate forest canopy and stand characteristics. Journal of Forestry **86**:31-38.

Nelson, R. F., T. G. Gregoire, and R. G. Oderwald. 1998. The effects of fixed-area plot width on forest canopy height simulation. Forest Science **44**:438-444.

Ni, W. G., X. W. Li, C. E. Woodcock, M. R. Caetano, and A. H. Strahler. 1999. An analytical hybrid GORT model for bidirectional reflectance over discontinuous plant canopies. IEEE Transactions on Geoscience and Remote Sensing **37**:987-999.

Ni, W. G., X. W. Li, C. E. Woodcock, J. L. Roujean, and R. E. Davis. 1997. Transmission of solar radiation in boreal conifer forests: Measurements and models. Journal of Geophysical Research-Atmospheres **102**:29555-29566.

Nicotra, A. B., R. L. Chazdon, and S. V. B. Iriarte. 1999. Spatial heterogeneity of light and woody seedling regeneration in tropical wet forests. Ecology **80**:1908-1926.

Niklas, K. J. 1994a. Plant Allometry: The Scaling of Form and Process. University of Chicago Press, Chicago, IL.

Niklas, K. J. 1994b. Size-dependent variations in plant-growth rates and the "3/4- power rule". American Journal of Botany **81**:134-144.

Nilsson, M. 1996. Estimation of tree heights and stand volume using an airborne lidar system. Remote Sensing of Environment **56**:1-7.

Oberbauer, S. F., D. B. Clark, D. A. Clark, P. M. Rich, and G. Vega. 1993. Light environment, gas-exchange, and annual growth of saplings of 3 species of rainforest trees in Costa Rica. Journal of Tropical Ecology **9**:511-523.

Oliver, C. D., and B. C. Larson. 1990. Forest Stand Dynamics. McGraw Hill, New York.

Olson, J. S., J. A. Watts, and L. J. Allison. 1983. Carbon in Live Vegetation of Major World Ecosystems. ORNL-5862, Oak Ridge National Laboratory, Oak Ridge, TN.

O'Neill, R. V., and D. L. DeAngelis. 1981. Comparative productivity and biomass relations of forest ecosystems. Pages 411-449 *in* D. E. Reichle, editor. Dynamic properties of forest ecosystems. Cambridge University Press, Cambridge.

Oohata, S., and K. Shinozaki. 1979. A statical model of plant form– Further analysis of the pipe model theory. Japanese Journal of Ecology **29**:323-335.

OTS, Organization for Tropical Studies. 2001. La Selva Biological Station: Meterological data (1957-2001). Available at: http://www.ots.duke.edu/en/laselva/

Paloscia, S., and P. Pampaloni. 1992. Microwave vegetation indexes for detecting biomass and water conditions of agricultural crops. Remote Sensing of Environment **40**:15-26.

Pare, D., and Y. Bergeron. 1995. Above-ground biomass accumulation along a 230-year chronosequence in the southern portion of the Canadian boreal forest. Journal of Ecology **83**:1001-1007.

Parker, G. G. 1995. Structure and microclimate of forest canopies. Pages 73-106 *in* M. D. Lowman and N. M. Nadkarni, editors. Forest Canopies. Academic Press, New York.

Parker, G. G., M. A. Lefsky, and D. J. Harding. 2001. Light transmittance in forest canopies determined using airborne lidar altimetry and in-canopy quantum measurements. Remote Sensing of Environment **76**:298-309.

Perry, D. A. 1994. Forest Ecosystems. Johns Hopkins University Press, Baltimore.

Peterson, B. E. 2000. Recovery of forest canopy heights using large-footprint lidar. M.A. thesis. Department of Geography, University of Maryland, College Park.

Pierce, S. 1992. La Selva Biological Station history: colonization/landuse/deforestation of Sarapiqui, Costa Rica. M.S. thesis. Colorado State University, Fort Collins, CO.

Potter, C. S. 1999. Terrestrial biomass and the effects of deforestation on the global carbon cycle - Results from a model of primary production using satellite observations. BioScience **49**:769-778.

Potter, C. S., and S. A. Klooster. 1999a. Detecting a terrestrial biosphere sink for carbon dioxide: Interannual ecosystem modeling for the mid-1980s. Climatic Change **42**:489-503.

Potter, C. S., and S. A. Klooster. 1999b. Technical Comments: North American carbon sink. Science **283**:1815.

Prince, S. D., S. J. Goetz, and S. N. Goward. 1995. Monitoring primary production from earth observing satellites. Water Air and Soil Pollution **82**:509-522.

Prince, S. D., and S. N. Goward. 1995. Global primary production: A remote sensing approach. Journal of Biogeography **22**:815-835.

Pyke, C. R., R. Condit, S. Aguilar, and S. Lao. In press. Floristic composition across a climatic gradient in a neotropical lowland forest. Journal of Vegetation Science.

Ranson, K. J., G. Sun, J. F. Weishampel, and R. G. Knox. 1997. Forest biomass from combined ecosystem and radar backscatter modeling. Remote Sensing of Environment **59**:118-133.

Rich, P. M., D. B. Clark, D. A. Clark, and S. F. Oberbauer. 1993. Long-term study of solar radiation regimes in a tropical wet forest using quantum sensors and hemispherical photography. Agricultural and Forest Meteorology **65**:107-127.

Richards, P. W. 1996. The Tropical Rain Forest: An Ecological Study. Cambridge University Press, New York.

Running, S., D. L. Peterson, M. A. Spanner, and K. B. Teuber. 1986. Remote sensing of coniferous forest leaf area. Ecology **67**:273-276.

Sader, S. A., R. B. Waide, W. T. Lawrence, and A. T. Joyce. 1989. Tropical forest biomass and successional age class relationships to a vegetation index derived from Landsat TM data. Remote Sensing of Environment **28**:143-156.

Saldarriaga, J. G., D. C. West, M. L. Tharp, and C. Uhl. 1988. Long-term chronosequence of forest succession in the upper Rio Negro of Colombia and Venezuela. Journal of Ecology **76**:938-958.

Sanford Jr., R. L., P. Paaby, J. C. Luvall, and E. Phillips. 1994. Climate, geomorphology and aquatic systems. Pages 106-119 *in* L. A. McDade, K. S. Bawa, H. A. Hespenheide, and G. S. Hartshorn, editors. La Selva: Ecology and Natural History of a Neotropical Rain Forest. University of Chicago Press, Chicago.

Schutz, B. E. 1998. Spaceborne laser altimetry: 2001 and beyond. *in* H. P. Plag, editor. Book of Extended Abstracts, WEGENER-98. Norwegian Mapping Authority, Honefoss, Norway.

Shippert, M. M., D. A. Walker, N. A. Auerbach, and B. E. Lewis. 1995. Biomass and leaf-area index maps derived from SPOT images for Toolik Lake and Imnavait Creek areas, Alaska. Polar Record **31**:147-154.

Skole, D. L., W. H. Chomentowski, W. A. Salas, and A. D. Nobre. 1994. Physical and human dimensions of deforestation in Amazonia. BioScience **44**:314-322.

Smith, G., and L. M. H. Ulander. 2000. A model relating VHF-band backscatter to stem volume of coniferous boreal forest. IEEE Transactions on Geoscience and Remote Sensing **38**:728-740.

Smith, T. M., W. P. Cramer, R. K. Dixon, R. Leemans, R. P. Neilson, and A. M. Solomon. 1993. The global terrestrial carbon-cycle. Water Air and Soil Pollution **70**:19-37.

Smith, W. B., and G. J. Brand. 1983. Allometric biomass equations for 98 species of herbs, shrubs and small trees. NC-299, USFS North Central Forest Experimental Station.

Spies, T. A. 1997. Forest stand structure, composition and function. Pages 11-30 *in* K. A. Kohm and J. F. Franklin, editors. Creating a Forestry for the 21st Century. Island Press, Washington DC.

Steffen, W., I. Noble, J. Canadell, M. Apps, E. D. Schulze, P. G. Jarvis, D. Baldocchi, P. Ciais, W. Cramer, J. Ehleringer, G. Farquhar, C. B. Field, A. Ghazi, R. Gifford, M. Heimann, R. Houghton, P. Kabat, C. Korner, E. Lambin, S. Linder, H. A. Mooney, D. Murdiyarso, W. M. Post, I. C. Prentice, M. R. Raupach, D. S. Schimel, A. Shvidenko, and R. Valentini. 1998. The terrestrial carbon cycle: Implications for the Kyoto Protocol. Science **280**:1393-1394.

Steininger, M. K. 1996. Tropical secondary forest regrowth in the Amazon: age, area and change estimation with Thematic Mapper data. International Journal of Remote Sensing **17**:9-27.

Steininger, M. K. 2000. Satellite estimation of tropical secondary forest above-ground biomass: Data from Brazil and Bolivia. International Journal of Remote Sensing **21**:1139-1157.

Strahler, A. H. 1997. Vegetation canopy reflectance modeling- Recent developments and remote sensing perspectives. Remote Sensing Reviews **15**:179-194.

Sun, G., D. S. Simonett, and A. H. Strahler. 1991. A radar backscatter model for a discontinuous coniferous forest. IEEE Transactions on Geoscience and Remote Sensing **29**:639-650.

Sun, G. Q., and K. J. Ranson. 1995. A 3-Dimensional radar backscatter model of forest canopies. IEEE Transactions on Geoscience and Remote Sensing **33**:372-382.

Sundquist, E. T. 1993. The global carbon dioxide budget. Science **259**:934-941.

Tans, P. P., I. Y. Fung, and T. Takahashi. 1990. Observational constraints on the global atmospheric CO2 budget. Science **247**:1431-1438.

Ulaby, F. T., K. Sarabandi, K. McDonald, M. Whitt, and M. Dobson. 1990. Michigan Microwave Canopy Scattering Model (MIMICS). International Journal of Remote Sensing **11**:1123-1253.

Wang, Y., F. W. Davis, J. M. Melack, E. S. Kasischke, and N. L. Christensen. 1995. The effects of changes in forest biomass on radar backscatter from tree canopies. International Journal of Remote Sensing **16**:503-513.

Waring, R. H., J. B. Way, E. R. Hunt, L. Morrissey, K. J. Ranson, J. F. Weishampel, R. Oren, and S. E. Franklin. 1995. Biologists toolbox - Imaging radar for ecosystem studies. BioScience **45**:715-723.

Weishampel, J. F., K. J. Ranson, and D. J. Harding. 1996. Remote sensing of forest canopies. Selbyana **17**:6-14.

Weltz, M. A., J. C. Ritchie, and H. D. Fox. 1994. Comparison of laser and field measurements of vegetation height and canopy cover. Water Resources Research **30**:1311-1319.

Whittaker, R. H., and G. M. Woodwell. 1968. Dimension and production relations of trees and shrubs in the Brookhaven Forest, New York. Journal of Ecology **56**:1-25.

Whittaker, R. H., and G. M. Woodwell. 1969. Structure, production and diversity of the oak-pine forest at Brookhaven, New York. Journal of Ecology **57**:155-174.

Wickland, D. E. 1991. Global ecology: The role of remote sensing. Pages 723-750 *in* G. Esser and D. Overdieck, editors. Modern Ecology, Basic and Applied Aspects. Elsevier, New York, NY.

Wigneron, J. P., A. Chanzy, J. C. Calvet, and W. Bruguier. 1995. A simple algorithm to retrieve soil moisture and vegetation biomass using passive microwave measurements over crop fields. Remote Sensing of Environment **51**:331-341.

Wigneron, J. P., P. Ferrazzoli, J. C. Calvet, Y. Kerr, and P. Bertuzzi. 1999. A parametric study on passive and active microwave observations over a soybean crop. IEEE Transactions on Geoscience and Remote Sensing **37**:2728-2733.

Wigneron, J. P., Y. Kerr, A. Chanzy, and Y. Q. Jin. 1993. Inversion of surface parameters from passive microwave measurements over a soybean field. Remote Sensing of Environment **46**:61-72.

Wu, Y. C., and A. H. Strahler. 1994. Remote estimation of crown size, stand density, and biomass on the Oregon transect. Ecological Applications **4**:299-312.

Yamakura, T., M. Kanzaki, A. Itoh, T. Ohkubo, K. Ogino, E. Chai, H. S. Lee, and P. S. Ashton. 1996. Forest structure of a tropical rain forest at Lambir, Sarawak with special reference to the dependency of its physiognomic dimensions on topography. Tropics **6**:1-18.

Yang, J. L., and S. D. Prince. 1997. A theoretical assessment of the relation between woody canopy cover and red reflectance. Remote Sensing of Environment **59**:428-439.

Zar, J. H. 1996. Biostatistical Analysis, 3rd edition. Prentice-Hall, Upper Saddle River, NJ.